C.P. No. 275
(16,679)
A.R.C. Technical Report

C.P. No. 275
(16,679)
A.R.C. Technical Report

MINISTRY OF SUPPLY

AERONAUTICAL RESEARCH COUNCIL

CURRENT PAPERS

The Hot-Wire Anemometer for Turbulence Measurements

Part III

by

B. Wise, M.A., and D. L. Schultz

LONDON : HER MAJESTY'S STATIONERY OFFICE

1956

PRICE 9s 6d NET

C.P. No. 275

The Hot-wire Anemometer for Turbulence Measurements Part III

- By -
B. Wise, M.A., and D. L. Schultz

O.U.E.L. No. 69.

Communicated by Prof. A. Thom

24th March, 1954

Summary

Further investigation of the operation of the hot-wire anemometer has shown that there are only two systems which are both statically stable and capable of improving the frequency response. A description is given of further experiments which have been made to verify the theory of operation of the wire, using both radio-frequency and direct current heating. An analysis of some feedback systems is given, and it is shown how these techniques may be used in the measurement of turbulence at high air speeds.

Contents

Section No.			Page No.
1.1		Static Stability	3
1.2		Dynamic Stability	6
1.3		Effect of Amplifier Characteristics	6
2.	Overall Feedback Systems		8
2.1		Constant Voltage Systems. Negative Feedback	8
	2.1.1	Frequency-independent Feedback	9
	2.1.2	Amplifier Characteristics	9
	2.1.3	Differentiated Feedback	10
	2.1.4	Phase-compensated Feedback	11
2.2		Constant Resistance System	11
	2.2.1	Frequency-independent Feedback	11
	2.2.2	The Effect of the Demodulator	12
	2.2.3	Compensated Feedback	13
	2.2.4	Differentiated Feedback	14
2.3		Doubly-differentiated Feedback	14

3./

Section No.			Page No.
3.	Improvements in the Radio Frequency System		14
	3.1	Feedback from the Wire Voltage	14
	3.1.1	Radio Frequency Analysis	15
	3.2	Impedance Transformation	17
	3.3	A Note on the Maximum Attainable Bandwidth with Constant Resistance Heating	18
4.	Experimental Verification of the Approach to Constant Resistance Operation		19
5.	Frequency Response of Typical Oscillator at Low Radio Frequencies		20
	5.1	Effect of $(R_1 - R_c)$ on Response	21
	5.2	Effect of Tuned Circuit Inductance on Response Bandwidth	21
6.	Overall Feedback Applied to Constant Resistance Systems		22
	6.1	Experimental Results. Negative Feedback	22
	6.2	Experimental Results. Differentiated Feedback for Stabilization	23
7.	Overall Feedback applied to Constant Current and Constant Voltage Systems		23
	7.1	Experimental Results. Negative Feedback applied to Constant Voltage System	25
	7.2	Constant Voltage System with Differentiated Feedback	25
	7.2.1	Experimental Results. Constant Voltage System with Differentiated Feedback	26
8.	The Use of High Frequency and Very High Frequency Oscillators		26
	8.1	The Push-pull Oscillator	27
	8.2	Power Valves for Use in Very High Frequency Oscillators	27
	8.3	The Push-pull 807 Oscillator	28
	8.4	Negative Feedback applied to the Push-pull 807 Oscillator	29
	8.5	Experimental Plot of the Nyquist Diagram	29
	8.6	The Transmission-line Oscillator	30
	8.7	High Frequency Characteristics of Hot-wire Probes	32
9.	The Production of Variations in Velocity for Testing Purposes		33
	9.1	Transient Testing of the Wire in an Airstream	33
	9.2	The Hot Wire in a Shock Tube	33
	Conclusion		34
	References		34
	Appendix		35

Introduction/

Introduction

In a previous paper[1] an analysis has been given of the operation of a hot-wire anemometer using radio-frequency heating and direct current heating, and experimental evidence in support of this theory has also been given[2]. The present paper deals with further theoretical and practical aspects of anemometer operation. In Section 1 it is shown that there are only two stable feedback systems which will improve the frequency response, one suitable for radio frequency applications and the other for direct current heating. The latter is analysed in detail in Section 1.3. In Section 2 overall feedback systems are analysed. Two methods of improving the radio frequency oscillator system are described in Section 3. In Section 4 a description is given of some elementary checks made on the zero-frequency operation of the self-oscillatory radio-frequency system to verify the equivalent circuit developed in Ref. 1.

Experimental results are presented in the remainder of the paper. Some of these results were obtained with platinum wires of resistance 10 to 25 ohms, such as were used in the experiments previously described in Ref. 2. These wires are, however, only suitable for use at low airspeeds and for use at transonic and supersonic speeds tungsten wires of resistance 2 to 5 ohms have been used. The development of a welding technique for these wires has been reported[6]. With these low resistance wires it is more difficult to create a practical embodiment of the theory, but by the use of high radio frequencies considerable progress has been made.

1.1 Static Stability

In Ref. 1 it was shown that, to approach ideal operation, a hot-wire should be connected in a circuit which gives a straight-line relation between voltage and current. This is shown in Fig. 1, which is reproduced here for convenience from Fig. 7 of Ref. 1.

It was shown how such a relation could be obtained by positive feedback from voltage to current. We now consider the general case of feedback from both voltage and current.

If a wire is connected to a voltage source V, which has an internal resistance ρ, the wire voltage v and current i are given by:

$$v + \rho i = V.$$

Similarly, if a wire is connected to a current source I, which has an internal admittance γ,

$$i + \gamma v = I.$$

In general, let us take the relation:

$$\alpha i + \beta v = \nu$$

where α and β are positive. We now add terms λi and μv to indicate feedsback from the wire current and voltage to the source, as follows:

$$\alpha i + \beta v = \lambda i + \mu v + \nu. \qquad \ldots (1)$$

This gives a straight line which intersects the hot-wire characteristic at the operating point (see Fig. 1). The slope of this line, R_c, is given by

$$R_c = \frac{\lambda - \alpha}{\beta - \mu}. \qquad \ldots (2)$$

If/

If the slope of the hot-wire characteristic at any point is R_W, small increments of wire current Δi and voltage Δv are connected by the relation:

$$\Delta v = R_W \cdot \Delta i .$$

The increment of the right-hand side of Eqn. (1), which results from a current increment Δi, is the incremental feedback, and, if this is less than the increment of the left-hand side, the operating point will be statically stable. This gives, as a necessary condition for stability,

$$\lambda + \mu R_W < \alpha + \beta R_W$$

i.e.,
$$\lambda - \alpha < (\beta - \mu) R_W . \qquad \ldots \quad (3)$$

We now consider two cases, first $\beta - \mu > 0$, and second, $\beta - \mu < 0$. When $\beta - \mu > 0$ we have from (3)

$$\frac{\lambda - \alpha}{\beta - \mu} < R_W \quad \text{i.e.,} \quad R_c < R_W \text{ from (2).}$$

In this case, therefore, the slope of the straight line must be less than the slope of the hot-wire characteristic for stability. When $\beta - \mu < 0$ we have from (2)

$$\frac{\lambda - \alpha}{\beta - \mu} > R_W \quad \text{i.e.,} \quad R_c > R_W .$$

Here, the slope of the straight line must be greater than the slope of the hot-wire characteristic for stability.

The two regions for stability are shown in Fig. 2. The region of stability given in the second case is not of practical interest, because to approach constant-resistance operation of the wire the slope of the straight line should approximate to v/i. In other words, the conditions $R_c > R_W$ and $R_c \simeq v/i$ are incompatible, because R_W is considerably larger than v/i. We therefore confine our attention now to the case $\beta - \mu > 0$.

Since in practice we require R_c to be positive, it follows from (2) that if $\beta - \mu > 0$, $\lambda - \alpha > 0$.

Two special cases of interest now arise, first $\alpha = 0$, second $\beta = 0$. The first implies pure voltage feedback, the second pure current feedback. When α is zero, λ must be positive, so we must feed back positively from current to voltage. There is no need for any voltage feedback, since μ can be zero. If any positive voltage feedback is used, it must not exceed a certain value, but there is no limit to its magnitude if negative.

On the other hand if β is zero, μ must be negative, that is we must feed back negatively from voltage to current. In this last case we must also have $\lambda - \alpha > 0$, so there must also be some current feedback. The connection of these two extreme cases with the general case can be seen from the following table.

	α	β	λ	μ
General Case	+	+	$>\alpha$	$<\beta$
Voltage Feedback	0	+	+	$<\beta$
Current Feedback	+	0	$>\alpha$	-

We/

We emphasize again the fundamental differences between the two extremes: in the first case the current-to-voltage feedback is positive and the voltage-to-voltage feedback can have either sign, whereas in the second case the voltage-to-current feedback is negative and the current-to-current feedback must be positive and exceed a certain value.

It has been shown in Ref. 1 that the first of these two cases, that of voltage feedback, lends itself to radio-frequency systems, whereas it is evident that if direct currents are to be used the second case, that of current feedback, would be more practical owing to the low impedance of the wire.

An embodiment of the second case is shown in Fig. 3 (Refs. 3, 4). Here H is the hot-wire, P, Q, S are fixed resistances, and the block represents a direct-coupled amplifier of gain m. If the resistances P, Q are so large that the current through them is negligible compared with the hot-wire current, we have pure current feedback. The input to the amplifier is $(PSi - Qv)/(P + Q)$ so that, if the slope of the pentode is s,

$$i = sm\frac{PSi - Qv}{P + Q} + i_o \qquad \ldots (4)$$

where i_o is the current in the pentode when there is no input to the amplifier. This may be written:

$$v = R_c i + v_o \qquad \ldots (5)$$

$$\text{where } R_c = \frac{P}{Q} \cdot S - \frac{P + Q}{smQ} \text{ and } v_o = i_o \frac{P + Q}{smQ} . \qquad \ldots (6)$$

This is shown in Fig. 4.

It was shown in Ref. 1 that the response of a hot-wire to velocity variations can be found from an equivalent circuit which is reproduced here as Fig. 5. In this circuit, i_a is a current generator which simulates the velocity variations, and Δi, Δv are changes in the hot-wire current and voltage. R_1 is the hot-wire resistance, and R_b is $R_w - R_1$ (see Appendix). C is a capacity such that CR_b is the time-constant in constant-current operation.

When v and i are related by Eqn. (5) the equivalent circuit reduces to that shown in Fig. 6.

The overall time-constant is now given by

$$T = CR_b\frac{R_1 - R_c}{R_b + R_1 - R_c} , \qquad \ldots (7)$$

It is evident from Fig. 4 that

$$R_1 - R_c = \frac{v}{i_1} - \frac{v - v_o}{i_1} = \frac{v_o}{i_1} \qquad \ldots (8)$$

so that

$$T = \frac{CR_b v_o}{R_b i_1 + v_o} \qquad \ldots (9)$$

When/

When $v_o << R_b i$, we have approximately

$$T = \frac{Cv_o}{i_1} . \qquad \ldots (10)$$

The smaller it is possible to make v_o, the smaller is T, but difficulties arise with dynamic instability, which is considered in the following Section.

1.2 Dynamic Stability

In the preceding Section, we have assumed that increments of wire current and voltage are related by $\Delta v = R_w \cdot \Delta i$, where R_w is the slope of the v/i characteristic. This is only true if thermal equilibrium is maintained. For rapid changes, we should take $\Delta v = R_1 \cdot \Delta i$, where $R_1 = v/i$.

This consideration modifies the criterion for stability when $\beta > \mu$ since $R_1 < R_w$, and it becomes

$$\beta > \mu, \quad R_c < R_1 .$$

The criterion when $\beta < \mu$ is not affected.

These two regions for stability are shown in Fig. 7. It is impossible to operate stably in the range $R_1 < R_c < R_w$. This result can also be obtained from the expression 7 for the time-constant, which is negative, indicating instability, when $R_1 < R_c < R_b + R_1$. It is shown in the Appendix that $R_b + R_1 = R_w$ so that this result is the same as the above.

In deriving the equivalent circuit Fig. 6, from which the expression (7) is derived, it has been assumed that the relation $v = R_c i + v_o$ is valid at all frequencies. In practice the frequency characteristic of the feedback amplifier will modify the equivalent circuit in a manner which is discussed in the next Section.

1.3 Effect of Amplifier Characteristics

Referring to Eqn. (6), when we consider that the amplifier gain m is a function of frequency, we will write

$$v = Z_c i + v_o$$

where $$Z_c = \frac{P}{Q} S - \frac{P + Q}{smQ} .$$

We will take $P = Q$, and let $2/s = r$, so that $Z_c = S - r/m$ and v_o is given by

$$v_o = i_o r/m . \qquad \ldots (11)$$

Suppose that at zero frequency $m = m_o$ and $Z_c = R_c$, so that

$$R_c = S - \frac{r}{m_o} , \quad \text{and} \quad R_c - Z_c = r\left[\frac{1}{m} - \frac{1}{m_o}\right]. \qquad \ldots (12)$$

From the equivalent circuit shown in Fig. 6, replacing R_c by Z_c, we find that

$$\frac{\Delta i}{i_a} = \left\{1 + (R_1 - Z_c)(1/R_b + pC)\right\}^{-1} . \qquad \ldots (13)$$

We now find $(R_1 - Z_c)$ in terms of m:

$$R_1 - Z_c = R_1 - R_c + R_c - Z_c$$

$$= \frac{v_o}{i_1} + r\left[\frac{1}{m} - \frac{1}{m_o}\right] \quad \text{from (8) and (12)}$$

$$= \frac{r}{m_o}\left[\frac{i_o}{i_1} + \frac{m_o}{m} - 1\right].$$

Substituting in (13),

$$\frac{\Delta i}{i_a} = \left\{1 + \frac{1}{A}\left[\frac{m_o}{m} - 1 + \frac{i_o}{i_1}\right](1 + pT_c)\right\}^{-1} = G_c \quad \text{say}$$

where $A = R_b m_o / r$ and $T_c = CR_b$

$$G_c = \left\{1 + \frac{1}{G_d}\right\}^{-1} \quad \text{where} \quad G_d = (1 + pT_c)^{-1} \cdot \frac{A\, m/m_o}{(1 - \gamma m/m_o)}$$

and $\gamma = 1 - i_o/i_1$.

The relation between Δi and i_a is thus the same as would be found in a feedback system with open-loop transfer function equal to G_d. The first factor in G_d represents a simple integrating time-constant, and the second a regenerative amplifier of gain Am/m_o and feedback factor γ/A. This equivalent circuit is shown in Fig. 8. When the dependence of m on frequency is neglected so that $m = m_o$, the overall response has a simple time constant approximately equal to $T_c(1-\gamma)/A$, i.e., it is reduced by a factor equal to the gain of the regenerative amplifier.

We will consider first the special case given by $\gamma = 0$, i.e., $i_1 = i_o$. Since i_o is the current when the bridge is balanced, this condition implies that no change in wire current would occur if the feedback loop in Fig. 3 were broken.

At this point we indicate briefly how the response function $G_c = \dfrac{G_d}{1 + G_d}$ is obtained from G_d, by means of attenuation and phase plots. The modulus, in decibels, and phase of G_d are plotted against the logarithm of the frequency, and an approximate idea of the overall response G_c is obtained by taking $|G_c| = 1$ when $|G_d| > 1$, and $|G_c| = |G_d|$ when $|G_d| < 1$. The response G_c can be found accurately from the Nichol's Chart[5].

If we disregard the frequency characteristic of the amplifier, (1) in Fig. 9 is the straight line plot of $|G_d|$, which is greater than unity when $\omega T_c < A$. The above approximate reasoning therefore gives an overall response of unity for $\omega T_c < A$ and a response equal to $|G_d|$ for $\omega T_c > A$. This approximate plot for $|G_c|$ is shown as (2) in Fig. 9. This gives practically the same result as the accurate analysis.

The overall response will be very little altered with a practical amplifier if the latter has a reasonably uniform response, without excessive phase shift, up to $\omega T_c = A$.

Returning now to the general case when γ is not zero, the above analysis will apply to the regenerative amplifier which has a gain Am/m_o and

positive/

positive feedback factor γ/A. The actual amplifier used must therefore have characteristics such that, when this positive feedback is applied, the response still satisfies the requirement of uniformity and absence of excessive phase shift up to the breakpoint of the required overall response.

2. Overall Feedback Systems

It has been shown in Ref. 1 that when two types of heating are employed one of them may be used to simulate velocity variations, and the possibility arises of using overall feedback. We present here an analysis in which the response signal appears as a modulation of a radio-frequency voltage, and direct current is used for feedback. If the two roles are reversed some modification is required, in that a modulator is used instead of a demodulator, and this appears in a different part of the loop. Another possibility, which has been considered but will not be further referred to here, is that of using two radio-frequency currents, one controlled by the other through a mixer.

The system considered is shown schematically in Fig. 10, in which the blocks represent transfer functions. The wire is subject to a velocity variation proportional to i_a and also a variation in direct-current Δi_d. As a result there is a change in radio-frequency output which is to be found from the equivalent circuit, Fig. 11, and this is the output from G_1. The block G_2 represents the demodulator circuit and subsequent amplification. Blocks G_3 and H represent circuits whose purpose is to improve the frequency response.

$$\text{Evidently } \frac{i_b}{i_a} = \left\{ \frac{1}{G_1 G_2 G_3} + H \right\}^{-1} = (G_c), \text{ say.} \qquad \ldots \quad (14)$$

Feedback systems fall into two groups: first, those in which a constant radio-frequency heating voltage or current is supplied, so that the resistance changes with velocity, and secondly those in which it is arranged that the resistance is substantially constant at zero frequency.

2.1 Constant-voltage Systems. Negative Feedback

When the wire is supplied with a constant radio-frequency heating voltage, and the demodulated output fed back negatively to reduce resistance variation, the arrangement shown in Fig. 12 is convenient. The value V_1, which is driven by an external oscillator, supplies power to the wire R via the tuned circuit LC. Variations in air speed modulate the voltage across the tuned circuit, which is applied to the demodulator D. The output from this is amplified and controls a direct current in the wire via the value V_2. The equivalent circuit is shown in Fig. 13, where i_a represents the velocity input, Δi_r and Δi_d the resulting changes in radio-frequency and direct current respectively, and the chain connecting Δi_d with Δi_r is included in the symbol k'. It simplifies the algebra to modify the equivalent circuit as shown in Fig. 14, where:

$$R_g = \frac{R_1 R_b}{R_1 + R_b}, \quad i'_a = \frac{i_a R_b}{R_1 + R_b}, \quad k = \frac{k' R_b}{R_1 + R_b}.$$

Comparing this with the general system shown in Fig. 10, we have:

$$G_1 = \frac{\Delta i_r}{i'_a} = (1 + pCR_g)^{-1} = (1 + pT_v)^{-1}.$$

Where T_v is the constant-voltage time constant. Evidently $G_2 G_3 H = k$ and we will take $H = 1$, regarding the feedback current Δi_d as the final response. In practice, the input voltage to V_2 would be the response of the system. We should remark that, with this algebraic simplification, G_3

now/

now contains certain constants, so that our previous statement that G_3 is inserted to improve the frequency response has to this extent to be modified.

2.1.1 Frequency-independent Feedback

We consider first the demodulator to be perfect, and the amplifier to have a gain which is independent of frequency, so that k is a constant. From (14)

$$G_c = \left(1 + \frac{1 + pT_v}{k}\right)^{-1}$$

$$= \left(1 + \frac{1}{k}\right)^{-1} (1 + pT')^{-1},$$

where $$T' = T_v(1 + k)^{-1}.$$

The overall response is thus given by a simple time-constant which is less than the constant-voltage time-constant by a factor $(1 + k)$. The response, when plotted as a function of log ω, will have a break-point at $\omega \simeq k/T_v$. This result can easily be demonstrated by means of attenuation frequency plots. Suppose the loop gain $G_1G_2G_3H$, is G_1 and $H = 1$ so that $G_c = (1 + 1/G_1)^{-1}$ from (14).

Where $|G_1| > 1$, $|G_c| \simeq 1$, and where $|G_1| < 1$, $|G_c| \simeq |G_1|$. In Fig. 15, (1) is the straight line plot of $|G_1|$, and (2) is the plot of $|G_c|$ obtained by this approximate reasoning. The loop gain below the breakpoint is $20 \log_{10} k$ dB, and above the breakpoint at $\omega T_v = 1$ falls at a rate of 20 dB per decade, so that it reaches 0dB at $\omega T_v = k$. This gives practically the same result as the accurate analysis.

We will now relate k to the voltage amplification m used in the system, so as to find what gain is required for a specified increase in bandwidth. The output from the tuned circuit is a voltage $X\Delta i_r$ where X is the reactance of the tuned-circuit capacity. If η_d is the demodulator efficiency, and s is the transconductance of V_2,

$$k = X \eta_d m s \frac{v_d}{v_r} \cdot \frac{R_b}{R_1 + R_b}.$$

Thus for a bandwidth improvement of N times, we require a voltage gain given by

$$m \simeq \frac{Nv_r (R_1 + R_b)}{X\eta_d S r_d R_b}.$$

Typical values are $X = 50$ ohms, $s = 5$ mA/V, $\eta_d = 0.8$, $R_1 = R_b$, and $v_a = v_r$, giving $m = 10N$. For example, a hundred-fold improvement in bandwidth would require a voltage gain of 1,000 times.

2.1.2 Amplifier Characteristics

It is well known[5] that a feedback system is usually unstable if the phase margin is negative when the loop gain exceeds or is equal to unity. In practice it is desirable that the phase margin should exceed 30° when the gain is unity. In the system described above, the loop gain is unity when $|G_2G_3| \simeq \omega T_v$.

Assuming/

Assuming that the amplifier gain characteristic is substantially uniform up to this frequency, and equal to k, we have $\omega = k/T_v$ for a loop gain of unity, and this is the breakpoint of the overall response. The approximate attenuation-frequency plot of Fig. 15 is thus unaltered.

At the upper breakpoint, $\arg G_1(i\omega) \simeq 90°$, so that for a phase margin of 30° here we need $\arg G_2 G_3 > -60°$. This will probably be the case if the gain characteristic is level up to this frequency.

We conclude that it will be satisfactory if the voltage amplifier has a characteristic which is level up to the frequency at which the overall response begins to fall off. If the amplifier is directly-coupled the possibility of instability only occurs at high frequencies, but if there are condenser-resistance couplings there is a possibility of positive feedback at low frequencies. As the frequency falls there is an increasing phase lead, and if the loop gain is still greater than unity when the phase margin becomes negative instability will occur. We cannot use three equal time-constants in the amplifier because the loop gain would then be limited to 8 times, whereas we require something like 100 times for a hundred-fold bandwidth improvement. Although instability would not occur with two equal time-constants, the phase margin at unity loop gain would be so small as to cause an objectionable peak in overall response.

A solution to the difficulty is found by inserting a single time-constant into the loop, whose breakpoint is at a frequency which is well above that of all other time-constants, so that the loop gain is reduced below unity when the phase margin becomes negative. If all the other time-constants are equal and have breakpoints at $\omega = \omega_1$, the breakpoint of this single time-constant must occur at $\omega = k\omega_1$, approximately. The effect on the overall response is negligible at frequencies above the lower breakpoint $\omega = \omega_1$, since it is only below this that the loop gain falls below unity.

2.1.3 Differentiated Feedback

Suppose that it were possible to insert in the amplifier a perfect differentiator so that in Fig. 10 $G_3 = pT_e$. We take $G_2 = 1$, and $H = 1$.

Then $$G_c = \left\{\frac{1 + pT_v}{pT_e} + 1\right\}^{-1} \quad \text{from (14)}$$

$$= \left\{1 + \frac{T_v}{T_e}\right\}^{-1} \left\{1 + \frac{1}{p(T_v + T_e)}\right\}^{-1} .$$

The overall response has a breakpoint at a frequency given by $\omega[T_v + T_e] = 1$, and is level above this. Before the loop is closed the breakpoint is given by $\omega T_v = 1$ so that closing the loop lowers the breakpoint.

Fig. 16 shows the attentuation-frequency plots for this system. Curve (1) shows the $|G_1|$ characteristic, and (2) and (3) are possible lines for $|G_3|$. The products $|G_1 G_3|$ are given by curves (4) and (5), which correspond to (2) and (3) respectively. In the first case, closing the loop produces curve (6) which has a lower breakpoint than (2), while in the second case closing the loop makes no difference in this approximate analysis since the loop gain is never greater than unity.

In practice differentiation can be approximately attained by a condenser and resistance, and this modifies the curves, as shown in Fig. 17. Let $G_3 = \frac{pT_3}{1 + pT_3} k$. Curves (2) and (3) are drawn with the same value of k but

in/

in the first case $T_3 k > T_V$, and in the second case $T_3 k < T_V$. It will be seen that the upper breakpoint is at $\omega T_V = k$ if the loop gain exceeds unity, independently of the value of T_3, but the lower breakpoint depends on T_3. When the loop gain does not exceed unity, the lower breakpoint is at $\omega T_V = 1$, while the upper is at a frequency determined by T_3. In this latter case there is of course a loss of signal level, and the feedback is virtually inoperative. An accurate analysis shows that in the case when $kT_3 = T_V$ and k is large, the upper breakpoint is at twice the frequency given by this approximate method, while the lower breakpoint is at one half the approximate frequency.

2.1.4 Phase-compensated Feedback

If we include in the feedback loop a phase-compensation network we may take $G_3 = k\varepsilon \dfrac{1 + pT_4}{1 + p\varepsilon T_4}$, where k is the gain without the network. The attenuation-frequency plot is shown in Fig. 18 where $k\varepsilon > 1$. It can be shown that the point P is at $\omega T_V = k$ independently of the values of T_4 and ε, so that the breakpoint of the overall response is approximately given by $\omega T_V = k$. In the particular case where $k\varepsilon = 1$ and $T_4 = T_V$, this breakpoint acutally occurs at a frequency given by $\omega T_V = 2k$.

2.2 Constant-resistance System

The transfer function for the self-oscillatory radio-frequency system whose equivalent circuit is shown in Fig. 11 is as follows:

$$\frac{\Delta i}{i_a} = \left\{ 1 + \frac{R_1 - R_c}{R_b} + p\left(\frac{2L}{R_b} + C\sqrt{R_1 - R_c} \right) + p^2 2LC \right\}^{-1} \qquad \ldots (15)$$

and this we may write in the following standard form:

$$G_1(p) = \left(1 + \frac{R_1 - R_c}{R_b} \right)^{-1} \left(1 + 2\frac{\zeta p}{\omega_q} + \frac{p^2}{\omega_q^2} \right)^{-1} .$$

Logarithmic plots of the modulus and phase of $G_1(j\omega)$ for different values of the damping coefficient ζ are given in books on networks and servomechanisms[5]. The damping depends very much on $R_1 - R_c$ as has been remarked in Ref. 1, and under certain conditions it may become zero. The factor $\left(1 + \dfrac{R_1 - R_c}{R_b} \right)^{-1}$ in the expression for $G_1(p)$ differs little from unity. It could be incorporated in the current generator, as was done with the factor $\dfrac{R_b}{R_1 + R_b}$ in the constant-current system, but it will for simplicity be omitted.

In Fig. 19 is shown the polar plot of $\{G_1(j\omega)\}^{-1}$, which is a parabola, the arrow giving the direction of increasing frequency. It will be noticed that the intercept on the imaginary axis is 2ζ, and that this point corresponds to the breakpoint on the logarithmic plots.

2.2.1 Frequency-independent Feedback

We consider first a system in which the loop gain at zero frequency is k, and $H = 1$. For convenience the factor v_a/v_r is incorporated in the value of G_3.

To begin with, we shall disregard the effect of the demodulator, taking $G_2 = 1$.

Then/

Then the overall transfer function from (14) is given by

$$G_c = \left\{ \frac{1}{kG_1} + 1 \right\}^{-1}$$

$$= \left\{ 1 + \frac{1}{k} + \frac{2\zeta p}{k\omega_q} + \frac{p^2}{k\omega_q^2} \right\}^{-1} .$$

Evidently the frequency of the breakpoint has been increased by the factor $(1 + k)^{\frac{1}{2}}$ and the damping decreased by a factor $(1 + k)^{\frac{1}{2}}$. An increase in bandwidth is thus obtained, but it may be accompanied by an objectionable peak in the response, due to the reduction in damping. The effect is clearly seen on the inverse polar plot, (Fig. 20), where a constant k is to be added to (1), $\{G_1(j\omega)\}^{-1}$ giving the parabola (2) which on division by k gives the new response locus (3). The ratio OB'/OA' is less than OB/OA indicating a decrease in the damping.

Figs. 21, 22 show the attenuation and phase of G_1; above the breakpoint $|G_1|$ falls at a rate of 40 dB/decade so that the loop gain reaches zero decibels at an angular frequency $\sqrt{k} \cdot \omega_q$. At this point the phase margin is small, its value depending on ζ and k; as an example, when $\zeta = 1$ and $k = 100$, it is 12°. The overall response therefore has a peak at this point; with the figures quoted it would have a magnitude of 12dB. The actual response can be found in any given case from a Nichol's chart[5]. This is referred to again in Section 8.4.

2.2.2 The Effect of the Demodulator

We now consider what modification in the above analysis is required to include the inevitable time-constant T_d of the demodulator.

Taking $G_2 = \dfrac{1}{1 + pT_d}$, we have, from (14),

$$G_c = \left\{ \left(1 + \frac{2\zeta p}{\omega_q} + \frac{p^2}{\omega_q^2} \right) \left(\frac{1 + pT_d}{k} \right) + 1 \right\}^{-1} .$$

The inverse polar plot of $G_1 G_2$ is shown in Fig. 23, and when the constant k is added to this it is evident that k must not exceed the intercept OC, otherwise the system will be unstable. The angular frequency at point C is $\omega_q \left(1 + \dfrac{2\zeta}{\omega_q T_d} \right)$ and the intercept OC is $2\zeta \left(\omega_q T_d + \dfrac{1}{\omega_q T_d} \right) + 4\zeta^2$.

As an example, we take $\omega_q = 50{,}000$ rad/sec, $T_d = 1\ \mu$ sec and $2\zeta = 1$. This gives ω at C $= 4.6\omega_q$ and OC $= 21$. Thus a value of $k = 21$ will cause oscillation at a frequency equal to 4.6 times that at the original breakpoint. The effect of the demodulator time-constant can be clearly seen when the attenuation and phase of $G_1 G_2$ are plotted as shown in Fig. 24, which is drawn for $2\zeta = 1$, $\omega_q = 50{,}000$ rad/sec and $T_d = 1\ \mu$ sec.

Suppose the value of $|G_1 G_2|$ when the phase margin becomes zero, i.e., phase -180°, is $1/k_o$ in dB. Then k must not exceed k_o, otherwise the system will be unstable. With the above values for ω_q, T_d, and ζ, k_o is found to be 21 times, and the angular frequency at which the phase margin is zero is $4.6\omega_q$, as already found.

2.2.3/

2.2.3 Compensated Feedback

In order to avoid the resonant peak produced by direct feedback, three courses have been considered. First, the original transfer function G_1 may be so much overdamped that a sufficient amount of direct feedback can be employed to increase the bandwidth without producing a peak. This is done by using, instead of a radio-frequency oscillator, a circuit driven from an external source. Then $R_1 - R_c$ is no longer zero, and by varying the degree of radio-frequency feedback we vary $R_1 - R_c$ and hence the damping ζ.

It has been found difficult to implement this idea, and in any case the dependence for a good response on the rather critical adjustment of a radio-frequency feedback would be an undesirable feature. In practice it is found that the response in a push-pull circuit without feedback does not usually have a peak, and may be considerably damped, so that some direct feedback can be successfully applied. Some results are given later, where it will be seen that in fact greater improvements in bandwidth can be achieved than would be expected from the simple theory outlined above.

Just as in the constant-current feedback system, it is necessary to arrange the low frequency characteristics so that the loop gain does not exceed unity when the phase margin becomes negative. This can be done, as before, by providing a single small time-constant in the loop.

When the demodulator time-constant is neglected, the effect of having $R_1 - R_c$ not equal to zero is to increase the p term. This could be done instead by employing differentiated feedback in addition to direct feedback. The effect will not be quite the same owing to the fact that differentiation is imperfect, and also owing to modification of the transfer function by the demodulator.

A third approach is to compensate for the time-constant of the demodulator; this implies the introduction of a transfer function $\varepsilon \dfrac{1 + pT_d}{1 + p\varepsilon T_d}$ in the loop.

The result of this is to substitute a new time-constant εT_d for T_d but an additional gain factor $1/\varepsilon$ is required. It will still be necessary to have some differentiated feedback, and the two ideas can be combined by the provision of a transfer function $\varepsilon \dfrac{1 + pT_f}{1 + pT_f\varepsilon}$ where T_f is somewhat larger than T_d. This is the same sort of transfer function as will arise in any case when some differentiated feedback is added to direct feedback, because the practical transfer function for differentiated feedback is of the form $\dfrac{pT'}{1 + pT'}$. Thus the idea of additional feedback and the idea of compensating for the demodulator are complementary and come to much the same thing.

Suppose that a mid-frequency loop gain of N times is used, so that a bandwidth improvement $\sqrt{N}$ is aimed at, the breakpoint rising from ω_q to $\sqrt{N} \cdot \omega_q$. We have at our disposal T_f and require to introduce an adequate phase margin at the point of zero gain.

Fig. 25 illustrates the effect of choosing $\varepsilon = 0.10$ and $T_f = 43.5$ μ sec. This locates the upper breakpoint of the phase advancer at the frequency at which the original system oscillated. It should be noted that an increased gain is now necessary since at low frequencies an attenuation of 20 dB is introduced by the phase compensator. The original response, Fig. 25 (1) has a break point at $\omega = 50{,}000$, $2\zeta = 1$, $T_d = 1$ μ sec.

The original phase response is (2) and the amplitude and phase response of the compensating network are shown in (3) and (4). The loop amplitude and

phase/

phase response may now be obtained, (5) and (6), and by choosing that the phase margin at unity loop gain shall be 20° we may determine from (5) that the overall low frequency loop gain must not exceed 13.75 dB.

From the Nichol's Chart the closed loop response (7) is found and it is seen to have a peak of 8.5 dB at $\omega = 3.5 \times 10^5$, an improvement of 7 times.

The compensator has introduced an attenuation of 20 dB hence the gain of the feedback amplifier must be 33.75 dB. If the loop gain was restricted to 26.4 dB as in the previous example, Fig. 24, the bandwidth improvement would be only 3.8 times but there would be an adequate phase margin of 50° and instability could not occur.

2.2.4 Differentiated Feedback

If in the example just given, a smaller value of ε is chosen, the low frequency loop gain is less than unity, and if ε is made vanishingly small, keeping εT_f constant, the transfer function being then $\dfrac{p\,\varepsilon\,T_f}{1 + p\,\varepsilon T_f}$, the loop gain and overall gain fall off at low frequencies. We then have what may be called differentiated feedback, Fig. 26. For the same reasons as set out in the previous Section the breakpoint of the differentiating network should be at about the same frequency as the desired response breakpoint. The overall response will be level approximately from $1/\sqrt{N} \cdot \omega_q$ to $\sqrt{N} \cdot \omega_q$. The lower cut-off may be an advantage in practice because the signal from a hot wire below a certain frequency represents fluctuations in mean speed rather than turbulence.

2.3 Doubly-differentiated Feedback

If in the general equation (14) we put

$$G_1 = 1 + \frac{2\zeta p}{\omega_q} + \frac{p^2}{\omega_q^2}, \quad G_2 = G_3 = 1$$

and make H perform a perfect double differentiation, $H = -\dfrac{p^2}{\omega_q^2}$

we have $G_c = \left(1 + \dfrac{2\zeta p}{\omega_q}\right)^{-1}$.

The overall response here is that of a simple time-constant $2\zeta/\omega_q$, so that when ζ is small this would represent a considerable improvement. When we consider imperfect double differentiation, however, $H = k\left(\dfrac{pT_g}{1 + pT_g}\right)^2$ we find that instability cannot be avoided with realizable gains.

3. Improvements in the Radio Frequency System

3.1 Feedback from the Wire Voltage

In Section 3.1 of Ref. 1 the following relation for the radio frequency circuit was found

$$\Delta v = R_c \Delta i - 2L \frac{d\Delta i}{dt} \qquad \ldots (16)$$

and this gives the equivalent circuit of Fig. 11. The smaller the value of the inductance the larger the bandwidth obtained, but there is a limit to the value

which/

which may be conveniently used in practice (about 0.5 μH). Now suppose that a voltage $k.\Delta v$ were fed back negatively, and the positive feedback increased by a factor $1 + k$.

$$\text{Then} \quad \Delta v = (1 + k)R_c \, \Delta i - 2L \frac{d\Delta i}{dt} - k.\Delta v$$

$$\text{or} \quad \Delta v = R_c \, \Delta i - \frac{2L \, d\Delta i}{(1 + k)dt} . \qquad \ldots\ldots (17)$$

Evidently the effective inductance has been reduced by a factor $1 + k$.

A possible embodiment of this idea is shown in Fig. 27 in which the wire voltage is amplified in A and mixed with the positive feedback from the wire current at the grid of V_2.

Since the current in the oscillator valve is proportional to the wire voltage it was thought that to begin with a resistance in the cathode circuit would provide negative feedback which would be effective from the wire voltage, but this was later found to be fallacious. In the meantime cathode degeneration was tried and found to have a beneficial effect in most circuits, this being presumably due to a reduction in non-linear effects, which have been neglected in our analysis.

It can be shown, however, that a decrease in effective inductance is obtained if a suitable tuned circuit is connected in the cathode circuit.

In the following subsection we establish a method of analysing approximately radio-frequency systems which may be somewhat more complicated than the simple oscillator so far considered.

3.1.1 Radio Frequency Analysis

In Ref. 1 the equation (16) was established by energy considerations and this method would be more difficult to apply in a more complicated circuit. We therefore need to establish a more general method.

Consider the voltage and current relationship in a circuit consisting of a capacity C, inductance L and resistance R in series. Let the voltage $v = V\exp(j\omega_o t)(1 + \alpha \cos \Omega t)$ be split into carrier and sidebands as follows:

$$v = V\exp(j\omega_o t) + \frac{V\alpha\exp}{2} [j(\omega_o + \Omega)t] + \frac{V\alpha}{2} [\exp j(\omega_o - \Omega)t] .$$

The impedance of the circuit is given in general by:

$$Z = j\omega L + \frac{1}{j\omega C} + R .$$

If L and C resonate at the carrier angular frequency ω_o, we have $Z = R$ at $\omega = \omega_o$. In general let $\omega = \omega_o + \Omega$, where $\Omega << \omega_o$, so that, approximately, $\frac{1}{\omega} = \frac{1}{\omega_o} - \frac{\Omega}{\omega_o^2}$. Then $Z = j\omega_o L + j\Omega L + \frac{1}{j\omega_o C} - \frac{\Omega}{j\omega_o^2 C} + R = 2j\Omega L + R$.

Thus the carrier component of the current will be $V/R \exp(j\omega_o t)$, the upper sideband;

$V\alpha$/

$$\frac{V\alpha}{2\left\{R^2 + (2\Omega L)^2\right\}^{1/2}} \cdot \exp\left[j(\omega_o + \Omega)t - \tan^{-1}\frac{2\Omega L}{R}\right]$$

and the lower sideband;

$$\frac{V\alpha}{2\left\{R^2 + (2\Omega L)^2\right\}^{1/2}} \cdot \exp\left[j(\omega_o - \Omega)t + \tan^{-1}\frac{2\Omega L}{R}\right].$$

Combining these, we have;

$$i = \frac{V}{R}\exp(j\omega_o t) + \frac{V\alpha}{\left\{R^2 + (2\Omega L)^2\right\}^{1/2}}\exp(j\omega_o t)\cos\left(\Omega t - \tan^{-1}\frac{2\Omega L}{R}\right).$$

From this expression we see that the envelopes of voltage and current are related by an equivalent circuit consisting of an inductance $2L$ in series with a resistance R. A similar equivalent circuit can be found for any system which behaves in the same way on either side of the carrier frequency. Another example is the parallel tuned circuit with C, L and R in parallel, the equivalent circuit for which is a capacity $2C$ in parallel with R. Now consider the circuit shown in Fig. 28, in which an impedance Z_k is connected in the cathode circuit of the oscillator.

We have $$\Delta v = \left(j\omega L + \frac{1}{j\omega C}\right)\Delta i - \frac{i_a}{j\omega C},$$

and $$i_a = s\,(j\omega M\Delta i - i_a Z_k)$$

so that $$\Delta v = \left(j\omega L + \frac{1}{j\omega C}\right)\Delta i - \frac{sM}{C}\cdot\frac{\Delta i}{1 + sZ_k}.$$

When Z_k is a resistance R_k, we have for the modulation angular frequency Ω,

$$\Delta v = 2j\Omega L\Delta i - \frac{sM}{C}\cdot\frac{\Delta i}{1 + sR_k}. \qquad \ldots\ldots (18)$$

The effect of R_k is thus merely to reduce the effective slope by the factor $(1 + sR_k)$. The fallacious reasoning which first led us to believe that R_k would reduce the effective inductance was based on the first of the above equations, which at the carrier frequency reduces to $\Delta v = \frac{-i_a}{j\,\omega_o\,C}$. The cathode voltage is thus proportional to the wire voltage at the carrier frequency and it was thought that it would constitute negative feedback from the wire voltage. The fallacy lies in our neglect of the sideband terms.

When Z_k is a tuned circuit consisting of R_k, C_k, L_k in parallel for modulation frequencies we take

$$\frac{1}{Z_k} = 2j\Omega C_k + \frac{1}{R_k}$$

which gives

$$Z_k = R_k\,(1 - 2j\Omega C_k R_k) \quad \text{if} \quad 2\Omega C_k R_k << 1.$$

Then/

Then
$$\frac{\Delta v}{\Delta i} = 2j\Omega L - \frac{sM}{C}\,\frac{1}{1 + sR_k(1 - 2j\Omega C_k R_k)}$$
$$\simeq 2j\Omega L - \frac{sM}{C(1 + sR_k)}\left[1 + \frac{2j\Omega C_k R_k}{1 + sR_k}\right]$$
$$= 2j\Omega\left[L - \frac{sMC_kR_k}{C(1 + sR_k)^2}\right] - \frac{sM}{C(1 + sR_k)}. \qquad \ldots\ldots (19)$$

The effective tuned circuit inductance is thus reduced and a corresponding bandwidth improvement would be expected.

A bridge circuit could also be used to obtain the required voltage and current signals for feedback as shown in Fig. 29. From the figure it will be seen that the signs of current and voltage feedback are opposite as required. No such system has been tried in practice since the Q of the tuned circuit would be low and high gain necessary to maintain oscillation. Stray capacity in the bridge circuit would also constitute a serious difficulty.

3.2 Impedance Transformation

The theory of the behaviour of the wire in a self-oscillatory circuit demands that the resistance of the wire be much greater than that in the remaining tuned circuit elements, L and C. While this condition is relatively easy to satisfy with wires of high resistance, say 10 to 25 ohms made of platinum wire in diameters down to 0.0001 inch, it becomes increasingly difficult to attain when the shorter, thicker wires with resistances say 2 to 5 ohms needed for high speed flows are employed.

It is manifest that we can use such low resistance wires if the tuned circuit inductance is reduced since for a given Q the resistance of the inductance L will decrease with a decrease in L. However there is a practical limit to L and it may be more convenient to employ some impedance transforming device such as is now described.

Consider the network shown in Fig. 30(a) in which X_1 and $-X_1$ are pure reactances. The input impedance Z_1 of this circuit is X_1^2/R. If this network is preceded by a similar one as shown in Fig. 30(b), the input impedance is $(X_2/X_1)^2 R$, so that if X_2 is greater than X_1 we have an impedance multiplication.

A practical embodiment is to have inductances and capacitances as shown in Fig. 30(c). When the resistance of the inductances, say r_1 and r_2, are included in the analysis, it is found that the input impedance is

$$\frac{L_2 C_1}{L_1 C_2}(R + r_1) + r_2.$$

If an impedance multiplication factor of, say, 5 times is used, the resistance r_2 is evidently of less importance than r_1, and the usefulness of the device will depend on making r_1 considerably less than the wire resistance R. If the inductances and capacitances are transposed, a similar conclusion is reached, the most important resistance being that of the inductance in the section nearest to the wire.

At/

At high radio frequencies two transmission lines having different characteristic impedances may be used to produce a similar impedance multiplication.

3.3 A Note on the Maximum Attainable Bandwidth with Constant Resistance Heating

Consider the impedance of the tuned circuit at the hot wire terminals, Fig. 31, where Z is the negative impedance provided by the positive feedback loop.

Then the input impedance is Zi, where,

$$Zi = \frac{1}{j\omega C_1} + \frac{Zj\omega L}{Z + j\omega L}, \quad \omega = \text{radio angular frequency}$$

$$= \frac{Z(1 - \omega^2 LC1) + j\omega L}{-\omega^2 LC_1 + j\omega C_1 Z}.$$

This is real if:

$$\frac{\omega L}{Z(1 - \omega^2 LC_1)} = \frac{\omega C1Z}{-\omega^2 LC_1} = \frac{Z}{-\omega L}$$

i.e., $$1 - \omega^2 LC_1 = \frac{-\omega^2 L^2}{Z}.$$

This gives a resonance at $\omega = \omega_o$ where $\omega_o^2\left(LC_1 - \frac{L^2}{Z^2}\right) = 1$.

In general let $\omega = \omega_o + \Omega$ where $\omega_o >> \Omega$ the modulation frequency, and as an approximation in the expression for Zi above, we may put:

$$\omega^2 = \omega_o^2 + 2\omega_o\Omega$$

$$1 - \omega^2 LC_1 = -\frac{\omega_o^2 L^2}{Z} - 2\omega_o\Omega LC_1.$$

Then Z_1 is found to be $Zi = \frac{-L}{ZC_1}(1 - 2j\Omega C_1 Z)$

i.e., $$Zi = -\frac{L}{ZC_1} + 2j\Omega L = -R_c + 2j\Omega L$$

and hence, when the system is oscillatory and we assume $R_1 \equiv R_c$ we may find the maximum attainable bandwidth, since this is given by:

$$\omega_q^2 = \frac{1}{2LC} = \frac{1}{2C_1 Z \cdot T_c}, \quad T_c = \text{const. curr. time con.}$$

Thus if we choose $C_1 = 100$ pF and Z as $= 500$ ohms, as set, say, by a given oscillator, then $\omega_q = 10^7/T_c$ and for t say 0.5 millisecs this is 20 kc/s.

Thus it is seen that there is a limit to the response set by the oscillator for any given wire time-constant.

4./

4. Experimental Verification of the Approach to Constant Resistance Operation

It has been shown that in a system employing positive feedback the wire resistance should remain constant when the air velocity is changed, and it has also been shown that when two types of heating are employed, changes in air velocity may be simulated by controlled changes in one of them. This may be used to check the operation of the circuit. The circuit of a simple oscillator is shown in Fig. 32 where Rw represents the hot wire fed from the 6J5 oscillator and from the 6L6 triode-connector. The radio-frequency voltage across the wire was measured by means of a valve-voltmeter and the radio-frequency current deduced from the voltage across the tuned circuit. These two parameters are plotted in Fig. 33(1) where the changes in radio frequency current were obtained by varying the cathode bias on the 6L6, and show that the wire resistance is approaching the desired constant-resistance conditions, the discrepancy being evident from the intercept on the ordinate. Response measurements made on this circuit showed that, under the conditions pertaining in Fig. 33(1), the direct current in the wire was causing excessive damping.

According to the theory presented in Section 3 the introduction of an unbypassed resistance Rk into the cathode lead should reduce the slope of the hot wire characteristic by $(1 + sRk)$.

Here, again, a plot of radio frequency wire voltage against current should allow this theory to be checked. The circuit shown in Fig. 36 was used for this purpose as it was found more convenient to operate at low radio frequencies. The direct heating current was again altered to move the operating point up along the $v_w - i_w$ line and without degeneration a wire was found to have a resistance of 17.95 ohms, Fig. 33(2). A cathode degeneration resistance of 110 ohms was introduced and with $s = 5$ mA/V, $1 + sR_k = 1.55$, so that the hot wire resistance should now be 11.6 ohms, whereas in fact it was found to be 11.45 ohms, Fig. 33(3), before the positive feedback was restored to its original level. From Fig. 33, in which the two lines are shown, it will be seen that cathode degeneration has reduced the intercept v_o, the characteristic now approaching more closely to constant resistance operation than without degeneration.

When the wire is operated as in Fig. 32 the equivalent circuit for turbulence measurements is as shown in Fig. 34.

Here we may assume that the resistance to direct and radio frequency currents is the same and hence the ratio v_{d_1}/v_{r_1} is the same as i_{d_1}/i_{r_1}. It follows from Fig. 34 that we should have:

$$\Delta i_r = - \frac{i_{d_1}}{i_{r_1}} \cdot \Delta i_d \qquad \ldots\ldots (20)$$

where $i_{r_1}^2 + i_{d_1}^2$ is a constant, and that if in Fig. 32 the direct current in the wire is varied and plotted against the radio-frequency current the points should lie on a circle.

This relationship is illustrated in Fig. 35 where experimental points are seen to lie very closely on the circle.

It is also possible to test the validity of this equivalent circuit dynamically at low frequencies by injecting an audio-frequency voltage and measuring the resulting modulation of the radio-frequency current by means of a demodulator of known efficiency. In the following table of results, i_{d1} and i_{r1} are the mean direct and radio-frequency currents respectively, Δi_r

is/

.is the peak-to-peak radio frequency current response as calculated, while Δi_r^* is the response as deduced from the demodulator output. It will be seen that the relationship is approximately correct.

(20)

i_d mA	i_r mA,rms	Δi_d mA,100c/s	Δi_r mA,rms	Δi_r^* mA,rms
5.00	13.25	1.00	0.38	0.313
5.00	13.25	0.60	0.217	0.197
10.00	10.65	1.00	0.939	0.838
10.00	10.65	0.60	0.555	0.465
12.50	7.50	1.00	1.67	1.170
12.50	7.50	0.60	1.00	0.838

5. Frequency Response of Typical Oscillator at Low Radio Frequencies

Having established within reasonable limits the validity of the equivalent circuits which are shown in Figs. 11 and 13 for both pure radio-frequency and mixed radio-frequency and direct current heating we are now in a position to determine whether the expected response bandwidth is achieved. That is to say whether the values obtained for break-point frequency ω and damping ζ found from Eqn. (15) are realized in practice. In order to permit the constant voltage time constant $CR_bR_i/(R_b + R_i)$ of the wire to be found, and smooth control of positive feedback also achieved, the circuit shown in Fig. 36 was used, being driven from an external oscillator, and provided with variable positive feedback through V_2 and V_3.

The tuned circuit $R_w - L - C$ is driven from a pentode which provides a substantially constant current I_a in the valve V_2. The tuned circuit current is thus $Q \cdot I_a = \omega L \cdot I_a/r$. Hence the wire voltage is $\omega L \cdot I_a$, which is thus constant, and the time-constant observed under these conditions is $T_{cv} = CR_bR_i/(R_b + R_i)$, as above. Assuming $R_b = R_i$, the time-constant under constant-voltage conditions is half that under constant-current conditions, and C and R_b in the equivalent circuit may be calculated.

The tuned circuit is tapped at a suitable point to give the requisite phase change for positive feedback through the cathode follower V_3. When no gain is applied by means of positive feedback through V_2 and V_3 the wire is heated under constant-voltage conditions by V_1. In practice the audio-frequency test signal is injected through a high series resistance (1,000 ohms is convenient), and the response is measured by means of a wave-analyser at the demodulator output. The resistance in the cathode of V_2 may be wholly or only partially bypassed at radio frequencies, and its effect has been analysed in Section 3. In general it will be seen that the results follow the predicted more closely when this resistance is in use.

With the regeneration in Fig. 36 advanced so that oscillations commence, and with the external oscillator removed, the results shown in Fig. 37 were obtained. The inductance in the tuned circuit was 97μH and the frequency of oscillation about 700 kc/s. Little difference, apart from a slightly lower peak in the response, was observed when an inductive feedback system was substituted for the cathode follower shown. The constant-voltage response of the wire used is also shown, and from it the values of C and R_b in the equivalent circuit may be calculated if the resistance at the operating point is known; this may be found from a single current and voltage measurement on the wire. With $L = 97\mu H$, $C = 23\ \mu F$, and $R_b = 20\Omega$ respectively the break-point should

occur/

occur at 2,400 c/s whereas in practice it is seen to occur at about 2,300 c/s. An increase in R_k caused the response to become more peaked, and the frequency at which the maximum response occurs approaches the break-point. The values of R_k used are shown in Fig. 37.

5.1 Effect of $(R_1 - R_c)$ on Response

In an attempt to determine the exact values of $(R_1 - R_c)$ in Eqn. (15), gain-frequency measurements were made on the circuit fed from an external oscillator, which was accurately calibrated, for various settings of the positive feedback control. From Eqn. (15) it is evident that, if $(R_1 - R_c)$ is not in practice vanishingly small, then it should be considered when calculation of the break-point is made. From the apparent Q of the circuit, the 3 dB bandwidth and the inductance, $(R_1 - R_c)$ may be found. With the hot wire in the tuned circuit a value of 6.5 ohms was obtained with the circuit on the verge of oscillation and 17.1 ohms when only moderate feedback was applied. The value of 6.5 ohms with the circuit about to oscillate seemed to be extremely high as something of the order of 0.05 ohms had been thought attainable. The hot wire was removed altogether and the circuit operated as a regenerative amplifier. Under these circumstances a gain of 9,500 could be achieved quite simply with low input levels, of the order of 1 mV, indicating a tuned circuit resistance of 0.02 ohms.

A linear resistance and then a hot wire were next inserted and the gain with maximum feedback for no oscillations measured over a range of inputs from 0.25 to 100 mV, the results being shown in Fig. 38. Apparently high gain, and hence low values of $(R_1 - R_c)$, are not obtainable with the large inputs necessary to provide adequate heating of the wire. The reasons for this behaviour are not fully understood at present, and the phenomenon is an obvious limitation to any system which attempts to reduce the time-constant of a hot wire by such means.

5.2 Effect of Tuned Circuit Inductance on Response Bandwidth

The fundamental equation expressing the response of an oscillatory system, Eqn. (15), shows that the bandwidth is inversely proportional to the square root of the tuned circuit inductance, and to check this a series of response measurements was made with the circuit shown in Fig. 36, the external oscillator not being required. Inductances of 97, 11 and 6.65 μH were used and in each case the cathode degeneration resistance was adjusted to give the optimum peaked response. A wire of 20 ohms cold resistance was used which had a constant-voltage time-constant of 1.43 millisecs, and with the inductance of 6.65 μH the observed break-point was seen to be at about 5,700 c/s, while a value of 5,200 c/s was indicated theoretically. With the inductance 11 μH the observed and calculated bandwidths were 4,000 and 4030 c/s respectively. The results are shown in Fig. 39 and the result with $L = 97$ μH has been replotted from Fig. 37. It will be seen that for the lowest and highest inductances the observed bandwidth is wider than the expected, while with the central value the results agree fairly well with theory. When the uncertainty in evaluating R_b and C is considered the agreement between theory and practice is seen to be reasonable.

To summarize the preceding experiments, the equivalent circuit current generators for both direct current and radio frequency heating have been verified, and an approximate check on the values of the circuit elements C, R_b, $R_1 - R_c$, 2L obtained. Reasonable faith can thus be placed in further analyses based on this circuit, and it is not proposed to conduct any further investigations along these lines. No attempt has been made to take into account non-linearities in circuit components, although a method of reducing the effect of one of these, the valve transconductance, has been demonstrated.

Further/

Further reduction in the tuned-circuit inductance is of course quite possible, and in a later section it will be shown that oscillators operating at very high frequencies (up to 110 Mc/s) are feasible, and indeed, necessary. The circuit so far used is not ideally suited to the higher radio frequencies and it was abandoned in favour of push-pull and transitron oscillators.

6. Overall Negative Feedback Applied to Constant Resistance Systems

Before presenting experimental results we show how the operation of the system may be more readily understood by reference to the Nyquist diagram. Such a diagram is shown in Fig. 40 and the values assumed for the coefficients are as follows: $L = 50\ \mu H$, $C = 50\ \mu F$, $R_b = 60\Omega$, $R_1 - R_c = 30\Omega$. The total time lag in the feedback loop which includes the demodulator and feedback amplifier has been taken as $10\ \mu s$ and the factor K as 66. $(R_1 - R_c)$ has been taken as unusually large to clarify the diagram, but the action of negative feedback is unaffected.

In Fig. 40 K_1G_1 is the initial response transfer function $\Delta i/i_a$, here plotted as the inverse $(K_1G_1)^{-1}$ for convenience. The negative feedback loop transfer function is K_2G_2 where K_2 is K in Section 2.2.1 and is frequency-independent while G_2 is the frequency-dependent factor $(1 + pT)^{-1}$.

By addition of K_2 to $(K_1G_1)^{-1}$ the inverse function is transformed into $(K_1G_1)^{-1} + K_2$, and this is illustrated in Fig. 40, when time lags are neglected, it will be seen that the locus is shifted K_2 to the right, thereby increasing the range over which the response is linear. When the loop time lag is taken into account, the locus K_2G_2 lags in phase and is reduced in amplitude, so that the sum $(K_1G_1)^{-1} + K_2G_2$ is asymptotic to $(K_1G_1)^{-1}$. The direct locus, which is $K_1G_1\ (1 + K_1K_2G_1G_2)^{-1}$ can be quickly replotted from the inverse locus on polar co-ordinate paper and this is also illustrated in Fig. 40.

6.1 Experimental Results. Negative Feedback Applied to Constant Resistance Systems

To test the elementary theory of overall negative feedback the circuit shown in Fig. 41 was used. It comprises a straightforward inductive feedback oscillator V_1 working at approximately 1.5 Mc/s, a demodulator V_5, and a feedback amplifier $V_2V_3V_4$ with a 3dB bandwidth of 50 kc/s. The final stage of the amplifier is a power valve which is also used to set the operating level of direct current in the wire.

The hot wire is operated at earth potential for convenience. With mixed heating the response is at the same frequency as the injected test signal but in general pick-up from direct modulation of the oscillator anode voltage was much below the level of the response.

With a hot wire of 20 ohms cold resistance (0.0001 in. Pt. Woll. wire) the responses shown in Fig. 42 were obtained, the negative feedback being increased from (1) to (3). It will be seen that the initial response before the application of negative feedback is highly damped, due to the presence of 8 mA direct current in the wire. It can be shown that $R_1 - R_c$, and therefore the damping ζ increases as the direct current is increased. This is readily seen from Fig. 43 in which the square wave response is seen to deteriorate as the direct current level in the wire is increased.

In order to obtain sufficient gain from the 6L6 a level of about 8 mA was required, as it was found that the transconductance was a linear function of the anode current up to about 7.5 mA, at which it had reached its final level of 3.5 mA/V. Similar characteristics were found for the type EL33 which did not reach full gain of 6 mA/V until the anode current was 12.5 mA.

In/

In Fig. 42 the inductive coupling in the oscillator has been maintained constant throughout and the calculated break-point occurs at 1.95 kc/s, whereas the actual response appears to have a break-point slightly lower than this. The figures -6 and -12 dB refer to the amount by which the low-frequency response has been suppressed, all curves being drawn with the same low-frequency response for convenience. The suppression of 12 dB achieved in curve (3) indicates that a value of $(1 + K) = 4$ has been reached, and that a bandwidth improvement of 2 times is to be expected. The actual improvement appears to be slightly better than this, although the attenuation after the break-point is at a rate greater than the 12 dB/octave predicted by the simple theory.

A further check on the theory of this type of feedback was obtained from measurements of the amplifier gain required in the feedback loop to produce a given suppression of the low-frequency response. It was noted in Section 2.1.2 that the value of K is $M s X_c \eta_d v_d/v_r$. With the oscillator shown in Fig. 41 M was in one example calculated to be 35.3 times to attain a suppression of 4 times in the response while a gain of 30 times was actually found necessary.

6.2 Experimental Results. Differential Feedback for Stabilization

The damping term ζ may be directly controlled by means of differentiated feedback and this has been discussed in Section 2.2.4. An experimental check on this theory was obtained by using the circuit shown in Fig. 41 with the addition of an R-C differentiating stage and amplifier as shown in Figs. 44 and 45. The negative feedback loop is tapped at a suitable point and the signal differentiated, amplified and mixed with the negative feedback signal at the grid of V_4. Typical responses are shown in Fig. 46 where (1) is the original response with the maximum permissible negative feedback for stability. The addition of differentiated feedback has the effect shown in (2) and it will be seen that the peak has been reduced in amplitude and a slight reduction in bandwidth has also occurred. From response (2) the negative feedback may now be increased and a widening of the bandwidth results. The reduction in the peak with differentiated feedback is seen to be 2.5 dB, the 3 dB bandwidth being reduced from 8 kc/s to 7.3 kc/s. Further negative feedback enables the 3 dB bandwidth to be increased to 11.5 kc/s. The optimum differentiated feedback is most readily found when a square wave testing signal is used and the responses in Fig. 47 show some results obtained. Responses a and c show the effect of increasing negative feedback while b and d have increasing amounts of stabilizing feedback in addition. The square wave is 1,000 c/s and the radio frequency 1.2 Mc/s, with L = 50 μH.

7. Overall Feedback Applied to Constant Current and Constant Voltage Systems

The methods described in the previous Sections, 6 - 6.1, for applying overall feedback are general in so far as the operation of the wire can be constant-current, -voltage, or -resistance. It has been shown that there are advantages to be gained from operation of the wire at constant resistance in a radio frequency oscillator and applying negative feedback through a direct-current loop.

It is now proposed to describe a system in which the wire is heated by a radio-frequency current under constant-voltage conditions and overall negative feedback is applied, again through a direct-current loop, to reduce resistance variations.

The circuit arrangement shown in Fig. 48 is a convenient embodiment of this principle; V_1, which is driven from an external oscillator, supplies power to the wire R under constant-voltage conditions. This enables sufficient heating current to be obtained from a low-power valve; if a large valve were used the wire could be operated under constant-current conditions by omitting L and C.

Variations/

Variations in air velocity modulate the voltage across the tuned circuit, and this is applied to the demodulator D. The output from the domodulator is amplified in A and controls a direct current in the wire via V_2. The equivalent circuit is shown in Fig. 49(a), where i_a represents the velocity input, Δi_r and Δi_d are the resulting changes in radio-frequency and direct current respectively, and the tuned circuit, demodulator, amplifier chain connecting Δi_d with Δi_r is included in K_1.

To simplify the algebraic analysis of the circuit it is modified to the form shown in Fig. 49(b), where:

$$R_g = \frac{R_1 R_b}{R_1 + R_b}, \quad i'_a = \frac{i_a R_b}{R_1 + R_b},$$

$$K = \frac{K_1 R_b}{R_1 + R_b} \qquad \ldots (21)$$

CR_g = Tv, the constant voltage time constant.

The overall response now becomes:

$$(i'_a - K\Delta i_r) \frac{R_g}{1 + pCR_g} = \Delta i_r \cdot R_g \qquad \ldots (22)$$

Thus,
$$\frac{\Delta i_r}{i'_a} = \frac{1}{(1 + K) + pCR_g} \qquad \ldots (23)$$

and the time-constant is reduced by $(1 + K)^{-1}$, the response being still that of a simple time-constant as shown in Fig. 50.

The factor K is given by:

$$K = X \cdot \eta_d \cdot m \cdot s \cdot \frac{v_d}{v_r} \cdot \frac{R_b}{R_1 + R_b} \qquad \ldots (24)$$

where

X = reactance of the tuned circuit condenser

η_d = demodulator efficiency

m = gain of amplifier

s = transconductance of V_2

v_d = initial direct voltage across wire

v_r = initial radio frequency across wire.

Thus if we are to attain a bandwidth improvement of, say, 100 times, with X = 50 ohms, η_d = 80%, s = 5 mA/V, $v_d = v_r$ and $R_b = R_1$, m must be 1,000. So far it has been assumed that the amplifier has a perfect characteristic. Inevitably the feedback loop must have a finite phase lag, and when the loop is closed the phase margin must be greater than 30° for stability when the loop gain is unity. This occurs when $\omega T_v \doteq K(j\omega)$ in Fig. 50 and here the phase angle of the wire is nearly -90°. Thus for a phase margin of 30° at this frequency the phase angle of K must be less than 60°. Since the latter frequency is below 50 kc/s this condition can be met if the amplifier has a level response up to $\omega T_v = K$.

If/

If the amplifier has resistance-capacitance coupling a phase lead will occur at low frequencies, and with more than two such couplings positive feedback, and subsequent oscillation, may occur, if, when the phase margin becomes negative, the loop gain is greater than unity. If one small time constant is inserted somewhere in the loop with a break-point much beyond all the others the loop gain may be reduced below unity before the phase margin becomes zero. The response should now be taken at some point after this time-constant if a rise at low frequencies is to be avoided.

7.1 Experimental Results. Negative Feedback Applied to Constant Voltage System

To test the simple theory given in Section 7 the circuit shown in Fig.51 was employed. V_1 is an amplifier which enables V_2 to provide sufficient heating current in the wire. The anode voltage of V_2 is demodulated, amplified in A and fed back in the correct phase by V_3 which provides the direct current heating in the wire. The amplifier shown as the block A in Fig. 51 is the cathode-coupled feedback triple in Fig. 52 which has a gain of 32 dB and a bandwidth from 25 c/s to 4 Mc/s, and was developed for general use in such feedback loops.

A typical response is shown in Fig. 53, where (1) is the constant-voltage response of the wire, exhibiting a break-point at 900 c/s. Drawing the tangent to (2) at the 6 dB attenuation point the second break-point is seen to be at about 6 kc/s. From the suppression obtained, 14 dB, we may calculate $(1 + K)$ which is thus 5, and the new break point should occur at 4.5 kc/s. The position of the constant-voltage break-point is somewhat uncertain, due to the fact that the attenuation is at 5 instead of 6 dB/octave. It is also difficult to measure R_1 and R_b accurately so that close agreement between theory and practice cannot be expected. The rise at low frequencies was due to the response being taken, for convenience, before the small time-constant (not shown in Fig. 51), which was inserted to prevent low-frequency instability.

7.2 Constant Voltage System with Differentiated Feedback

The low-frequency instability with high loop gains remarked upon in the previous Section may be avoided if the pure negative feedback is replaced by differentiated feedback $KpT_2(1 + pT_2)^{-1}$ and the overall response is taken from the output of the differentiating circuit. A block diagram is shown in Fig. 54 and we may write down the overall response directly from this as:

$$\frac{i_2}{i_a} = \frac{K}{K + (1 + pT_1)\left(1 + \frac{1}{pT_2}\right)} \qquad \ldots (25)$$

$$= \frac{K}{K + pT_1 + \frac{1}{pT_2} + \frac{T_1}{T_2} + 1} \qquad \ldots (26)$$

where K has the same identity as in the previous Section.

If now we put $K = 100$, say, and $T_2 = T_1/100$ the denominator of Eqn. (26) becomes $(200 + pT_1 + 100/pT_1)$ which may be factorized as:

$$201\left(1 + \frac{pT_1}{201}\right)\left(1 + \frac{1}{2.01pT_1}\right) \qquad \ldots (27)$$

and/

and the response exhibits two break-points at $\omega_1 T_1 = \frac{1}{2.01}$ and $\omega_2 T_1 = 201$, say 1/2 and 200, respectively, as shown in Fig. 55.

There is a low-frequency cut-off at $\omega_1 = \frac{1}{2T_1}$ which limits the useful bandwidth of the circuit, but it appears that if K is made sufficiently large a considerable improvement in the high frequency response is obtained without danger of instability. By considering the integrating time-constant in the feedback amplifier, normally very much less than T/200, it can be shown that a third break-point occurs, causing attenuation at 12 dB/octave but that this is above the second at $\omega_2 = 200/T_1$, and is thus of minor significance.

7.2.1 Experimental Results. Constant Voltage System with Differentiated Feedback

The theory was tested using the circuit shown in block diagram form in Fig. 56, the various stages being identical with those shown in Fig. 51, with the addition of a capacitance-resistance differentiating stage. To make the gain requirements as low as possible a high-resistance wire was used (30 ohms cold) and the differentiating time-constant was made variable.

The response (2) in Fig. 57 is the output at the differentiating network with no gain in the feedback loop, while (3) relates to maximum attainable gain and a differentiating time-constant of 50 μsecs. The constant-voltage response is shown in (1). In general it will be seen that the expected type of result is obtained, although the attenuation above the second break point is much steeper than predicted even by a more complete theory which includes the loop integrating effects. However, the 3 dB bandwidth has been extended to 17 kc/s and the low frequency break-point is at 180 c/s. Attempts to reduce the differentiating time constant still further were only partially successful, due to the noise level in the amplifier.

8. The Use of High Frequency and Very High Frequency Oscillators

Most of the experimental work described in the preceding Sections has been concerned with the use of Wollaston wire anemometers having cold resistances typically between 15 and 30 ohms and nominal diameters of 0.0001 and 0.0002 inches. It was realized that validity of the equivalent circuit demanded a wire resistance at least several times that of the tuned circuit resistance, which is mainly present in the inductance, and hence wires of this order of resistance generally gave results consistent with theory when coils with a Q greater than 150 and inductances less than 100 μH were used. The bandwidths are more than adequate for turbulence measurements at the air speeds at which these wires can be used (up to 200 ft/sec) and apart from the checking of the theory there is little to be gained in increasing the bandwidth beyond, say, 15 kc/s, since this corresponds to a spatial resolution of 0.08 inches at 200 ft/sec and this is of the same order as the length of the wire. Corrections can be applied to measurements made under these conditions but it is more convenient to reduce the length of the wire.

When the possibility of applying this method of anemometer operation to flow investigations at high air speeds was examined it became apparent that the wire material currently used, platinum, would prove to have too low an ultimate tensile strength to withstand the higher aerodynamic stresses imposed upon it. It has been shown in Ref. 6 that for high speed measurements it is necessary to use tungsten wires whose resistance is in the range 2 - 5 ohms.

Thus/

Thus attention became focussed on oscillators which would enable wires of this low resistance to be used and the tuned circuit inductance was progressively reduced from about 100 μH to 0.5 μH and the frequency of oscillation increased from about 1 Mc/s to over 100 Mc/s.

8.1 The Push-pull Oscillator

Single-sided oscillators are not ideally suited to operation at the higher radio frequencies because of the difficulty of manipulating the small inductances, and a push-pull system has much to recommend itself.

The circuit shown in Fig. 58 was developed for the initial measurements at higher radio frequencies, a double triode type CV1102 being used which had separate cathodes suitable for degeneration. The wire is located between the split section of the tuning capacitance, one end being earthed for convenience to the positive high tension rail. Provision was made for overall negative feedback via the 6L6 and the amplifier A was the A_1 amplifier of a Cossor 1035 oscillograph. Responses were first obtained with platinum wires of quite high resistance, 20 ohms being typical; later tungsten wires of 4 to 10 ohms were used. It was found that with this oscillator and an inductance of 2.15 μH the responses obtained were limited by the valve and not by the wire if the valve was operated at a low anode current. The best operation is obtained if the standing anode current is greater than the radio-frequency current in the valve, but if the standing current is much above the rated value the resporses are again limited by the valve.

An inductively-coupled demodulator was used throughout, and the measured frequency of oscillation with L = 5 μH was 9.85 Mc/s. The responses shown in Fig. 59 were those typically obtained using wires of cold resistance 20 ohms in 0.0001 inch platinum and 9 ohms in 0.00015 inch tungsten. Responses (1) and (2) refer to the platinum wire, (3) and (4) to the tungsten wire. The oscillator operating conditions are shown on Fig. 59 and it will be seen that the use of cathode degeneration has a considerable effect on the bandwidth, the damping being reduced so that a peak appears in the response (2). If the direct anode current was not restored after the insertion of R_k the responses were typically peaked at a lower frequency than the original break-point and as the wire resistance was restored to its former operating level by increasing the anode current, the response peak moved upwards as shown in (2).

The effect of overall negative feedback, which suppressed the low-frequency response 11 dB, is shown in (4), the 3 dB bandwidth being 25 kc/s. There is an unexplained attenuation of 1.5 dB at 6 kc/s extending to 18 kc/s before falling the further 1.5 dB. Further feedback caused the sudden onset of oscillations, and few responses were obtained showing a peak.

8.2 Power Valves for Use in Very High Frequency Oscillators

The desire to decrease still further the tuned-circuit inductance and obviate the effects of non-linear valve operation led to the adoption of power valves for use in the oscillator circuit. For a given wire the tuned circuit Q decreases as the inductance is decreased and hence the dynamic impedance presented to the anodes falls, so that oscillations will cease when the product of the dynamic impedance and the slope becomes less than unity. A survey of all suitable valves, including receiving types such as the CV1102 already used, indicated that the slope increased with the maximum allowable anode dissipation.

A further reason for using power valves is that the larger the valve the smaller can be the ratio of oscillatory to direct current in the valve, and this minimizes the effect of non-linear characteristics.

A push-pull 807 oscillator was first used in this attempt, operating at 25 to 50 Mc/s. Later a double tetrode type QQV04/20 was found even more suitable at these frequencies with the added advantage that it could be used above 100 Mc/s.

8.3/

8.3 The Push Pull 807 Oscillator

The double triode CV1102 oscillator described in Section 8.1 had included a tuned circuit inductance of 2.15 μH operating at approximately 10 Mc/s and had given responses in accordance with theory with wire resistances above about 10 ohms, but attempts to reduce this figure gave responses limited by the valve. The value of 10 ohms is still too high for the type of anemometer contemplated, and the use of inductances less than 1 μH was indicated, the object being to reduce the inherent resistance of the inductance to a figure of 10% of the wire resistance or less.

The circuit in Fig. 60 comprises a pair of 807 valves in push-pull, and oscillations were possible with inductances down to 0.185 μH at frequencies up to 60 Mc/s. The wires used were typically of 2 to 5 ohms cold resistance in 0.0002 inch Wollaston wire with constant voltage time constants of 0.3 to 0.7 millisecs. The time-constants were obtained by reducing the positive feedback and driving the circuit from an external oscillator loosely coupled into the grid circuit.

Resistances of 50 ohms were needed in both grid and screen-grid connections to prevent parasitic oscillation. It was also found that for wire resistances greater than 2 ohms the Q of the tuned circuit was too low to allow oscillations with an untuned grid circuit and the modification shown in Fig. 61 was made, oscillation being then possible for the range zero up to 5 ohms.

It was soon noticed that the responses were very dependent on both cathode bias and grid tuning, when used, indicating that grid current was becoming a limiting factor.

A microammeter was inserted in one grid lead and the effect of even very low grid currents is illustrated in Fig. 62, where (1) is the response with the bias set beyond grid current cut-off and (2) corresponds to the just cut-off condition. By retuning the demodulator the response may be made to peak (3) with 0.05 mA in the grid, although at an octave below (2), while doubling the grid current made it impossible to obtain such a peak. The untuned grid circuit, Fig. 60, was used to get the responses shown in Fig. 62.

When a tuned circuit was used in the grid the response was little different so long as the circuit was correctly tuned, but on each side of resonance widely different results were obtained. The coupling between the circuits also had considerable effect on the response; too small a coupling produced a peaked response, too large a coupling an over-damped response.

Cathode degeneration in the form of fixed resistances attached at the cathode pins was also used and with this addition break-points close to those predicted by theory were obtained.

For example, a wire with an operating resistance of 3.0 ohms (0.0002 in. P_t) had a constant-voltage time-constant of 0.318 millisecs, so that, assuming $R_1 = R_b = 3$ ohms, $C = 212$ μF. The total tuned circuit inductance as determined from bridge measurements of total shunting capacitance and resonant frequency was 0.24 μH (nominal coil inductance 0.185 μH) hence a response break-point at 15.8 kc/s is expected. Actual response curves for this wire are shown in Fig. 63 where it will be seen that the break-point is at about 18 kc/s although there is a wide variation between the responses shown which were obtained with different amounts of cathode degeneration and positive feedback. The cathode degeneration and positive feedback. The cathode degeneration resistance could not be increased above 220 ohms or oscillations ceased even with the maximum possible positive feedback.

8.4/

8.4 Negative Feedback Applied to the Push-pull 807 Oscillator

With the possibility of attaining wide initial bandwidths with circuit dampings not very much less than 0.5, the additional use of negative feedback becomes an obvious method by which to extend the response. A means of isolating the wire from the direct connection to the valve anode is required and these must now be fed through chokes as shown in Fig. 64. The coupling condensers need only carry the carrier frequency and its sidebands and could be much less than the 0.01 μF shown but these were used since their physical size was less than smaller condensers (0.0001 μF) available, and it was desired to keep the lead inductance as low as possible.

The feedback amplifier used was the 32 dB wide-band unit in Fig. 52 and the loop connections were identical with those in Fig. 41. It has been shown that the initial response before the application of negative feedback should preferably be damped and with this in mind the oscillator was adjusted to provide the break-point at 12 kc/s and response shown in Fig. 65 (1). By means of negative feedback the response (2) was obtained, a mid-frequency of 2kc/s being suppressed 25 dB. The response (2) shows a peak of 5.5 dB which proved to be quite stable and the break-point is at 49 kc/s, any further increase in feedback above this causing oscillation at about 50 kc/s.

A check can be made on the performance of this system since the value of K corresponding to 25 dB is 16.8. Thus the break-point should have moved out (1 + K) or 4.22 times to 50.5 kc/s which is a very close agreement with that observed. Another check on the experimental results can be obtained by means of the Nichol's Chart[5] if the phase of the initial response can be found. The attenuation at the break-point of the initial response, Fig. 65 (1) is 2.5 dB, thereafter the response becomes asymptotic to a 10 dB/octave line. Thus $20 \log 2\zeta = 2.5$ and $\zeta = 0.667$. Assuming $\zeta = 0.7$ we may now draw the phase of the initial response and obtain the curve (3) on Fig. 65. The loop transfer function including the amplifier may now be plotted on the Nichol's Chart, Fig.66 (1) and from the constant M contours the closed loop response (4) in Fig. 65 found. The phase margin of C_1G_3 at unity loop gain is seen to be 20° resulting in a peak of 9 dB in the predicted response since the locus is tangential to the M = 9 dB contour at 52 kc/s. The observed response had a peak of 5.5 dB at 36 kc/s, Fig. 65 (2).

Locus (1) in Fig. 65 truly represents the amplitude response of the radio frequency system together with the demodulator but in assuming that the phase of this may be deduced from the amplitude using standard plots of phase and amplitude we are neglecting the phase lag of the demodulator. The time-constant in the demodulator was 2 μsecs with a break-point at 100 kc/s, and at 35 kc/s is seen to have a phase lag of about 20° so that the overall loop phase margin is now zero. The fact that a stable response was in fact obtained can only have been due to opposite rotation of phase elsewhere in the circuit or to the fact that (3) may be an incorrect deduction from (1) in Fig. 65.

As explained in Section 2.1.1, the initial response should be overdamped to avoid instability when negative feedback is applied. As an illustration of what happens when the initial response is underdamped, curve (2) of Fig. 66 shows the locus for $\zeta = 0.25$, corresponding to the response shown in Fig. 67 (1). Here the initial response has a 6 dB peak at 10 kc/s. The phase-margin at zero loop gain is very small, and curve (3) in Fig. 67 indicates roughly the large peak which would result.

8.5 Experimental Plot of the Nyquist Diagram

It was realized that the elementary theory giving rise to the equivalent circuit did not take into account the tuned demodulator which was found necessary in the preceding tests and in an attempt to find the actual vector locus of $\Delta i/i_a$

a/

a series of measurements was made of the phase and amplitude ratio of the input signal i_a with respect to the response Δi. This enabled the Nyquist diagram to be plotted and it was expected that the operation at high frequencies would be clarified. Referring to Fig. 68 which shows the essential features of the circuit, it will be seen that the input i_a and the response Δi are coupled to the horizontal and vertical deflecting plates respectively of an oscillograph which was fitted with identical amplifiers. The phase relationship between the two quantities was determined from the phase ellipse, Fig. 69, the amplitude being found from the attenuation required to maintain the ellipse size constant. Difficulty was experienced at both low and high frequencies due to the low level of the response and attenuation in the feedback amplifier and it was found that the phase and amplitude could not be determined with sufficient accuracy below about 25 c/s.

On Fig. 70 are plotted the direct and inverse loci of a response which was adjusted to have a 3 dB point at 15 kc/s and to be linear to 10 kc/s. No negative feedback has been employed in this case but it would be predicted that even a small suppression of say, $k > 1$, would cause severe peaking at 25 kc/s. At frequencies below 1 kc/s the phase is leading and at 25 c/s Δi leads i_a by 90° and the attenuation is due mainly to the feedback amplifier.

Inevitably the quadratic assumed for the initial response becomes a cubic when the demodulator is included and the inverse locus must be asymptotic to the negative imaginary axis at large ω but if the frequency at which the locus fell below the axis, i.e., the phase margin became negative, could be delayed a greater amount of negative feedback could be employed and the peak caused thereby would be at a higher frequency. Some experimental work along these lines was done but with the introduction of the transmission line tuned circuit and a direct coupled demodulator this was discontinued as it was thought that uncertainties in these relationships in the three coupled circuits would prevent anything but qualitative measurements. Apart from a loss of gain in the loop there appears to be no reason why a phase advancing network should not be effective in delaying the occurrence of a negative phase margin.

8.6 The Transmission Line Oscillator

The push-pull 807 oscillator suffered from disadvantages attributable to its low gain with wires of even moderate resistance, necessitating the use of a tuned grid circuit. Adjustment of the grid circuit had been found critical and it was impossible to connect a demodulator directly to the anodes. Further reduction of the total tuned circuit inductance below about 0.2 μH was impractical with lumped elements and since it was thought desirable to reduce this to the minimum attainable, both the 807 valve and the lumped inductance were abandoned in favour of a high frequency power valve, the QQV04/20, and a transmission line tuned circuit.

As an example the inductance of a co-axial array with internal diameter 0.5 inch and inner conductor diameter 0.075 inch, Fig. 71 (a) is 0.1151 μH/foot given by the usual formula $L = 0.1405 \log b/a$ μH/ft and its self capacitance by $C = 7.35/\log b/a$ μF/ft is 8.92 μF/ft.

In the case of the open wire line, Fig. 71 (b), the spacing needed to provide the same inductance per foot length is 0.1339 inch, since in this case $L = 0.28 \log \frac{d-r}{r}$ μH/ft and the self capacitance, given by $C = 3.67/\log \frac{d-r}{r}$ pF/ft is 8.95 pF/ft. The input impedance of the line when terminated by a resistance of, say, 2 ohms is L/CR, and hence, in both cases is about 6,450 ohms which is more than adequate to ensure oscillation with the QQV04/20 which has a transconductance of 4 mA/V. Apparently there is nothing to be gained in this case from the use of a co-axial line and open wire lines have been extensively used in the experiments described in the following Sections.

In/

In order to obtain a comparison between the 807 and the QQV04/20 at low radio frequencies two sets of coils used in the 807 oscillator were substituted directly into the circuit shown in Fig. 72. In all instances there was sufficient gain for oscillations to be possible with an untuned grid circuit and the majority of the work done with this valve was of this nature. Typical responses are shown in Fig. 73 and a response obtained with a similar wire in the 807 oscillator is shown for comparison. Reduction of the inductance, still lumped, to 0.3 μH increased the bandwidth by an amount less than that predicted, the table below summarizing the results.

Wire diam.	Cold res.	Change pt.	L μH	Ratio L_1/L_2	Ratio ω's
0.0003 in.	3.0	5500 c/s	0.57	1.38	1.28
0.0003	3.5	7000	0.30		
0.0002	3.5	8000	0.57	1.38	1.13
0.0002	3.5	9000	0.30		

A transmission line was constructed using 5/16 inch diam. tubing with centre spacing 1 inch, having a calculated inductance of 0.30 μH/ft and with a length of 1 ft gave the response shown in Fig.73 (4). The circuit is shown in Fig. 74 the transmission line being tuned by means of a small capacitance across its end and for the preliminary tests was fitted with a tuned grid circuit heavily damped with a 2kΩ resistance.

It was noticed that in this ocillator grid tuning had somewhat less effect on the response than was the case with the push-pull 807 and in view of the fact that there was adequate gain without this tuning even with wires of up to 5 ohms cold resistance it was eliminated for simplicity of operation, Fig. 75. A directly-coupled demodulator was added and the wire was isolated from the direct current in the valve by means of blocking condensers, choke feed being employed to supply the anodes. This isolation of the direct current was necessary as the finer wires, smaller than 0.0002 inch diam., have insufficient thermal overload capacity and when oscillations commence as the bias is reduced on the valves failure may occur. Wires of 0.0003 inch diameter could be operated satisfactorily without this precaution but it was found essential for tungsten wires in almost all diameters. Cathode degeneration is not possible with this valve since the two cathodes are connected inside the envelope, to reduce the effects of cathode lead inductance.

No accurate measurement of the tuned circuit inductance was possible with lengths of line less than about 3 inches, and no great improvement in bandwidth was achieved with these shorter lines. With 2.75 inches the frequency of oscillation was 110 Mc/s, and a bandwidth of 22 kc/s could be obtained with wires of about 3 ohms cold resistance (0.0002 in Tung.), mounted in a suitable probe. This appears to be about the practical limit for this oscillator without recourse to overall feedback.

Prior to the construction of this high frequency oscillator platinum wires had been supported on two stiff tinned copper leads attached to porcelain insulators. The wire was soldered across the support points and a suitable length etched off the silver coating. This enabled wires of various resistances to be made with the minimum effort, an important feature when the risk of a wire failure due to burn-out is great. A typical wire mount such as described

above/

above was found to have an inductance of 0.04 μH and with the total tuned circuit inductance as low as 0.30 μH this addition has to be considered when the predicted bandwidth is calculated.

The QQV04/20 oscillator was, however, intended to be a prototype for turbulence measuring equipment and it was thought desirable at this stage to make the wire support in the form which it would eventually take and to verify that the same bandwidth could be attained with this arrangement.

8.7 High Frequency Characteristics of Hot-wire Probes

The technique of production of hot-wire probes suitable for high air speeds is dealt with in Ref. 6 but a short discussion of their electrical characteristics is included here since the transmission line oscillator at 110 Mc/s makes the severest demands on low probe inductance.

Fig. 76 illustrates the manner in which the wire itself is supported on two steel needles, in turn held inside a 0.125 inch outside diameter brass tube by means of dental porcelain. This method of construction ensures that the supports are rigidly held and insulated from each other. Since one end of the wire itself is earthed for convenience, one needle is soldered to the brass case, and the case serves as the electrical connection to the wire. The probe unit above was tested by means of a Q-meter at 60 Mc/s, the highest frequency available, and found to have the following characteristics:

$$L = 0.027\ \mu H$$

$$R = 0.05\Omega$$

$$C = 9.0\ pF.$$

It will be seen that the inductance is appreciable when compared with the total tuned circuit inductance and little advantage will be gained from reducing the latter. The unit shown in Fig. 76 is, moreover, only part of the probe and the supporting strut must be included to conduct the leads into the centre of the working section of the tunnel.

A tunnel with a working section 2 inches square was to be used in a preliminary trial with the oscillator developed and the support must be long enough to allow traversing at least to the centre line. Two probes were finally used, as shown in Figs. 77 and 78. The first is suitable for the unit in Fig. 76 which may be replaced when a wire fails, while the second was designed for use at transonic speeds where the interference from the support must be reduced.

A dummy probe was made to the same dimensions as that in Fig. 78 but fitted with a static tube in place of the needles and it was found that the extension shown was necessary to avoid bow wave interference from the support.

A series of bandwidth measurements made using the replaceable probe unit showed that responses with 3 dB points at about 22 kc/s were consistently obtainable with tungsten wires of 0.00022 in. diam. A typical response is shown in Fig. 79. The feedback coupling for this example was set at about 20 pF, the total anode current was 60 mA and the anode voltage 250 V. The best responses were obtained with the lumped tuning capacitance set for maximum response amplitude, less than this causing squegging and greater, a damped response, as did a decrease in the anode voltage or an increase in the feedback coupling.

9./

9. The Production of Variations in Velocity for Testing Purposes

The need has long been recognized for some means of applying a known velocity variation to a hot wire in order to ascertain its frequency response.[7,8,9] Schuh[9] produced sinusoidal variations in air speed by means of a loudspeaker diaphragm but the frequency was limited to about 2 kc/s, and extension to higher frequencies would be difficult.

Various schemes have been considered for producing periodic variations in an airspeed using rotating discs, but the upper frequency limit was in all cases too low.

An alternative method of testing the hot wire is by the use of a velocity transient. This is anal gous to testing an amplifier with a step-function input instead of sine waves. A velocity transient can easily be obtained by disturbing the stream in front of the wire for a short period of time by shooting through it a small obstacle. This can be done by means of a needle projecting from the rim of a large disc rotating at high speed. Some practical results are given in subsection 9.1.

Another way of producing a change in speed in a supersonic stream would be to have a small wire forming an obstacle which is suddenly disintegrated by passing a current through it. Another possibility would be to have an obstacle which is moved very rapidly by electromagnetic means. Transient effects can also be produced by electric sparks, and some experimental work on this method has been done, but it was found impossible to eliminate pick-up voltages from the spark itself. The possibility of using a shock tube is referred to in subsection 9.2.

9.1 Transient Testing of the Wire in an Airstream

By disturbing the flow of an airstream past a wire by a small diameter needle it is possible to produce a pulse whose rise time gives an idea of the maximum frequency of response of the equipment.

Two needles of diameter 0.65 mm were attached symmetrically to a disc of diameter 4 inches which was rotated at 4,000 r.p.m. so that the needle was in front of a wire, whose length was 0.64 mm, for a period of about 65 μsecs. The output of the oscillator was applied to a cathode ray tube with the time-base running free so that the pulses appeared at random positions on the screen. A brief exposure was made on a camera and by projecting the film strip on to a graph sheet the shape of a single pulse could be determined from a calibration sine wave on the tube. The oscillator actually used was the transitron described in Ref. 2, which gave a bandwidth of about 12 kc/s without negative feedback. Rise times of about 60 to 70 μsecs were observed in practice as shown in Fig. 80 (a); this is a reasonable value for this bandwidth in view of the fact that the air velocity change is not a step function. The time to fall to zero is seen from Fig. 80 (a) to be about 180 μsecs and this could be reduced by the use of negative feedback, Fig. 80 (b). The application of negative feedback with this particular type of oscillator was not reported in Ref. 2 but its main effect was to increase the peak without greatly extending the bandwidth as evidenced from the overshoot seen in Fig. 80 (b).

9.2 The Hot Wire in a Shock Tube

A more truly square wave may be obtained from a shock tube although the disturbance amplitude in this case is very large and followed, in a short shock tube, by a period of unsteady flow. A simple 2 inch diameter shock tube exhausting to atmosphere was constructed and rise times of 50 μsecs were observed when the response bandwidth of the equipment was about 16 kc/s (QQVO4/20 oscillator Section 8.6). Since the signal is in this case so large there is no great

advantage/

advantage to be gained in the investigation of shock tube behaviour, using hot wires, from employing constant-resistance heating and a conventional constant-current system followed by a severe differentiating network would probably be quite adequate and give a reasonable signal-to-noise ratio.

However, the technique produces waves which have steeper fronts than any other device considered, and thus proves to be a useful testing facility. It has not so far been possible to photograph the responses obtained due to the high writing speeds involved, although observation showed a clear enough trace on the cathode-ray tube.

Conclusion

The theory of operation of a hot-wire anemometer using two types of heating has been dealt with in considerable detail, and experimental verification of the major part of this theory has been obtained. It has been shown that with a given wire there is a limit to the attainable signal-to-noise ratio at high frequencies, and this limit has been approached in practice.

A satisfactory method of testing the high frequency response of the wire to actual variations in air velocity remains to be found. Experimental results on turbulence in a high speed wind tunnel using the equipment described here will be reported in a further paper.

References

No.	Author(s)	Title, etc.
1	B. Wise	The hot-wire anemometer for turbulence measurements. Part I. O.U.E.L.52. Presented by Prof. A. Thom. C.P. 273. February, 1951.
2	B. Wise and D. R. Stewart	The hot-wire anemometer for turbulence measurements. Part II. O.U.E.L.54. Presented by Prof. A. Thom. C.P. 274. September, 1951.
3	J. C. Laurence and L. G. Landes	Auxiliary equipment and techniques for adapting the constant temperature hot-wire anemometer to specific problems in air flow measurements. N.A.C.A. T.N. 2843.
4.	E. Ossovsky	Constant temperature operation of the hot-wire anemometer. Rev. Sci. Ins. 9, 12, p.881.
5	H. Chestnut and R. Mayer	Servomechanisms and regulating system design. Vol.1. Wiley and Sons, N.Y.
6	D. L. Schultz	The design and construction of hot-wire anemometers for high speed flows. O.U.E.L.68. Communicated by Prof. A. Thom. A.R.C. 16,635 - 4th March, 1954.

7./

References (Contd.)

No.	Author(s)	Title, etc.
7	A. A. Hall	The measurement of the intensity and scale of turbulence. R. & M. 1842. August, 1938.
8	L. S. G. Kovásznay	Turbulence measuring equipment. N.A.C.A. 2839.
9	H. Schuh	Determination of the sensitivity and the time constant of hot wires for turbulence measurements. (MAP-VG33-165T). A.R.C. 10,046 - August 15th 1946.

APPENDIX

From Eqn. (1) in Ref. (1)

$$vi = f(R_1, V)$$

thus

$$\frac{dv}{di} i + v = \frac{df}{dR}\left[\frac{1}{i}\frac{dv}{di} - \frac{v}{i^2}\right], \quad R_1 = \frac{v}{i}$$

$$\frac{dv}{di} + R_1 = \frac{df}{dR} \cdot \frac{1}{i^2}\left[\frac{dv}{di} - R_1\right]$$

and from Eqn. (10) in Ref. (1)

$$\frac{df}{dR} = i^2\left[1 + \frac{2R_1}{R_b}\right] .$$

Hence

$$\frac{dv}{di}\left[\frac{2R_1}{R_b}\right] = 2R_1 + \frac{2R_1^2}{R_b}$$

and

$$R_w = \frac{dv}{di} = R_1 + R_b .$$

BW

FIGS. 1 – 7.

FIG. 1.

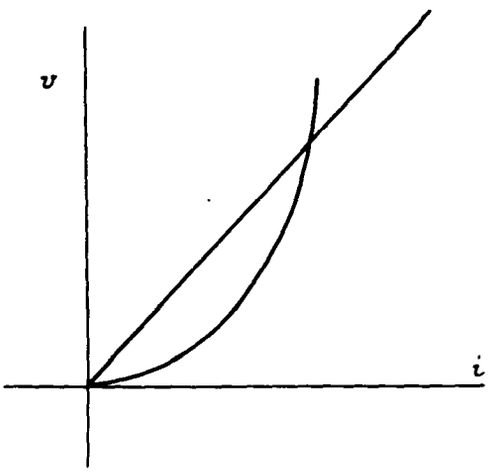

FIG. 2.

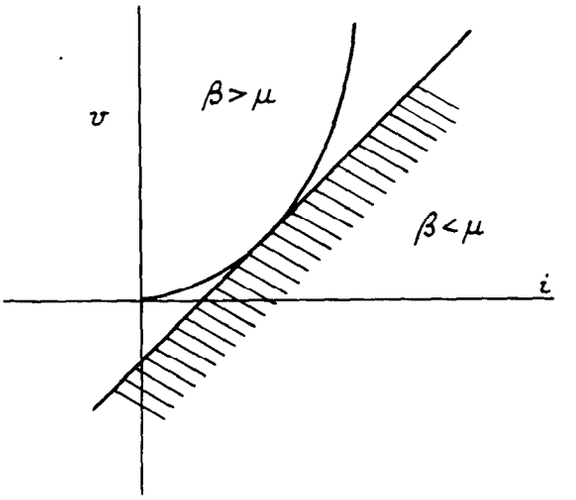

FIG. 3.

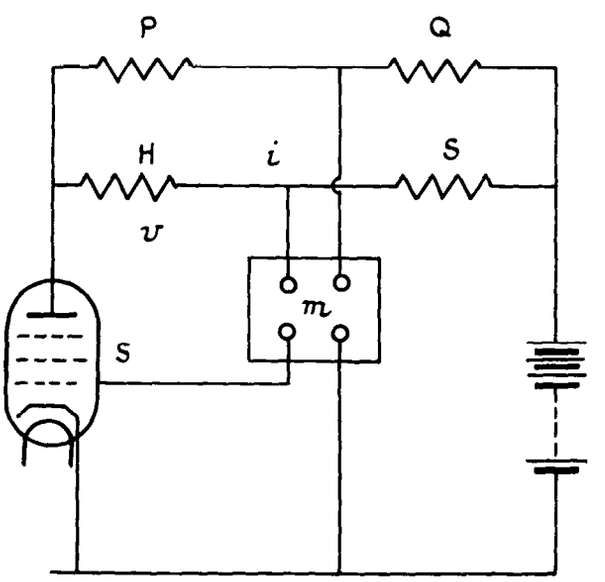

FIG. 4.

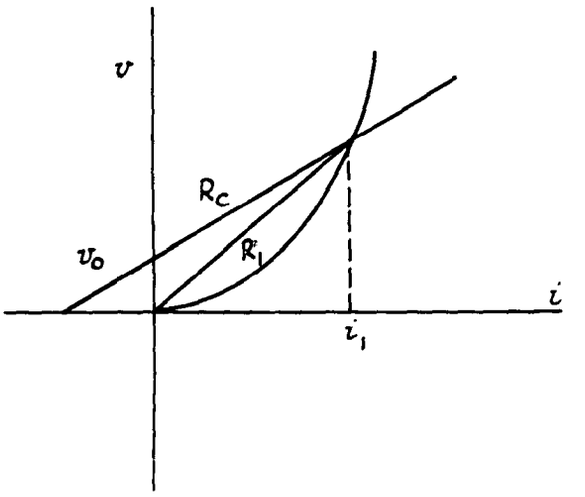

FIG. 5.

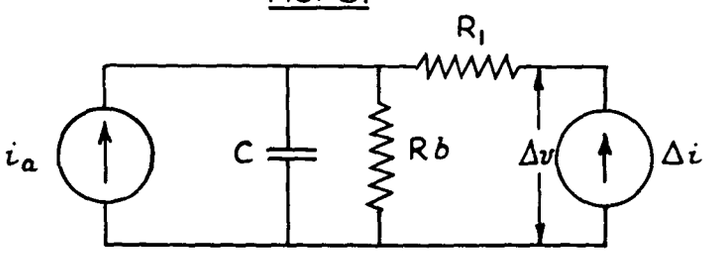

FIG. 6.

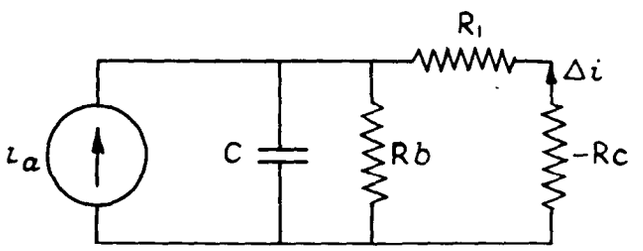

FIG. 7.

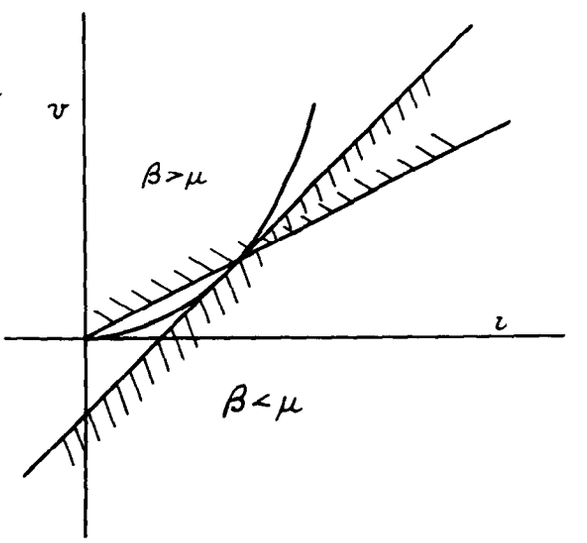

FIGS. 8 - 12.

FIG. 8.

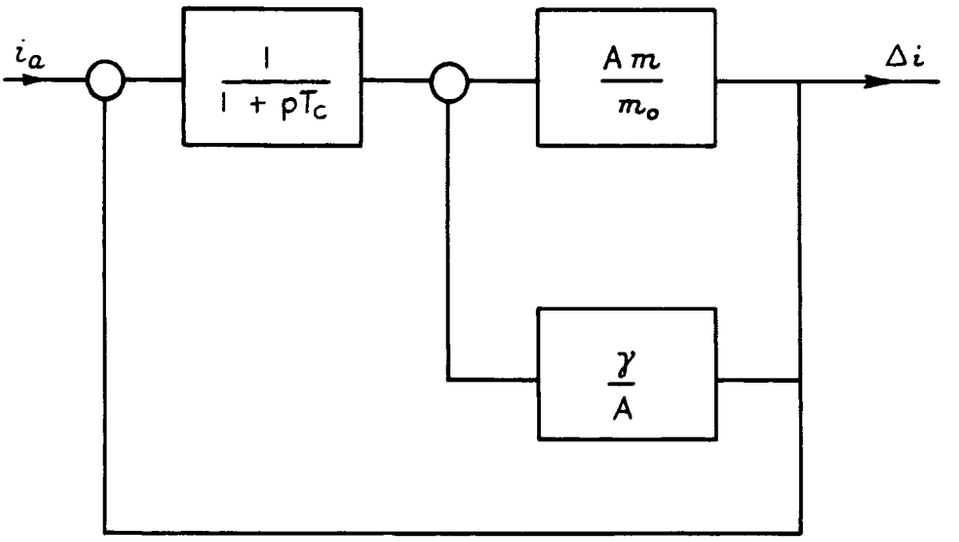

FIG. 9.

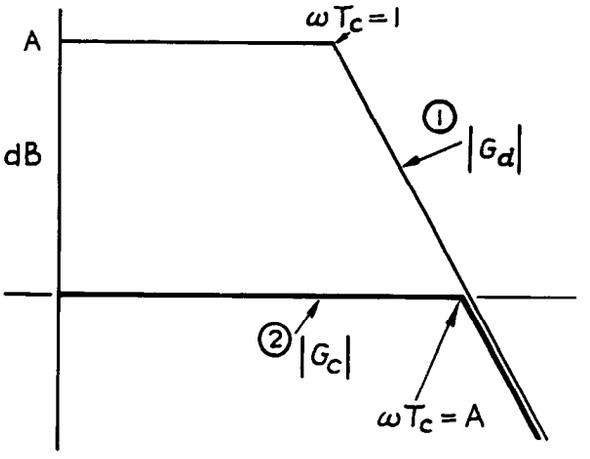

FIG. 10.

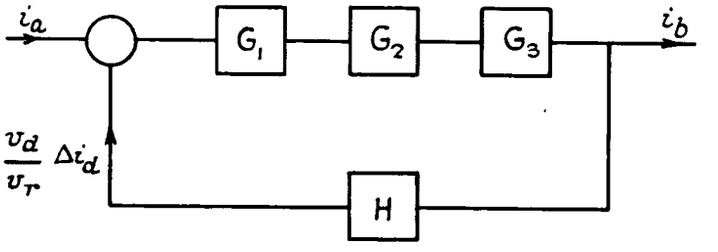

FIG. 11.

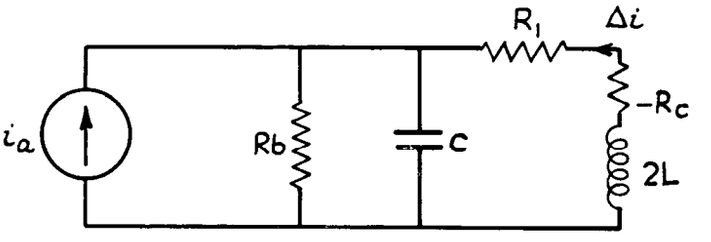

FIG. 12.

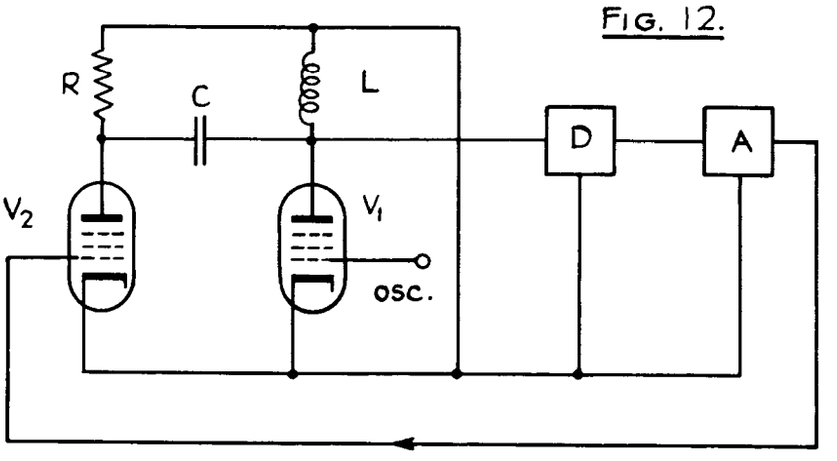

FIGS. 13 - 16.

FIG. 13.

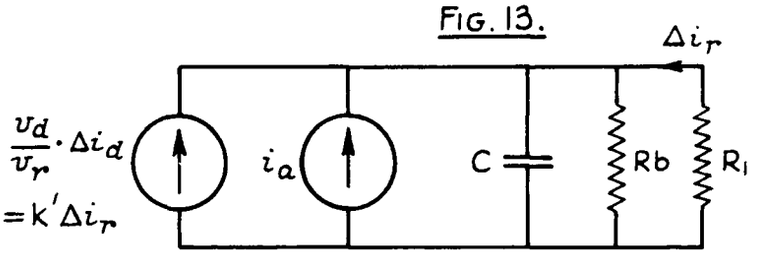

FIG. 14.

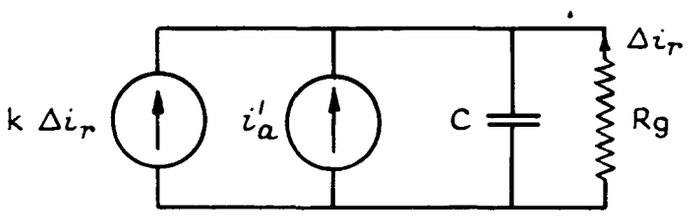

FIG. 15.

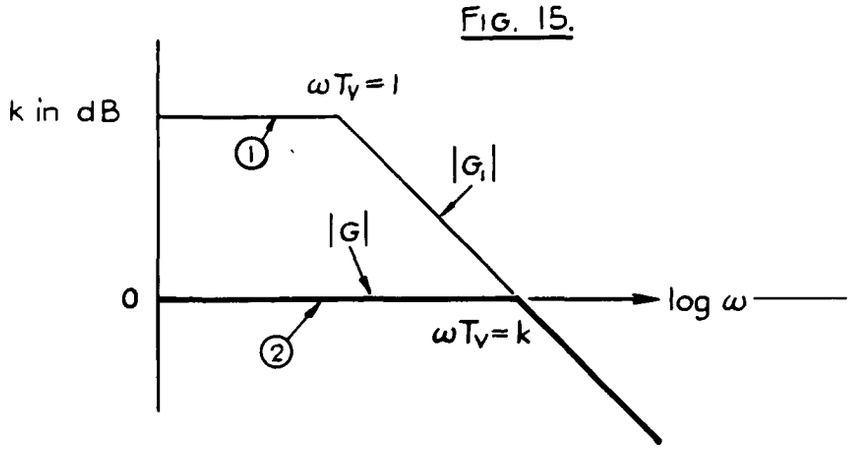

FIG. 16.

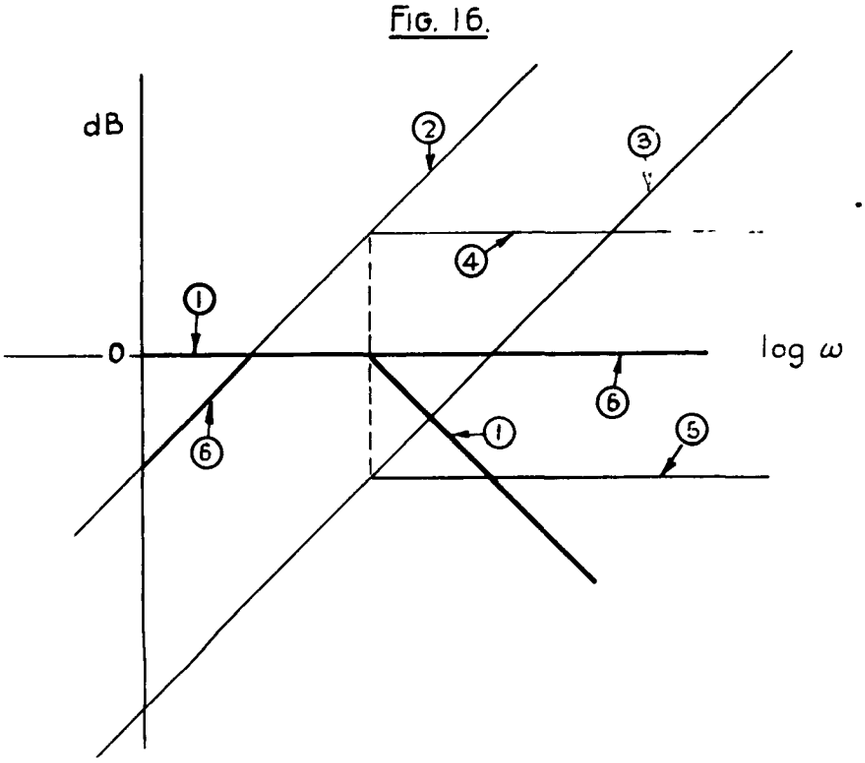

FIGS. 17 – 20.

FIG. 17.

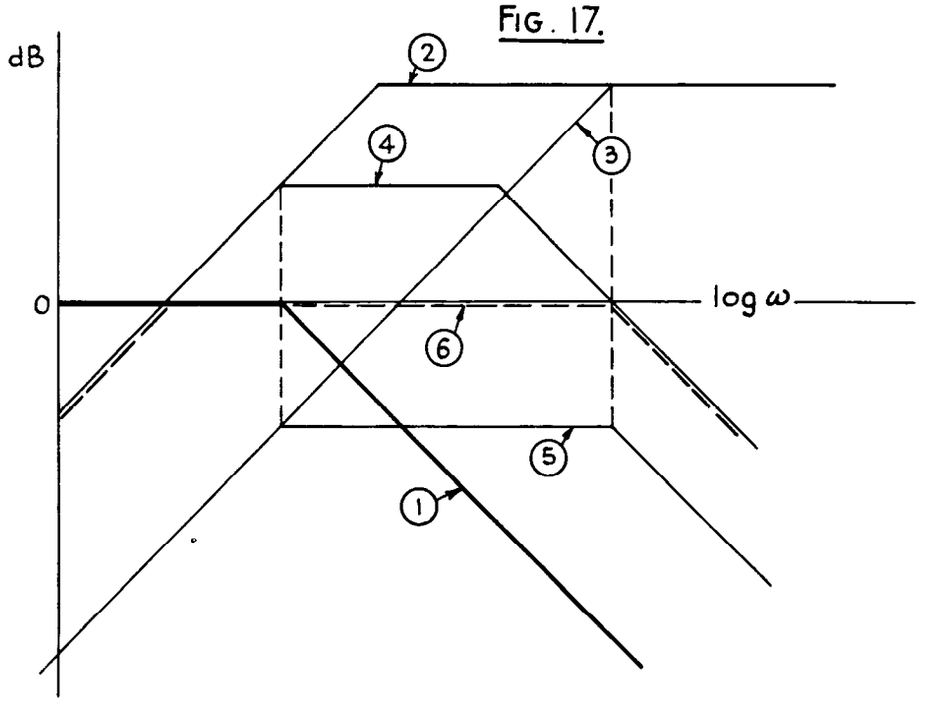

FIG. 18.

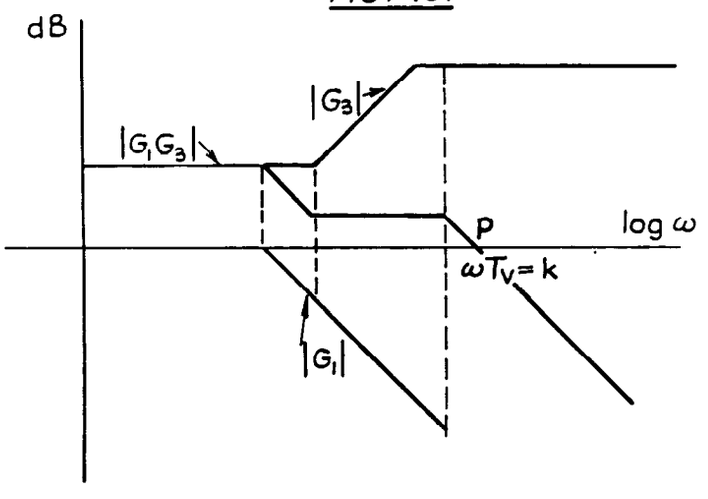

FIG. 19.

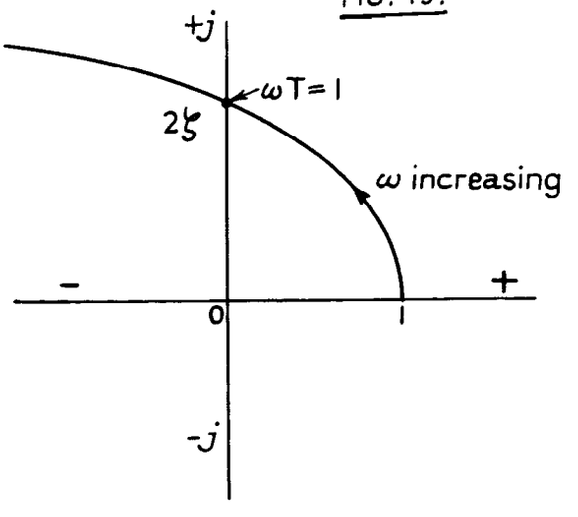

FIG 20.

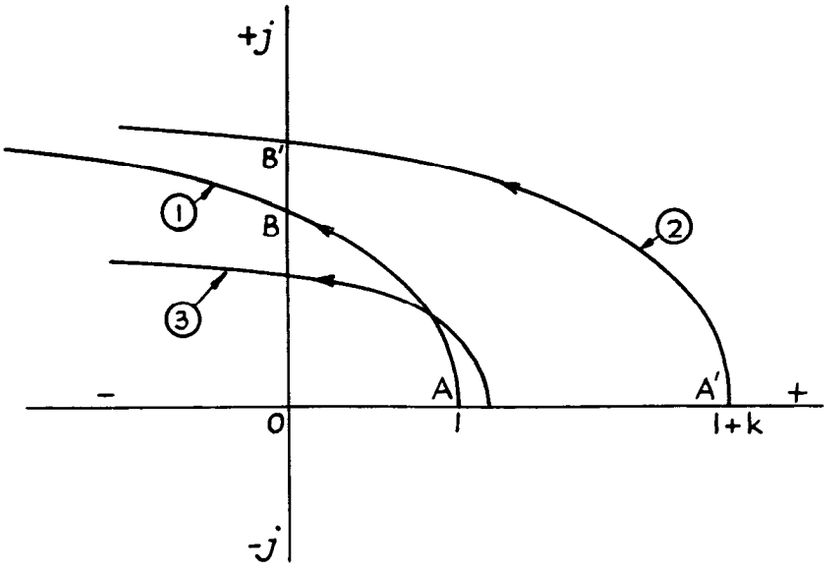

FIGS. 21 - 23.

FIG. 21.

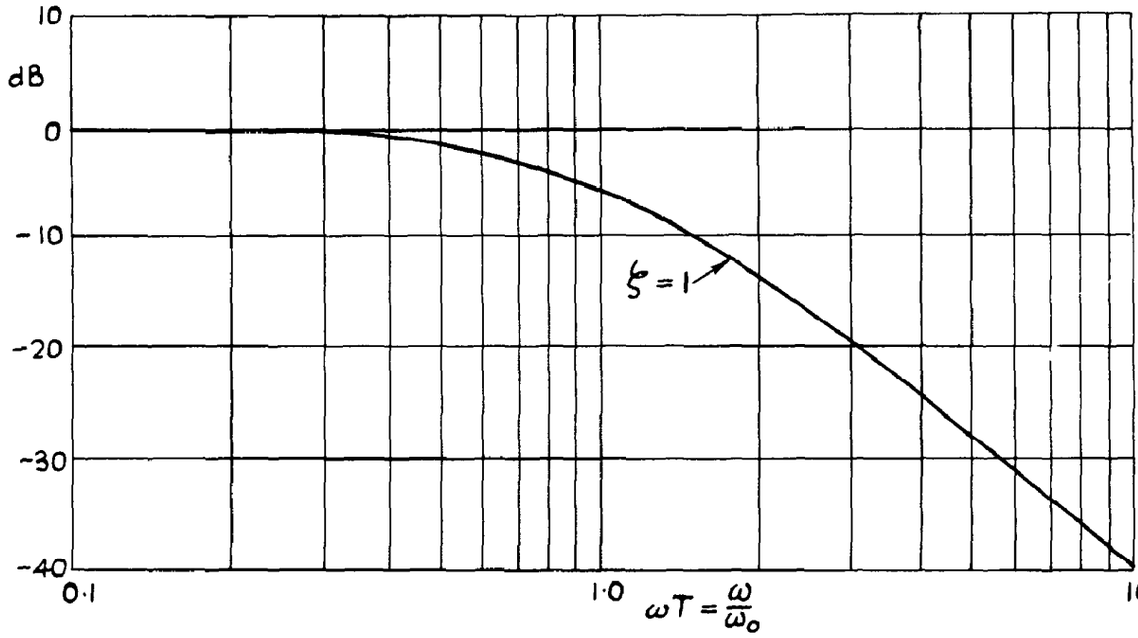

Amplitude response $|G_1 G_3|$

FIG. 22.

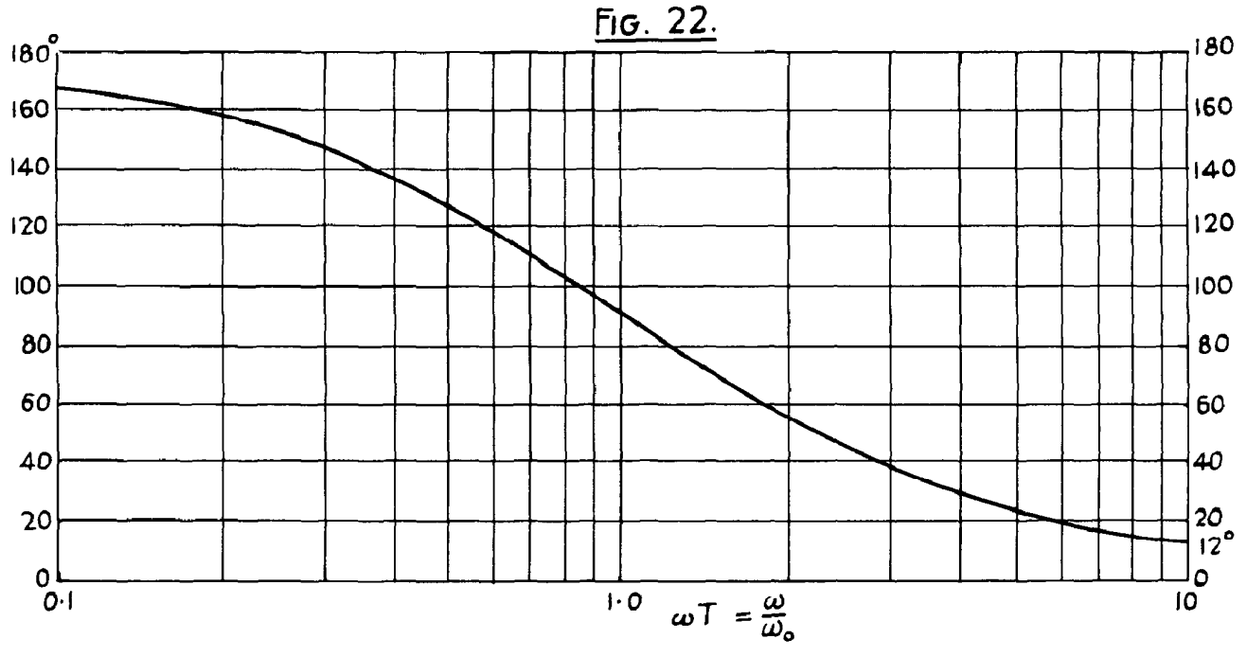

Phase response.

FIG. 23.

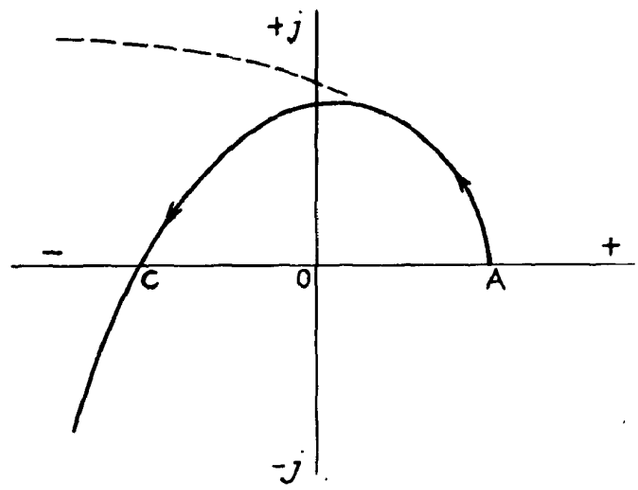

FIG. 24.

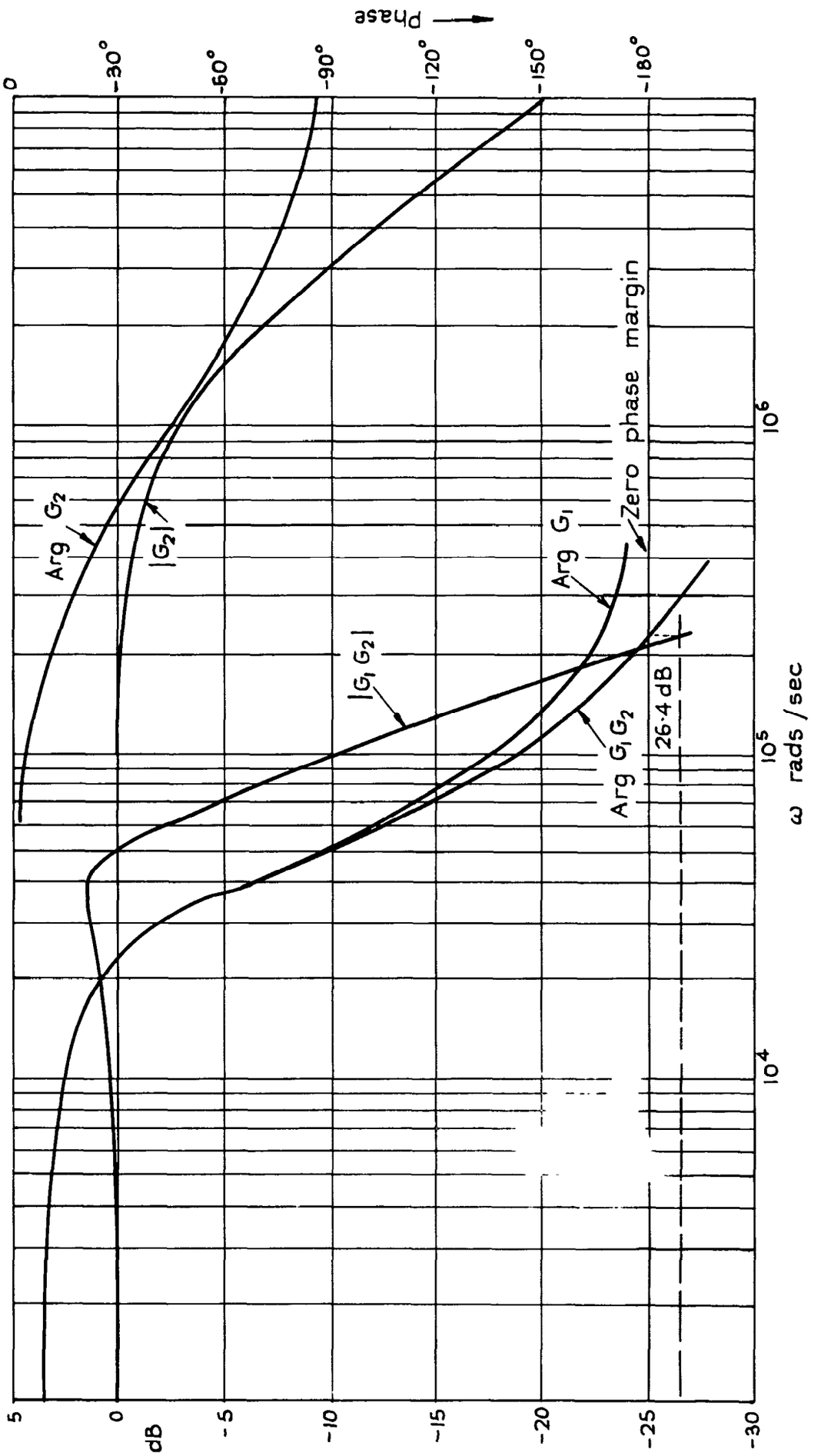
Phase
0
-30°
-60°
-90°
-120°
-150°
-180°
Arg G2
|G2|
|G1 G2|
Arg G1
Zero phase margin
Arg G1 G2
26·4 dB
10⁶
10⁵
10⁴
ω rads/sec
5
0
-5
-10
-15
-20
-25
-30
dB

FIG. 25.

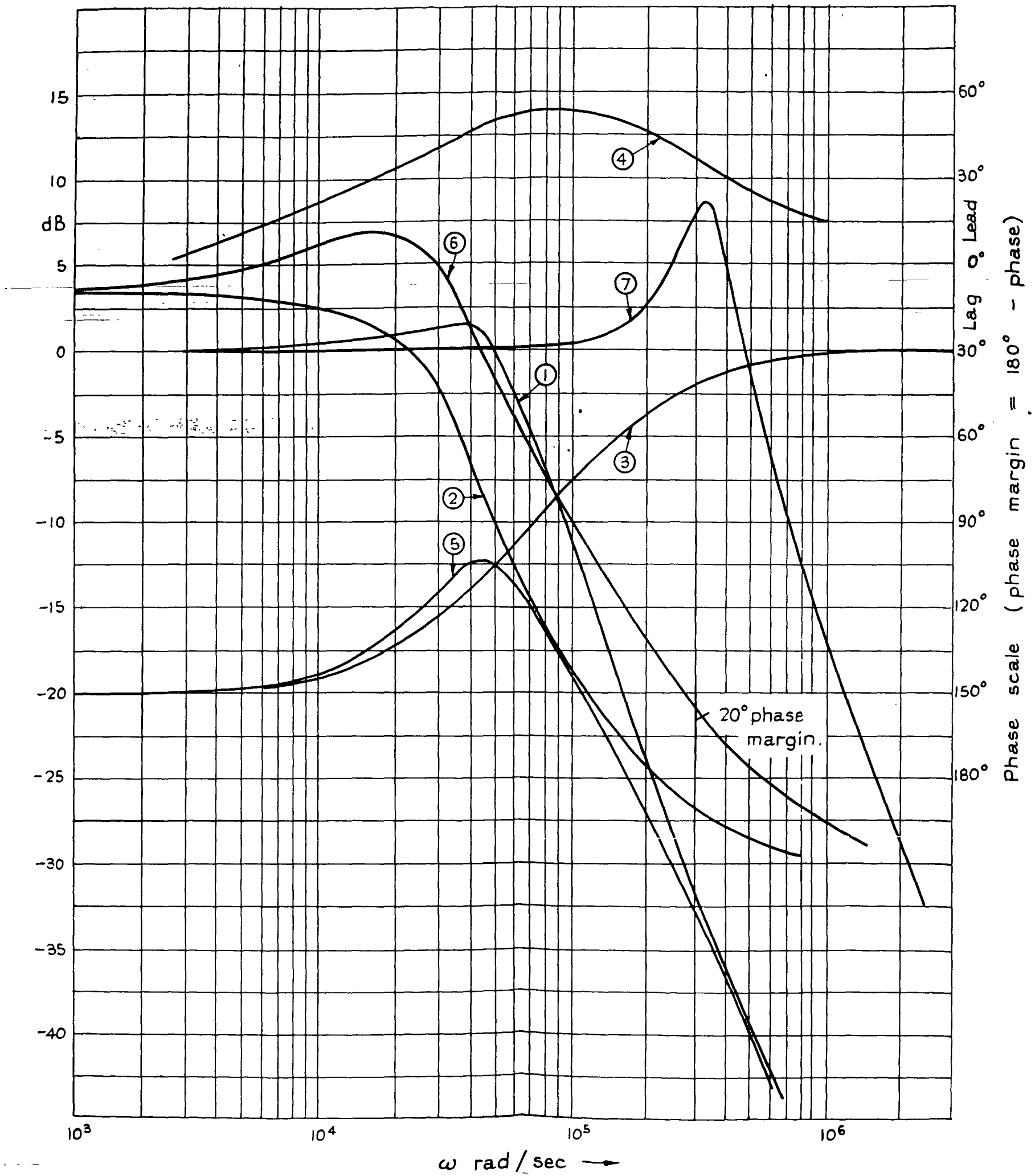

① Orig. amplitude response

② Orig. phase response

③ Modulus of phase advancing network.

④ Phase of (3)

⑤ Overall loop gain

⑥ Overall loop phase (open loop)

⑦ Closed loop response. Gain 34 dB

Phase advancer in feedback loop.

FIGS. 26 - 28.

FIG. 26.

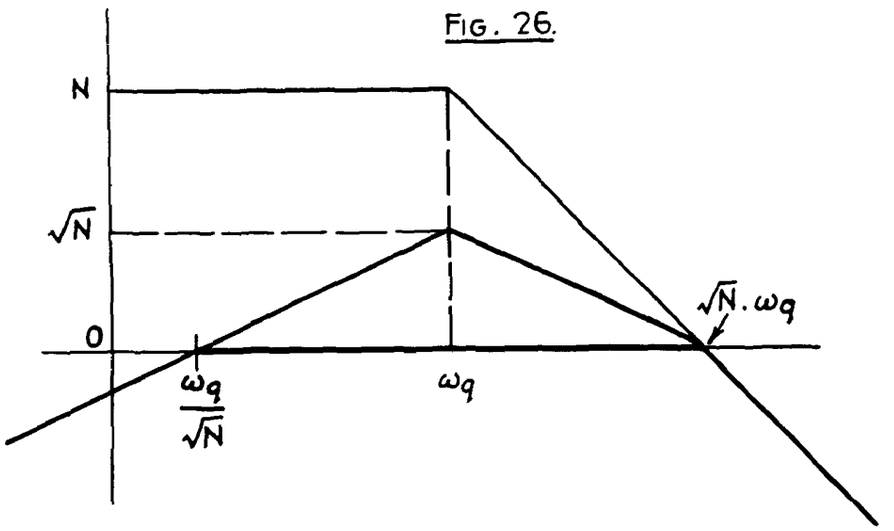

FIG. 27.

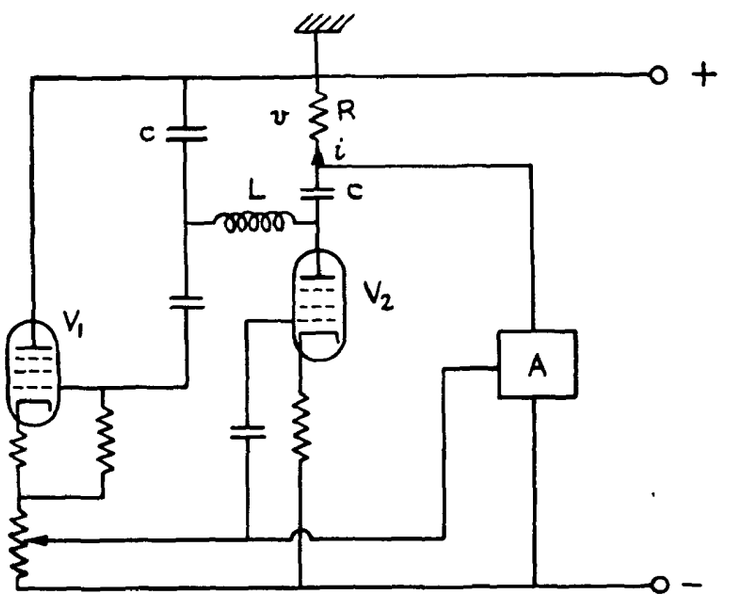

FIG. 28.

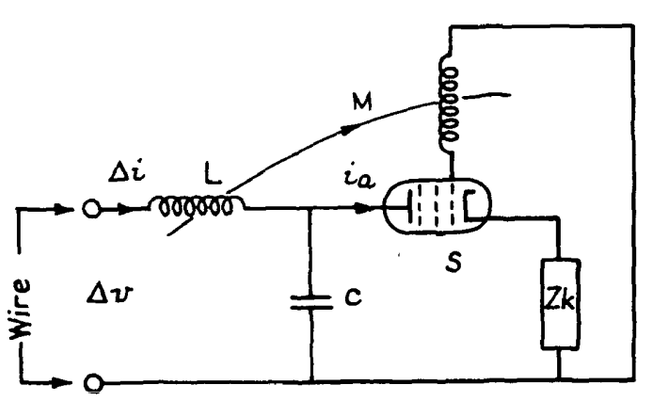

FIGS. 29.& 30.

FIG. 29.

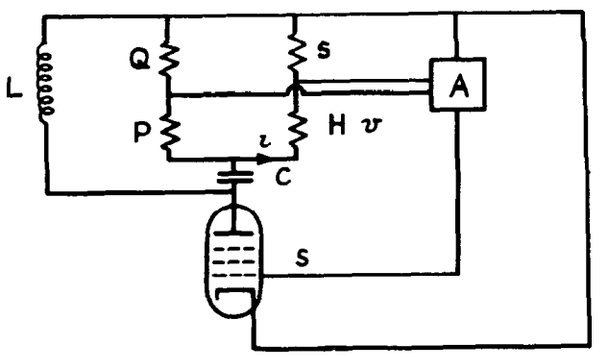

Input to a
$= \frac{SPi}{P+Q} - \frac{Q v}{P+Q}$

FIG. 30.

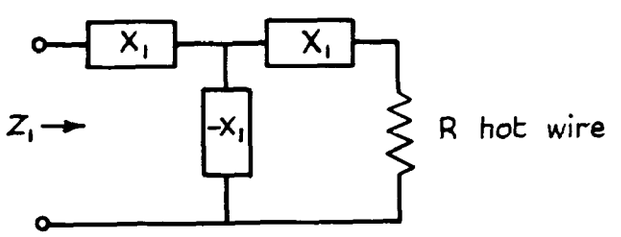

(a)

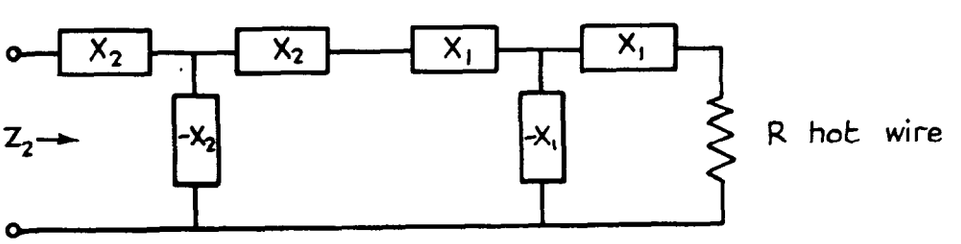

(b)

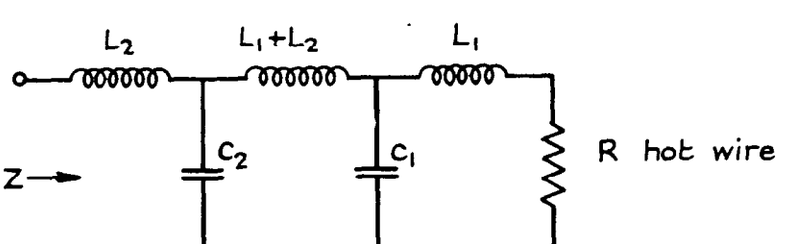

(c)

FIGS. 31 - 34.

FIG. 31.

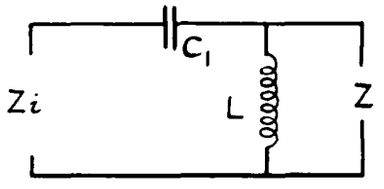

FIG. 32.

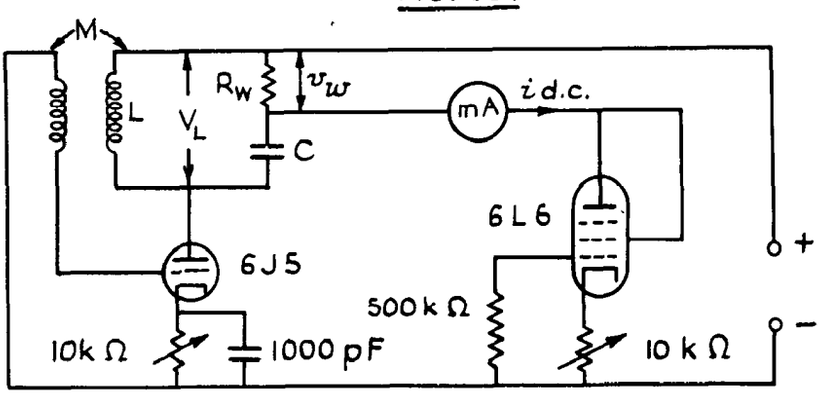

FIG. 33.

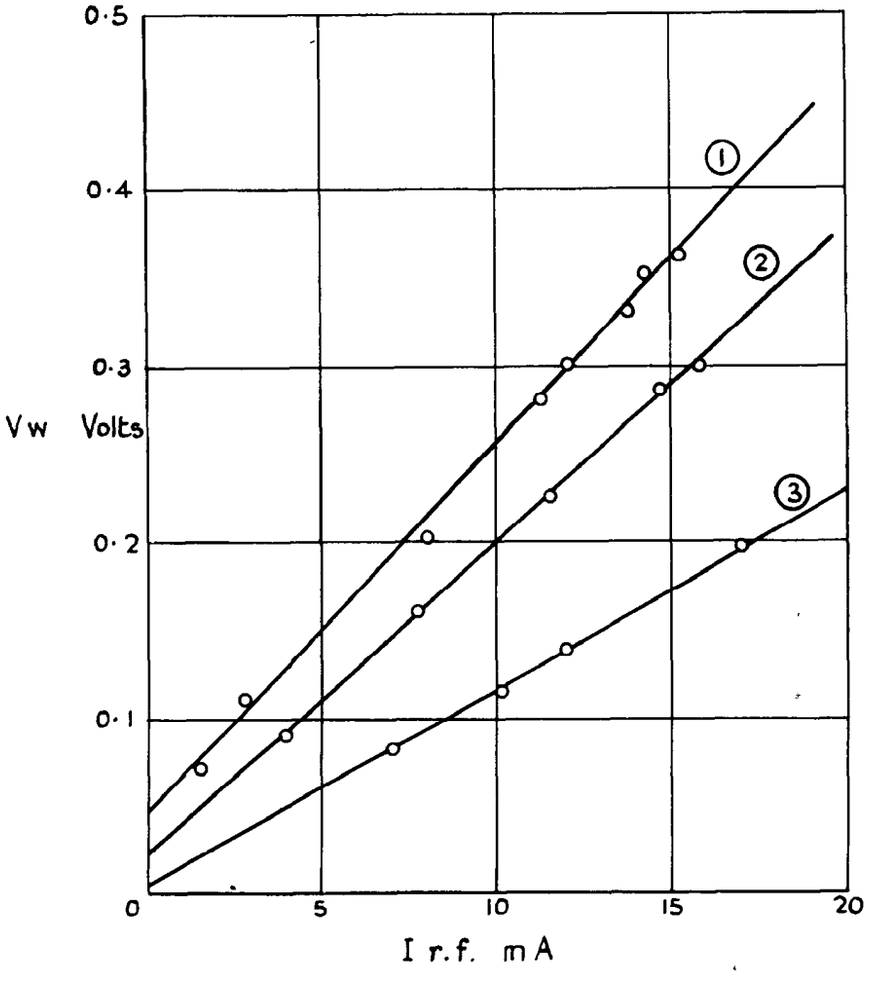

FIG. 34.

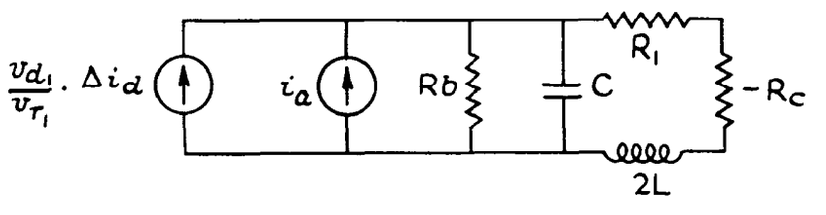

FIGS. 35 & 36.

FIG. 35.

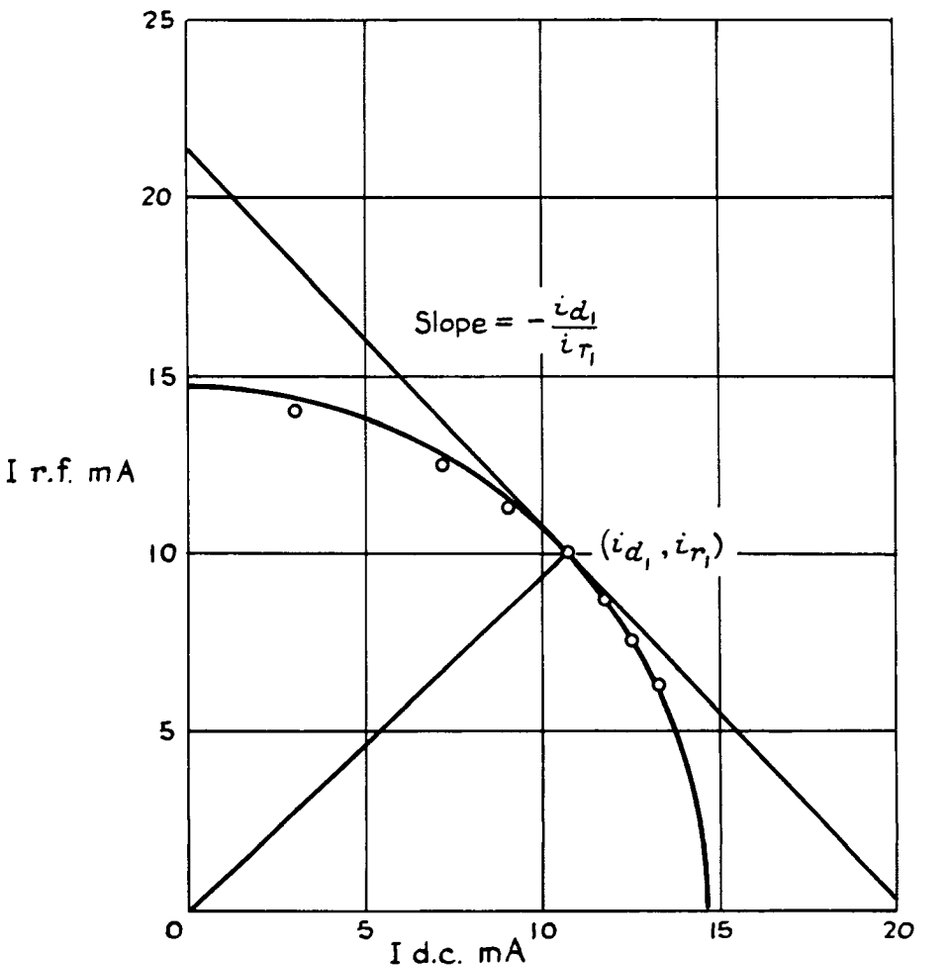

FIG. 36.

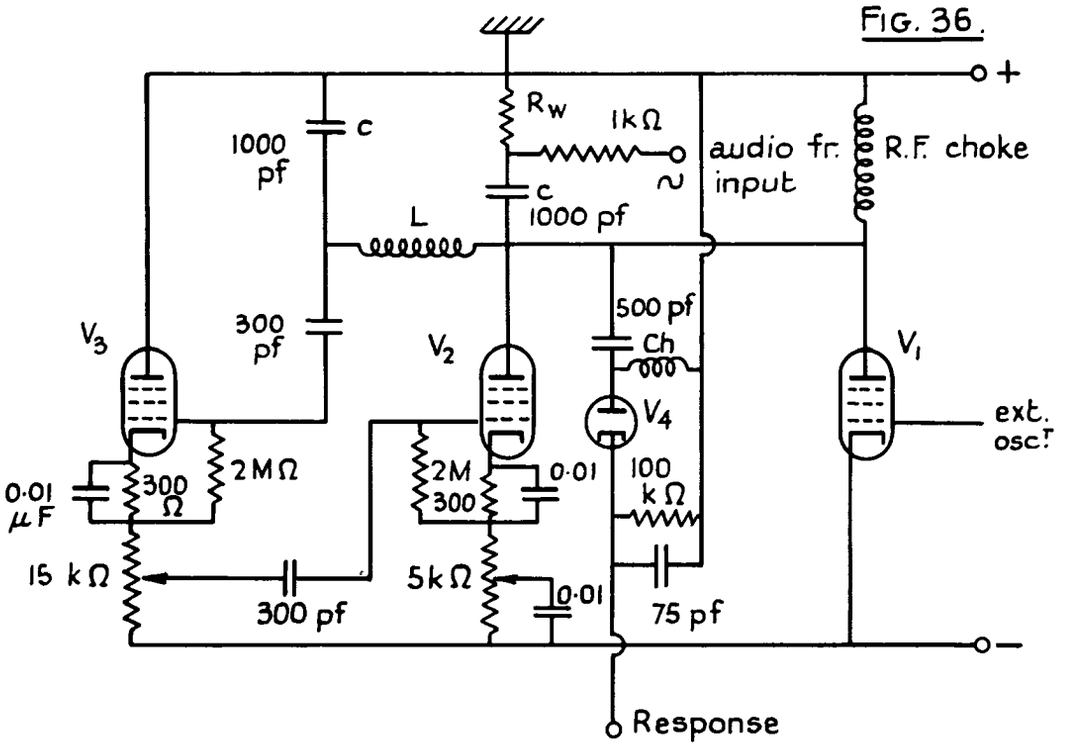

Oscillator at low radio frequencies.

L = 97 μH , Rw = 15 Ω , Fr. = 700 kc/s. V_1 , V_2 , V_3 EF50 V_4 EA50

V_1 and V_2 suppressor and screen grid connections are conventional and are omitted for clarity. V_1 cathode bias not shown. V_3 suppressor and screen grid tied to anode.

FIGS. 37 & 38.

FIG. 37.

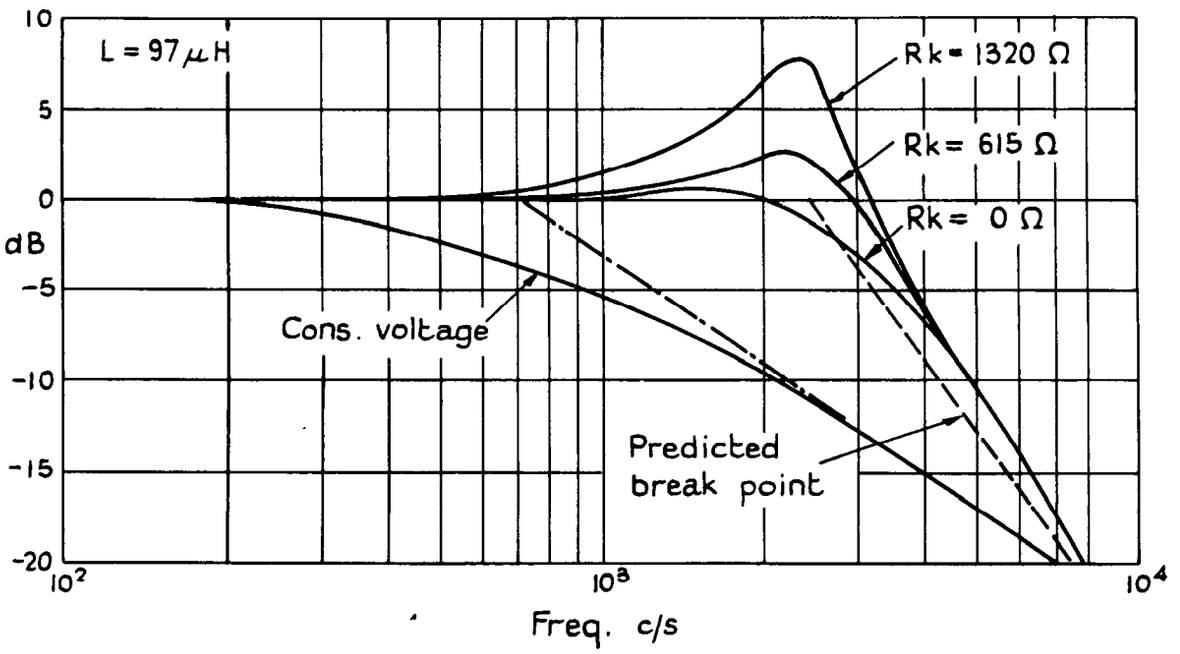

FIG. 38.

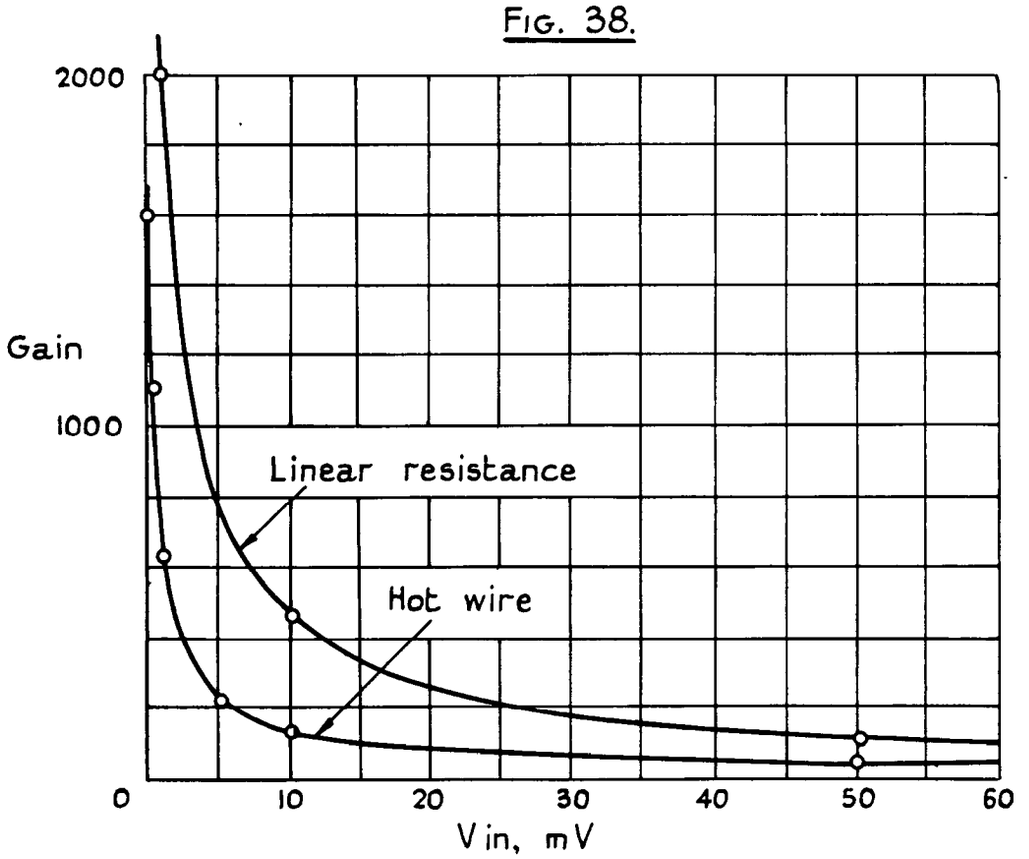

FIG. 39.

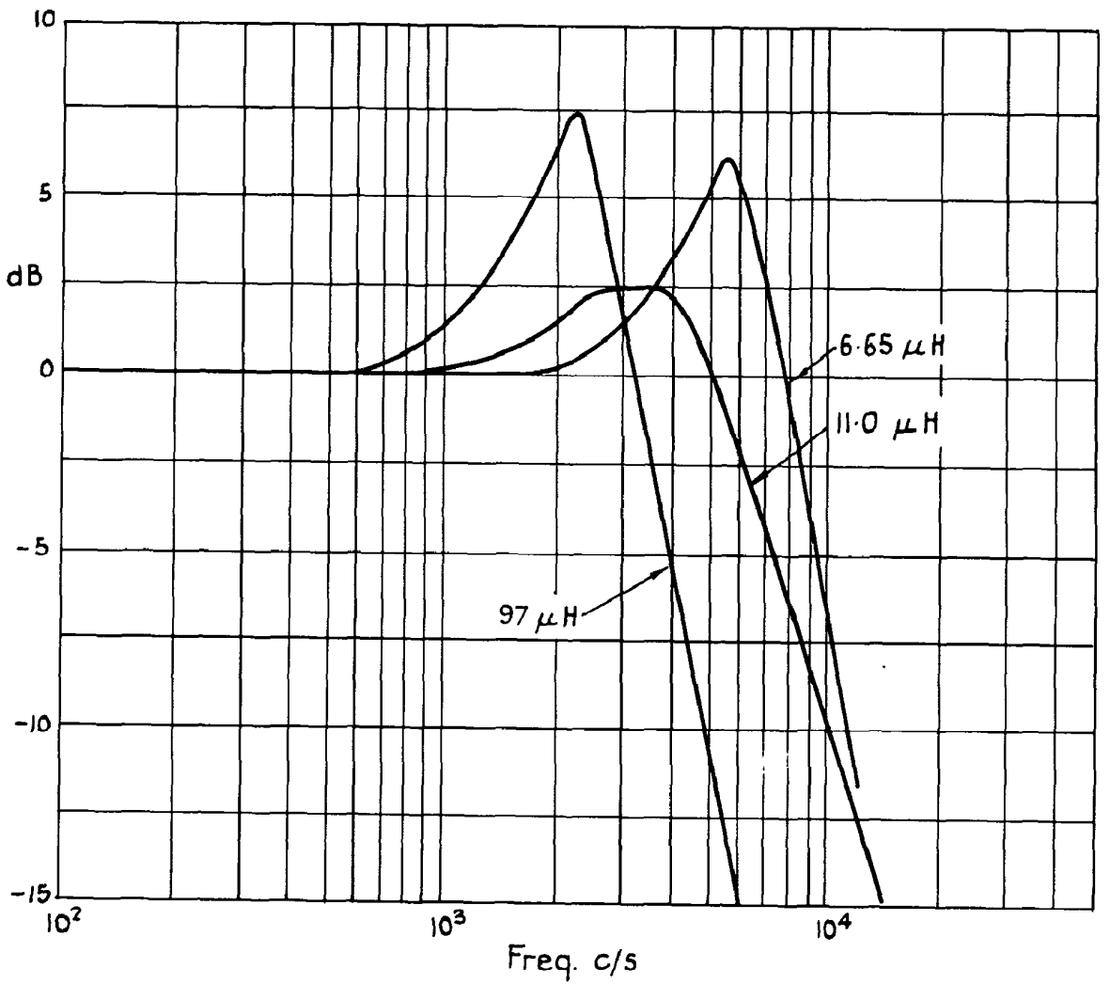

Oscillator at low radio frequencies, effect of inductance.

Wire time constant = 1·43 millisecs. Tuned circuit capacitances C-C= 105 pF for 11 and 6·65 μH coils, 1000 pF for 97 μH coils.
6·65 μH, Rk = 1600 Ω; 11 μH, Rk = 220 Ω; 97 μH, Rk = 1320 Ω.
Rk in each case adjusted to give optimum response.

FIG. 40.

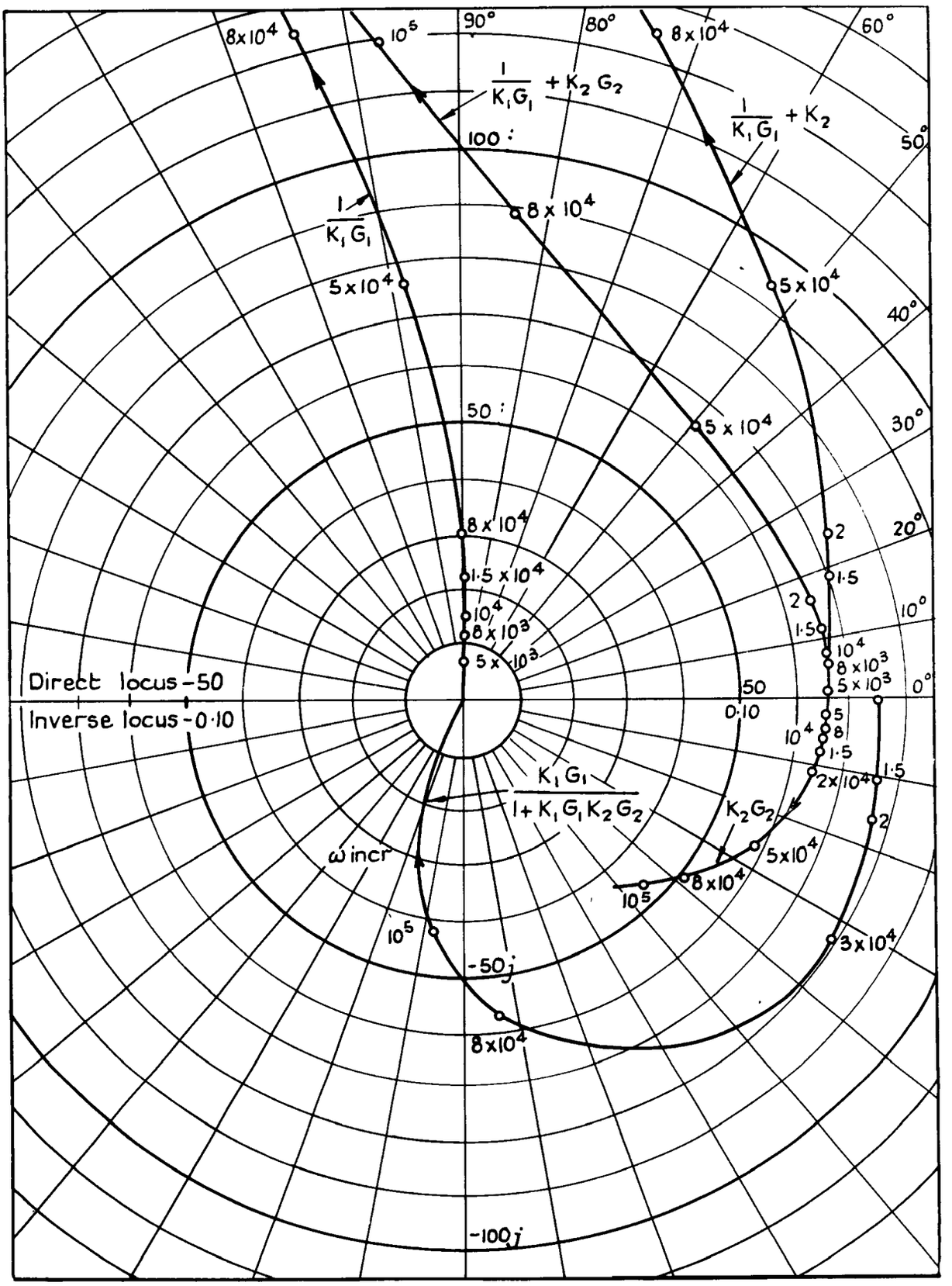
90°
80°
60°
50°
40°
30°
20°
10°
0°
100 :
50 :
$\frac{1}{K_1G_1} + K_2G_2$
$\frac{1}{K_1G_1} + K_2$
$\frac{1}{K_1G_1}$
$\frac{K_1G_1}{1+K_1G_1K_2G_2}$
K_2G_2
8x10⁴
10⁵
5x10⁴
1·5 x 10⁴
10⁴
8x10³
5x10³
3x10⁴
2x10⁴
2
1·5
5
8
50
0·10
Direct locus - 50
Inverse locus - 0·10
ω incr
-50j
-100j

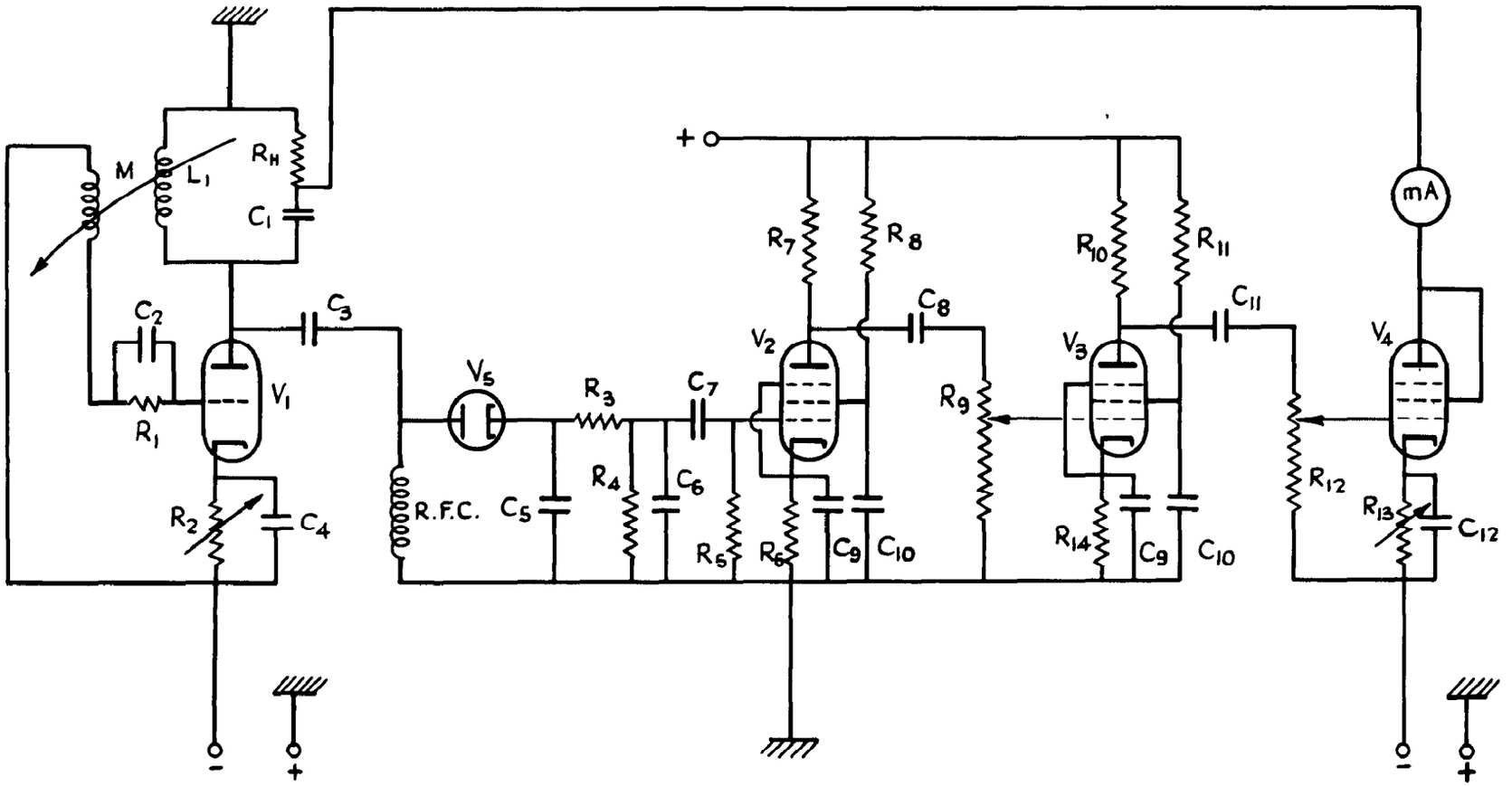

FIG. 41.

R_H	Hot wire	R_5	2 MΩ	R_{10}	30 kΩ	C_1	300 pF	C_6	75 pF	C_{11}	0·25 μF	V_4	6L6
R_1	1 kΩ	R_6	300 Ω	R_{11}	100 kΩ	C_2	300 pF	C_7	0·15 μF	C_{12}	25 μF	V_5	EA50
R_2	10 kΩ	R_7	10 kΩ	R_{12}	100 kΩ	C_3	1000 pF	C_8	0·25 μF	V_1	6J5	L_1	50 μH
R_3	10 kΩ	R_8	100 kΩ	R_{13}	10 kΩ	C_4	300 pF	C_9	25 μF	V_2	EF50		
R_4	100 kΩ	R_9	500 kΩ	R_{14}	300 Ω	C_5	75 pF	C_{10}	0·15 μF	V_3	EF50		

FIGS. 42 & 43.

FIG. 42.

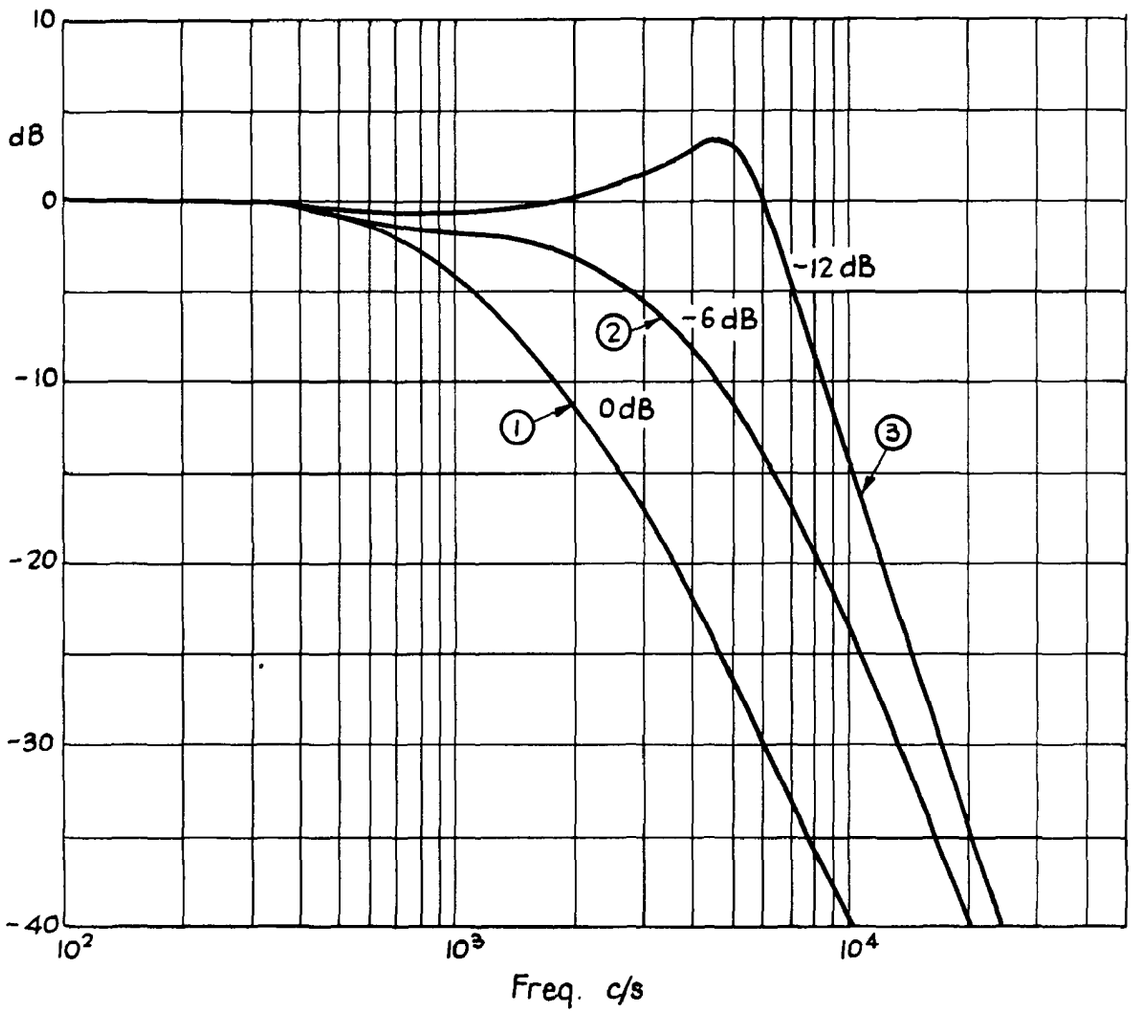

Overall negative feedback.

Response of circuit shown in fig. 31. Radio freq. = 1·5 M c/s
Rw = 20 Ω (0·0001 in. Pt.), L = 50 μH. $i_{d.c.}$ = 8 mA in the wire.

FIG. 43.

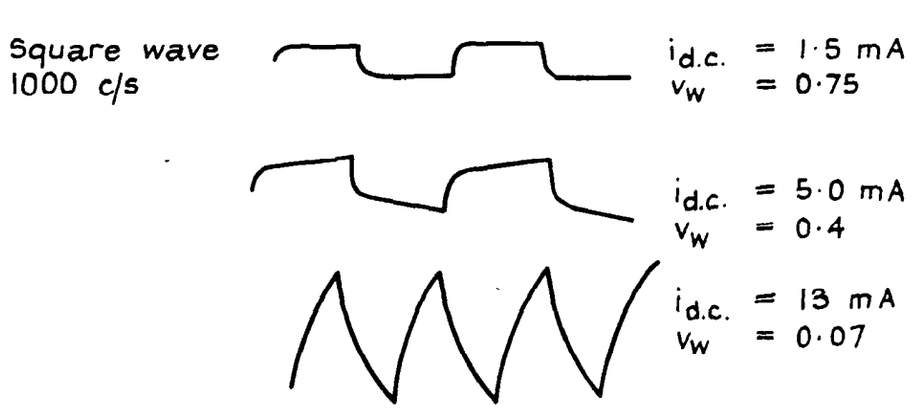

FIGS. 44 & 45.

FIG. 44.

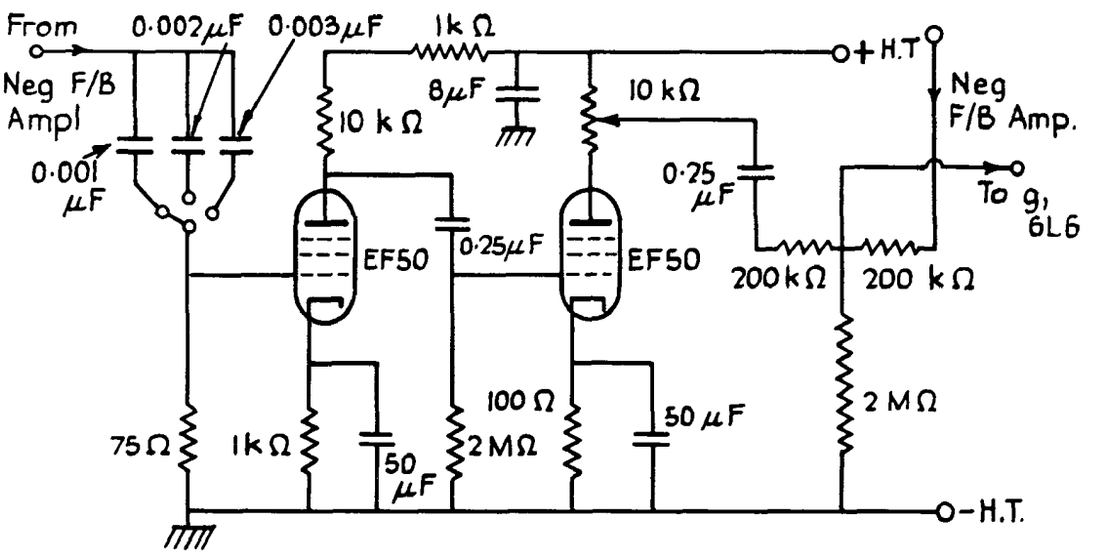

FIG. 45.

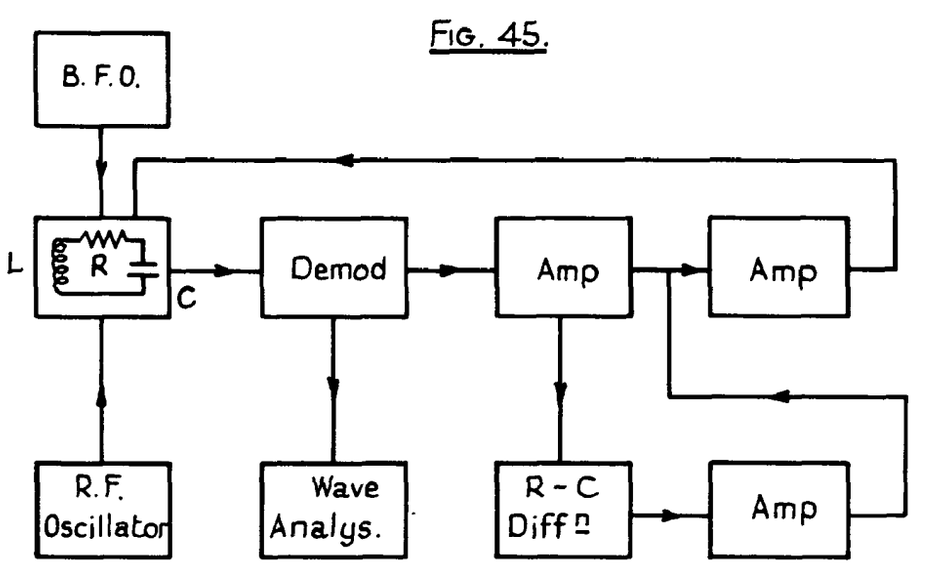

FIG. 46.

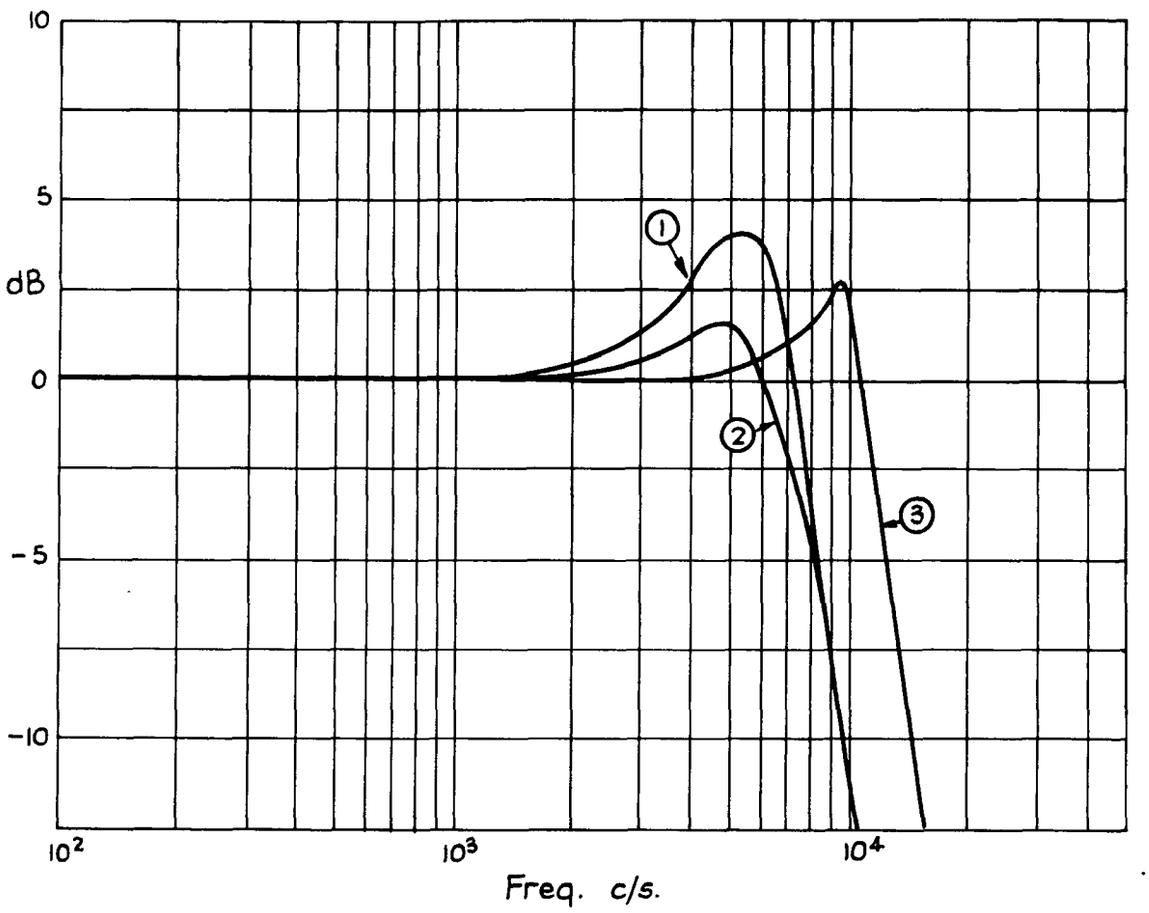

Overall negative feedback with differential stabilisation.

Response of system shown in figs. 41, 44. Rw = 35 Ω, L = 50 μH.

FIGS. 47 & 48.

FIG. 47.

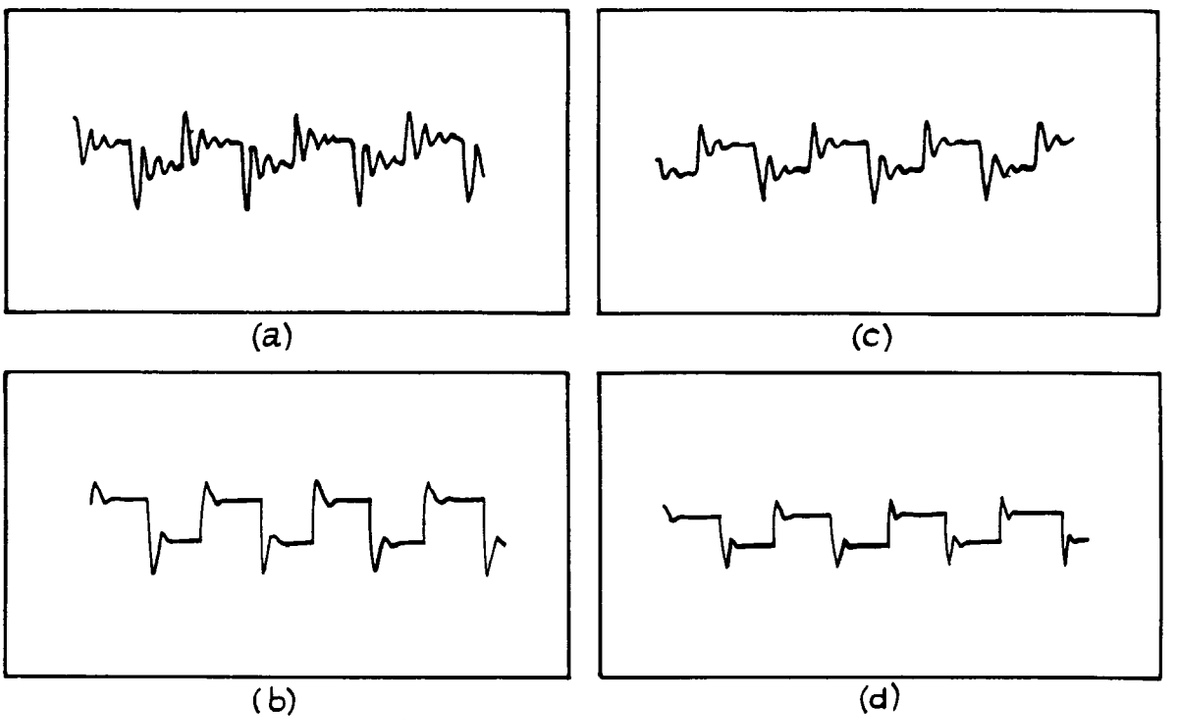

Differentiated feedback for stabilisation.

Square 1000 c/s. Radio frequency = 1·2 Mc/s. Rw = 30 ohms. L=47·6μH.
R.F. wire voltage = 0·046 V. D.C. in wire 12 mA.

(a) Negative feedback applied to initial response.
(b) Differentiated feedback applied to reduce peak.
(c) Further negative feedback applied.
(d) Increase in differentiated feedback.

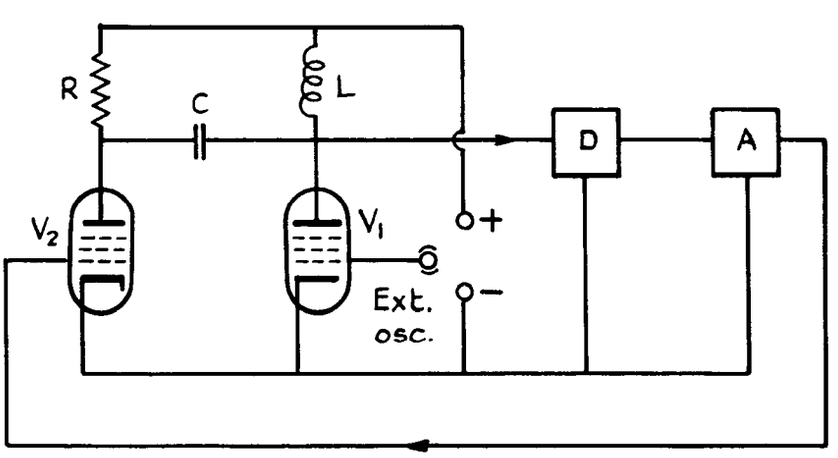

Overall negative feedback with constant voltage wire heating.

V_1 is driven from an external oscillator and supplies the wire R under constant-voltage conditions. D is a demodulator and A a voltage amplifier which drives V_2. V_2 supplies direct current to the wire along with the negative feedback signal.

FIGS. 49 - 51.

FIG. 49(a).

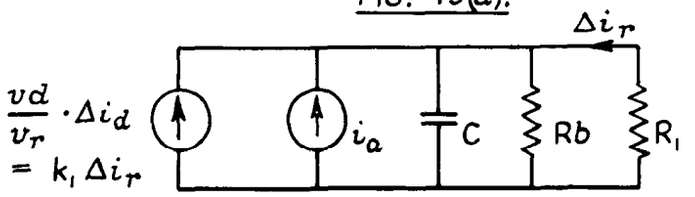

FIG. 49 (b).

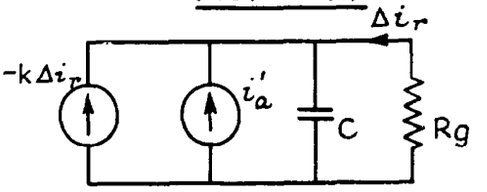

FIG. 50.

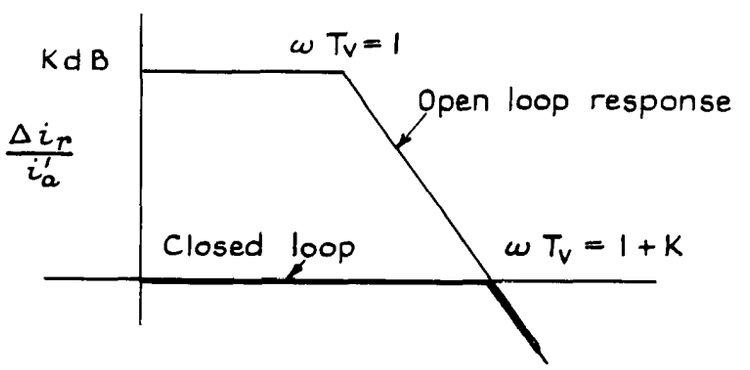

FIG. 51.

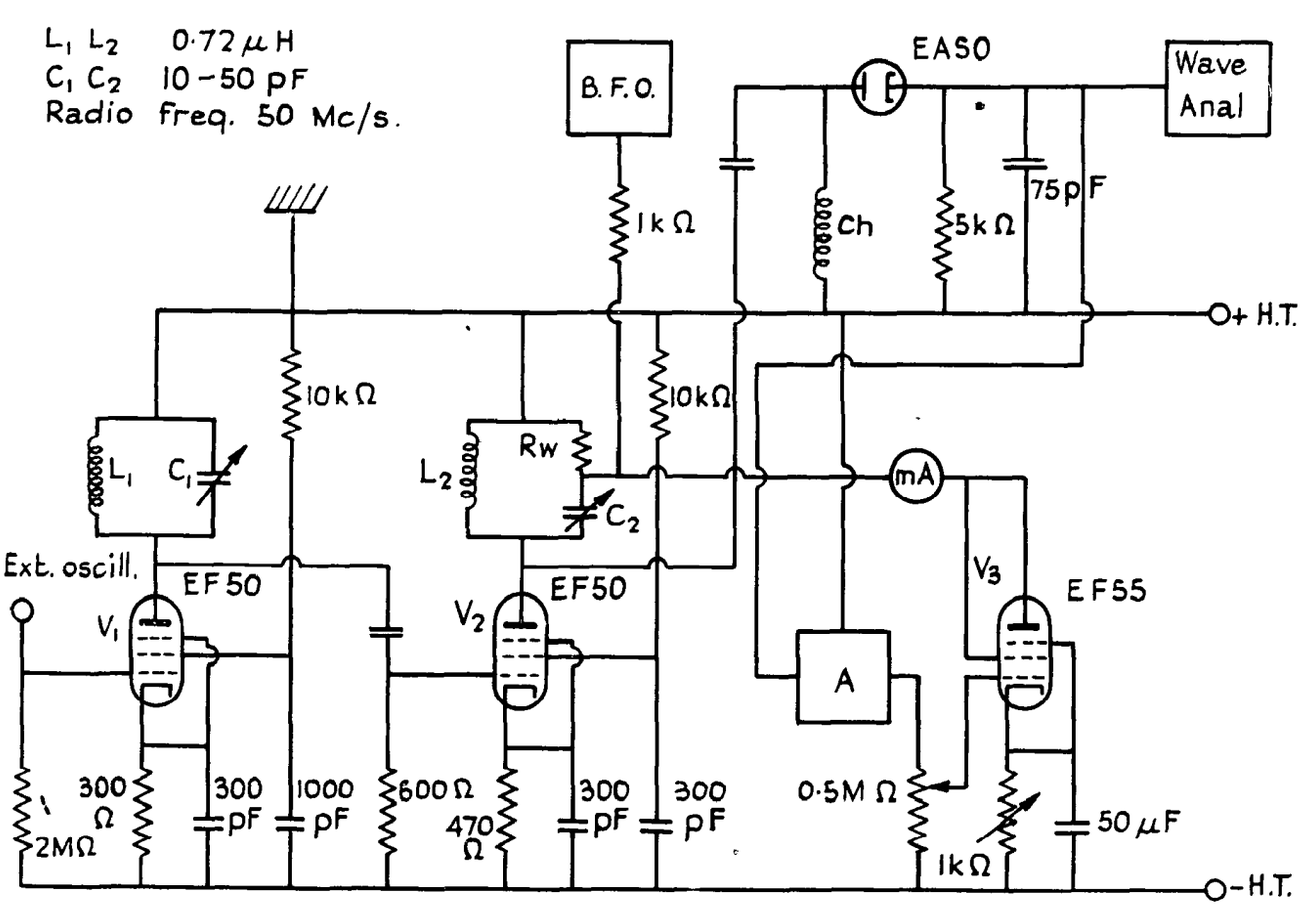

FIG. 52.

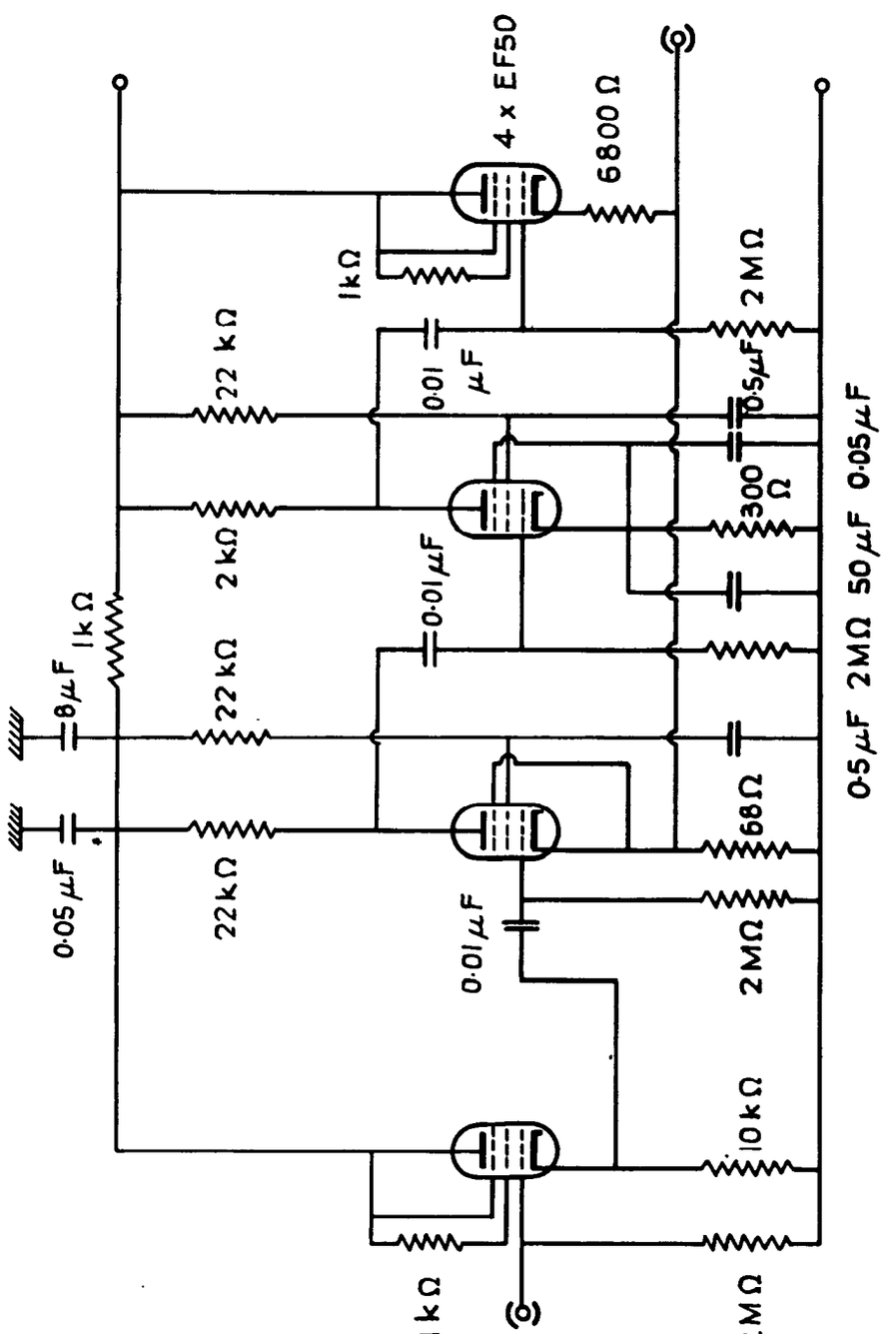
4 x EF50
6800 Ω
1kΩ
2 MΩ
22 kΩ
0·01 μF
0·5μF
300 Ω
0·05μF
2 kΩ
0·01μF
1k Ω
8μF
22 kΩ
68Ω
0·05μF
22kΩ
0·01μF
2MΩ
10 kΩ
1kΩ
2MΩ
0·5μF 2MΩ 50μF 0·05μF

FIG. 53.

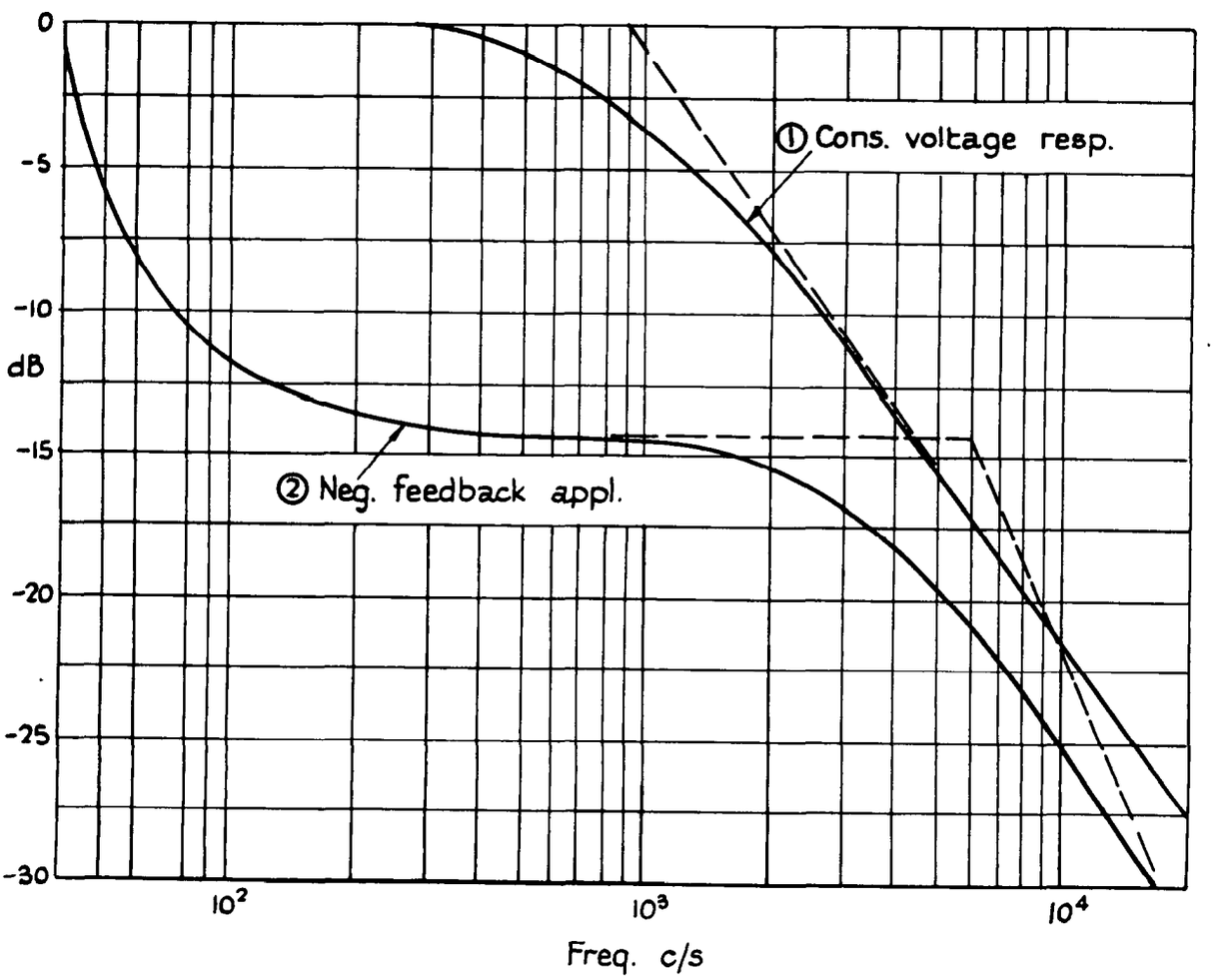

Response of constant voltage system, fig. 47, with overall negative feedback.

Rw = 30 Ω, 0·0001 Pt. Vw = 0·70 V Id = 10 mA Gain = 30 dB
1 + K = 5

FIGS. 54, 55 & 56.

FIG. 54.

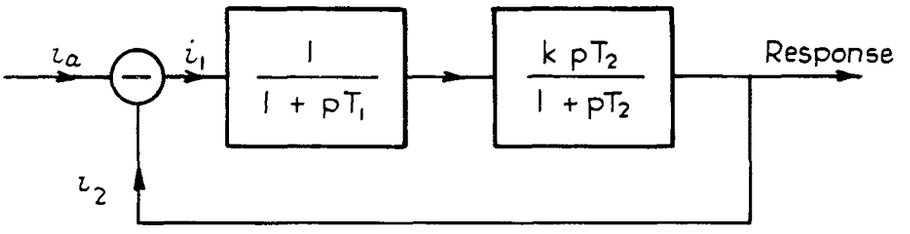

FIG. 55.

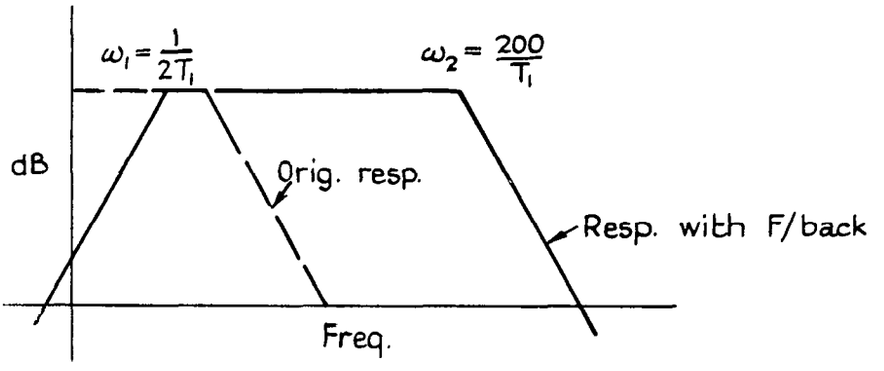

FIG. 56.

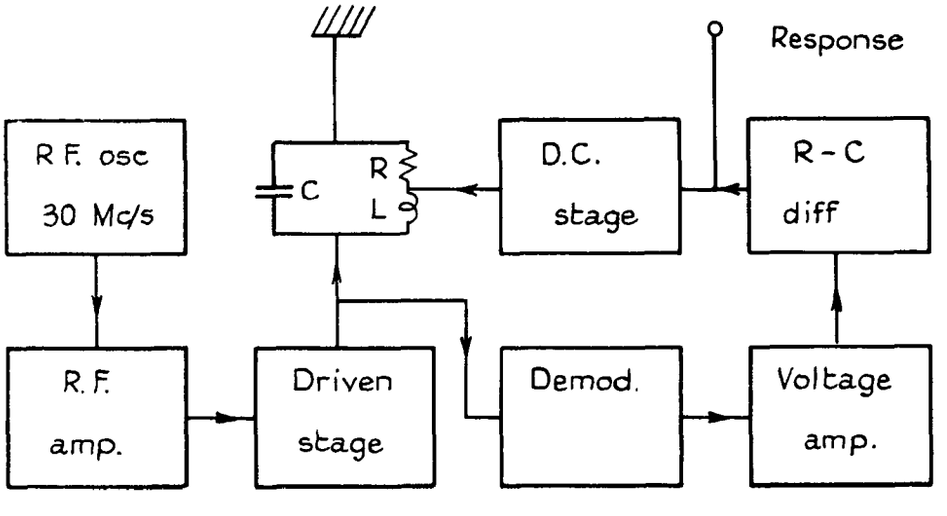

FIG. 57.

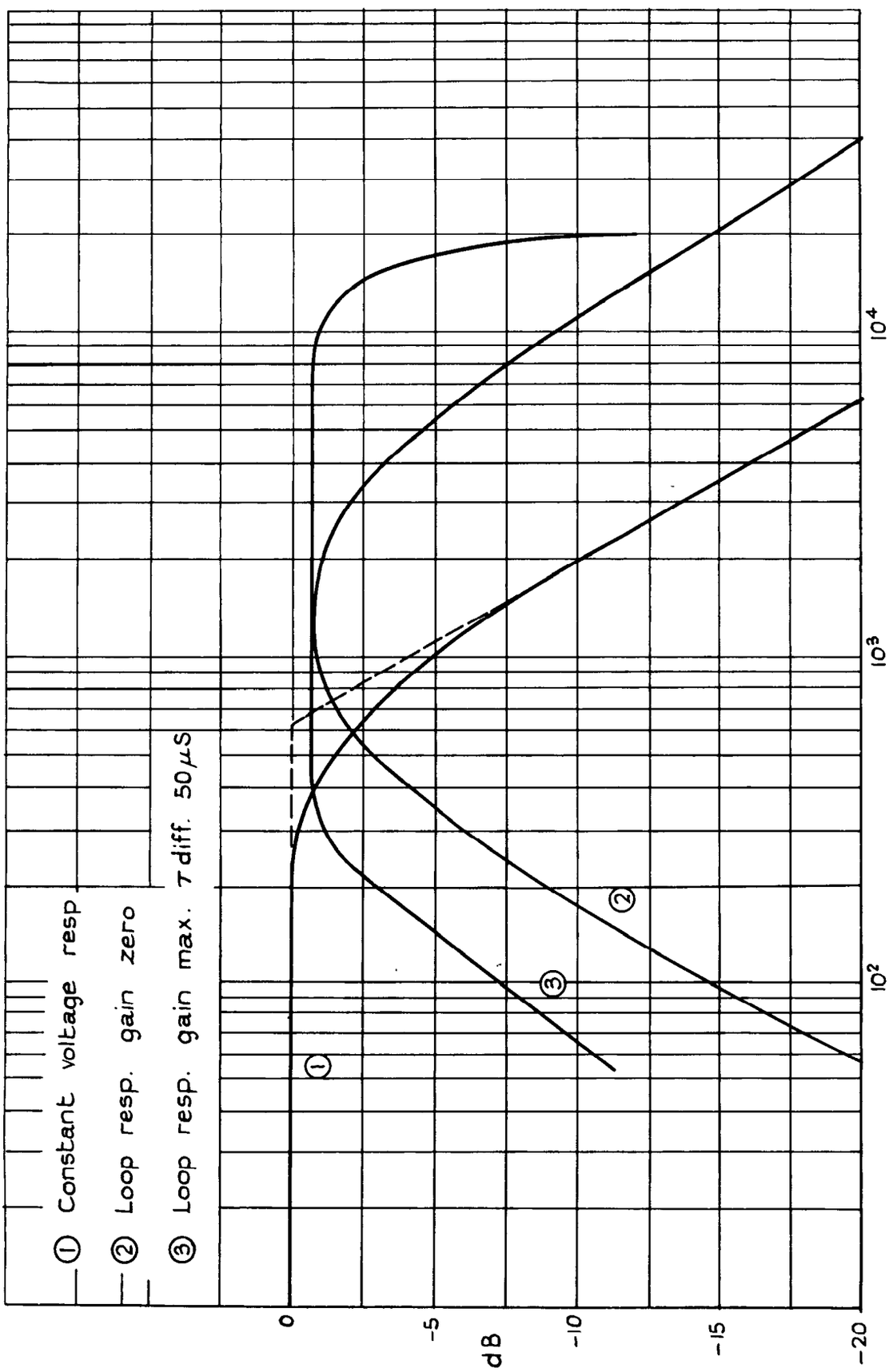

Rw = 30Ω 0·0001" Pt. I d.c. = 15 mA. V_w = 0·66 V. (R.F.).
Atten n levels relative only.

FIGS. 58 & 59.

FIG. 58.

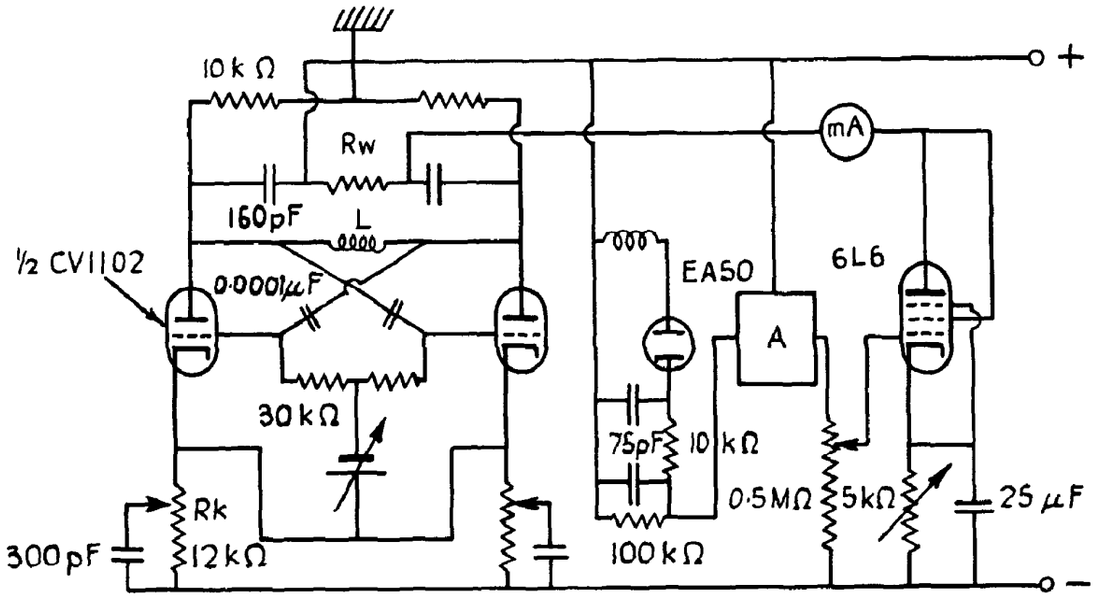

FIG. 59.

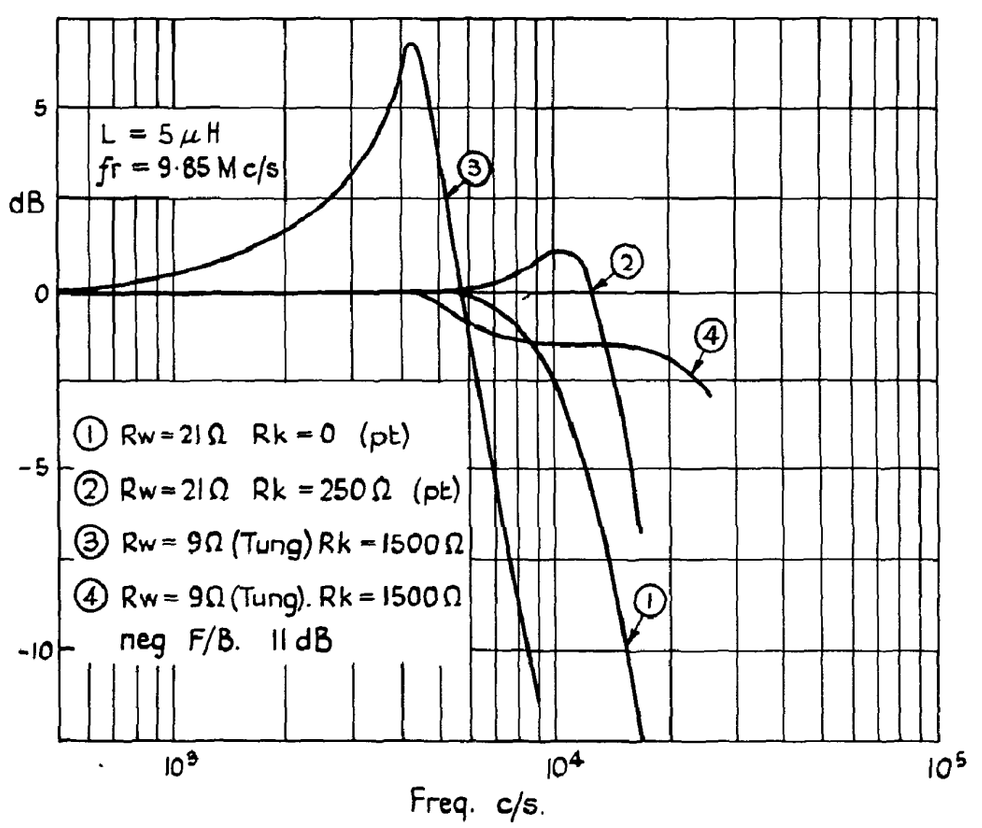

FIGS. 60 - 62.

FIG. 60.

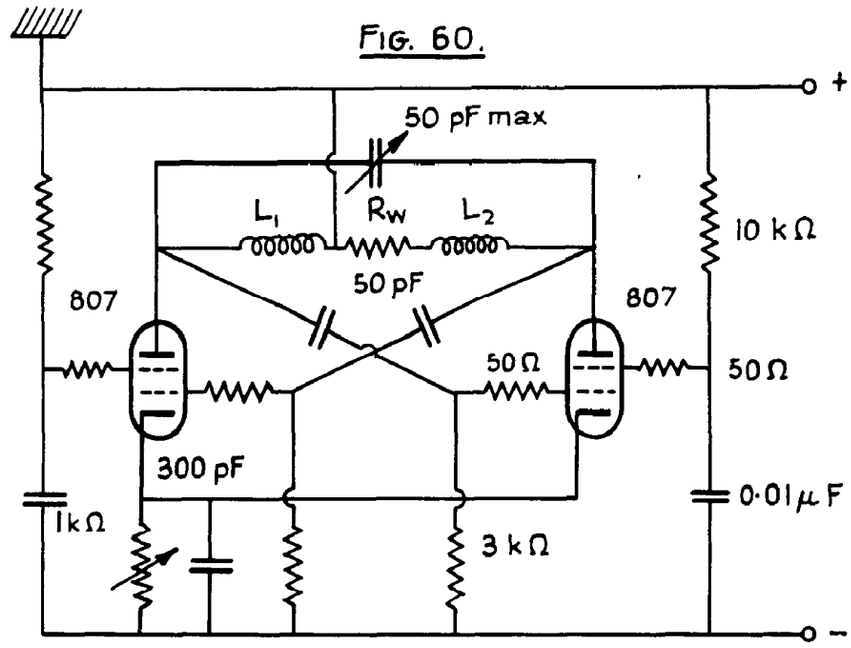

FIG. 61.

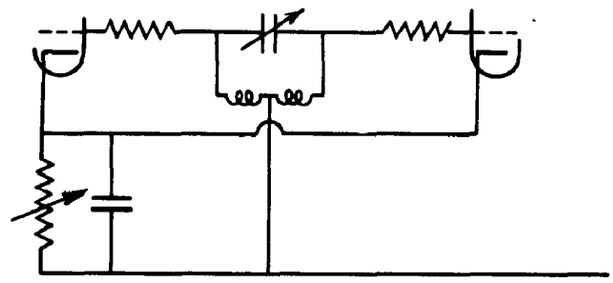

FIG. 62.

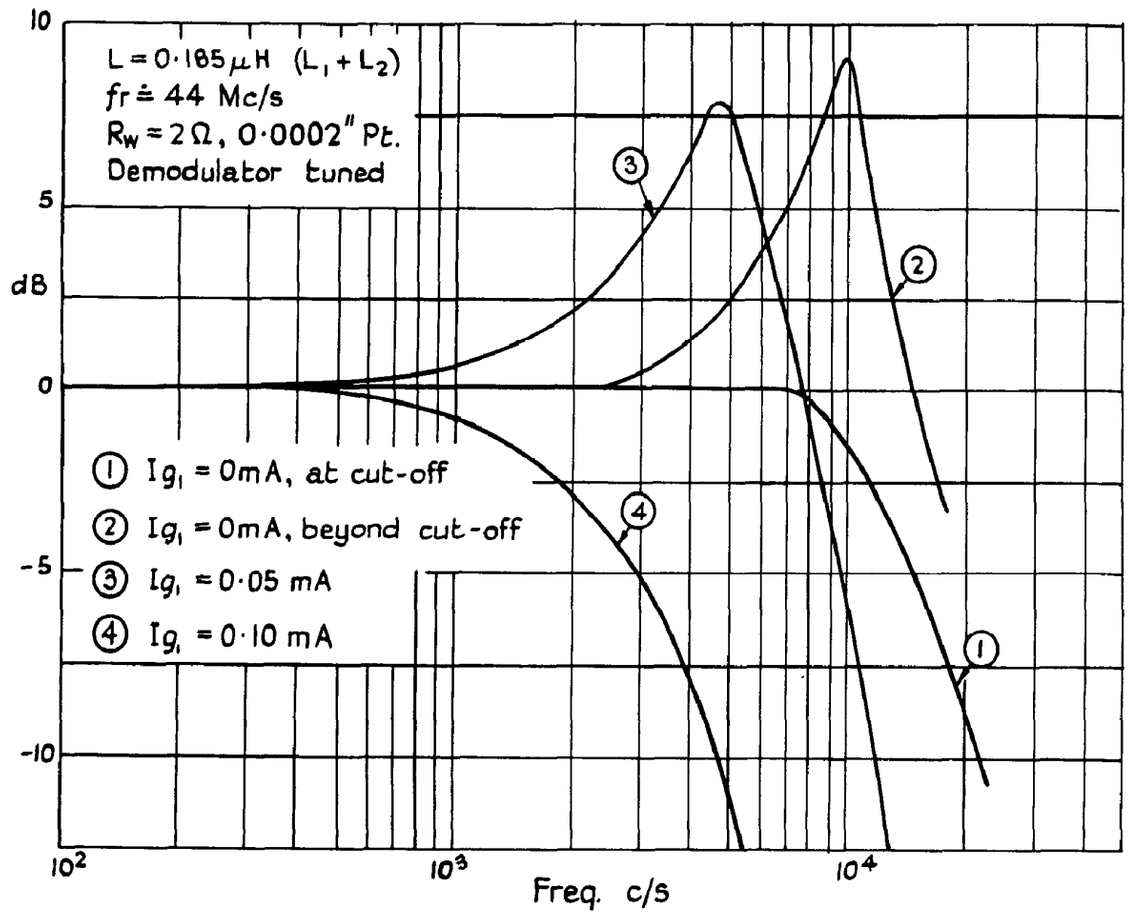

FIGS. 63 & 64.

FIG. 63.

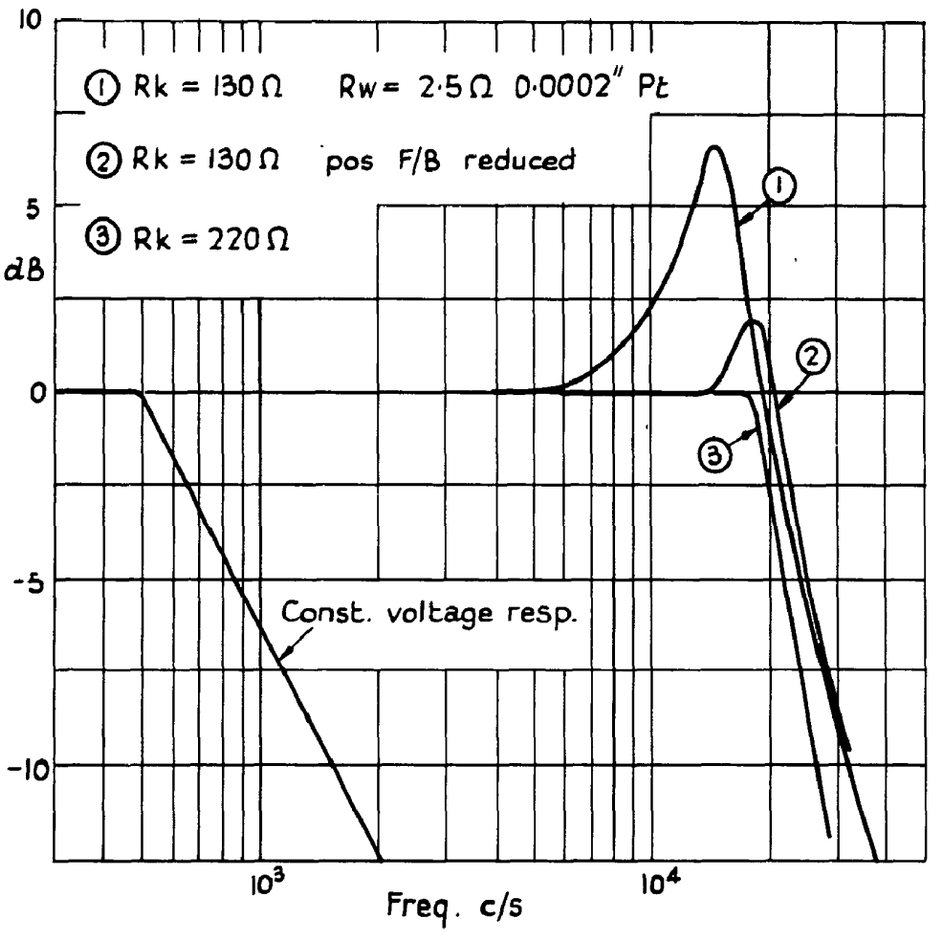

Response of push pull oscillator with cathode degeneration.

Total tuned circuit inductance = 0·24 μH. $T_{c.v.}$ = 0·318 millisecs.
Radio freq. = 50 Mc/s Rw = 3 Ω, 0·0002 in. Pt.

FIG. 64.

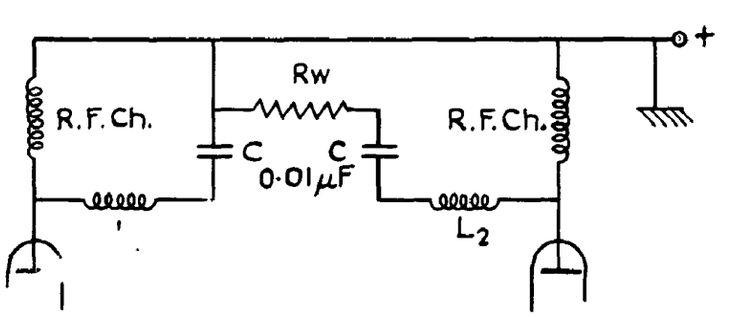

FIG. 65.

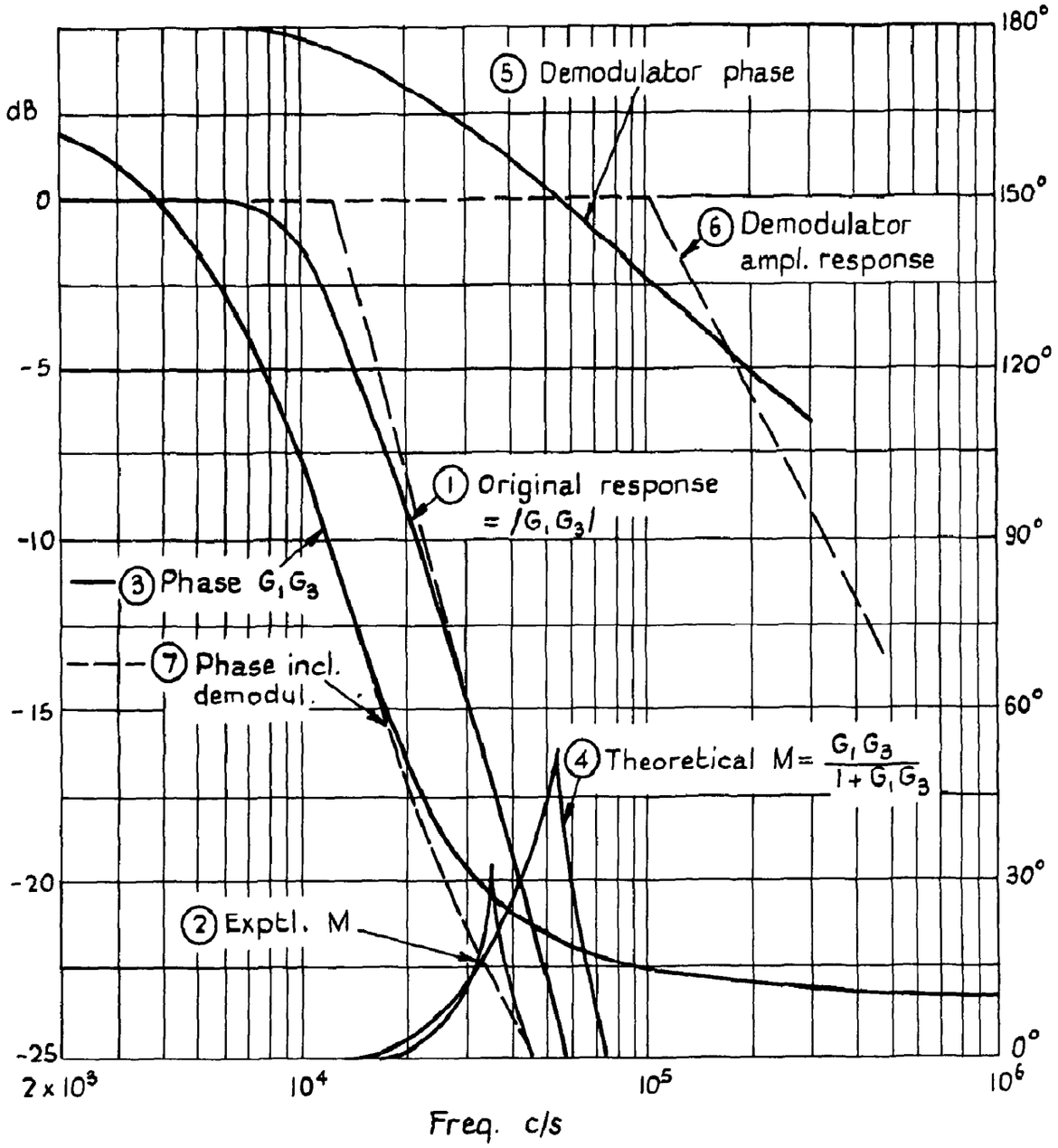

Experimental and theoretical responses.

Overall negative feedback applied to push-pull 807 circuit.

Phase response (3) obtained from ref. 5.

Rw = 2·5 , 0·0002 in. Pt. Rk = 220 Ω , L = 0·24 μH. $T_{c.v}$ = 0·318 m.sec.

FIG. 66.

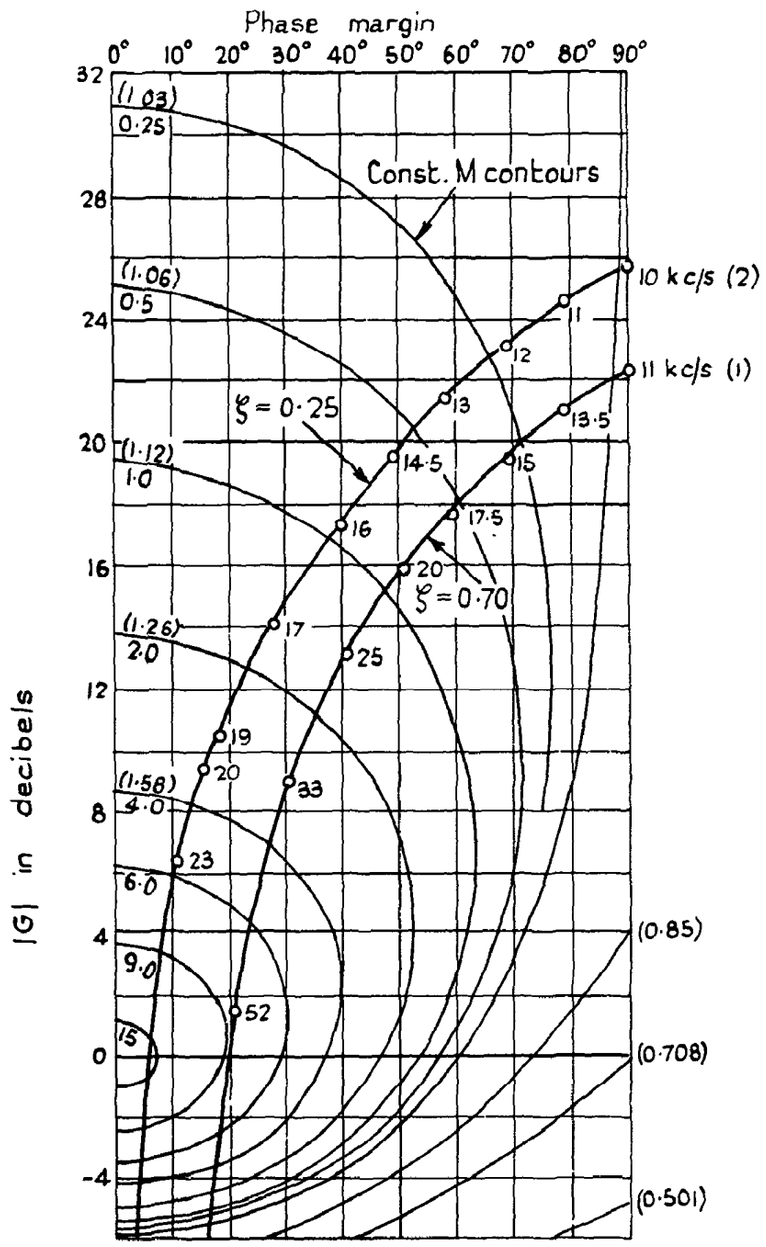

Nichol's chart showing response (4), fig. 65. 25 dB suppression at low frequencies, $\zeta = 0.70$.

Locus (2) above referring to fig. 63.

FIG. 67.

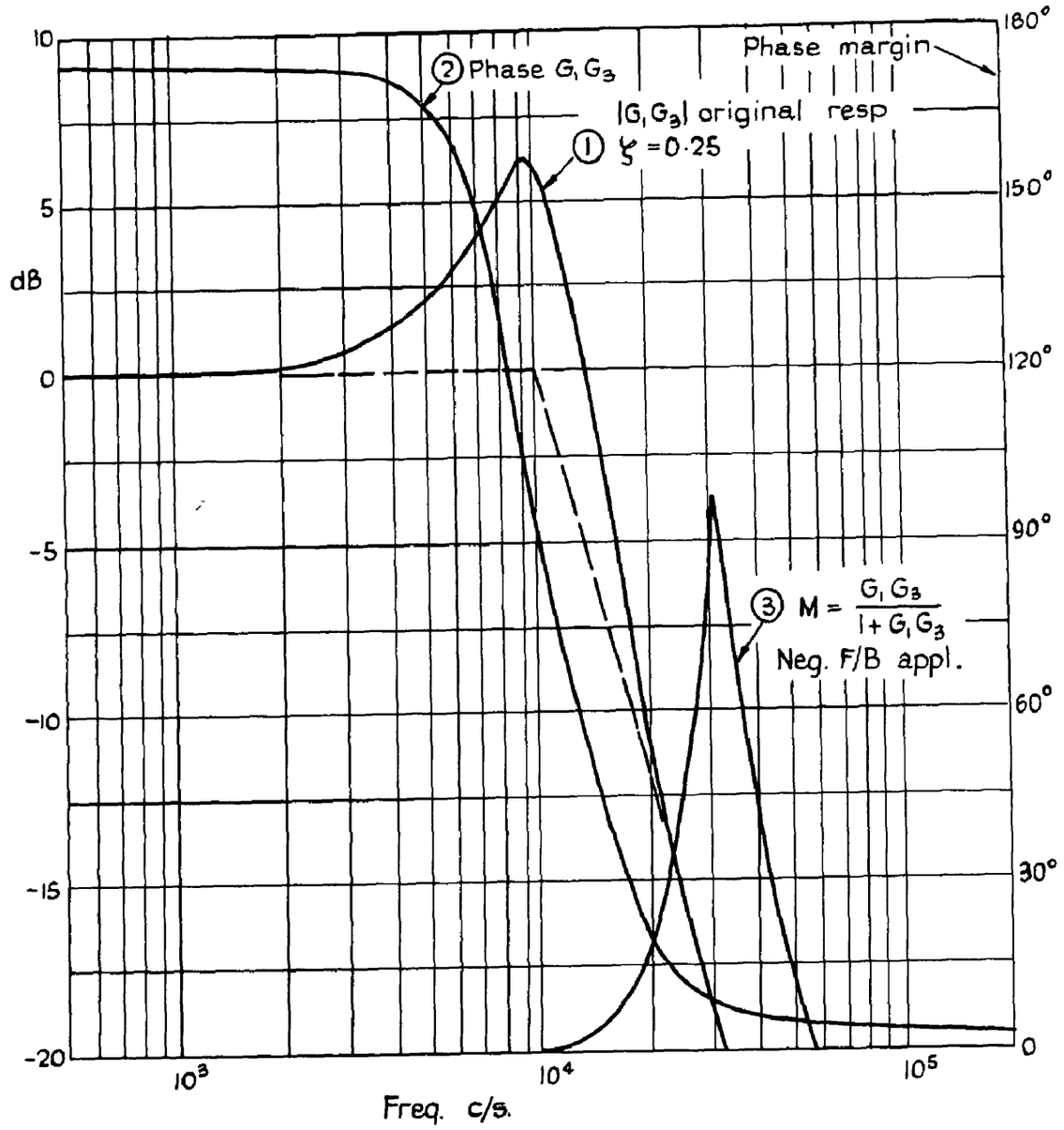

Negative feedback applied to underdamped response

$\zeta = 0.25$ in original response (1). Phase derived from Ref. 5. Locus of (3) plotted on Nichol's chart, Fig. 66.

FIGS. 68 & 69.

FIG. 68.

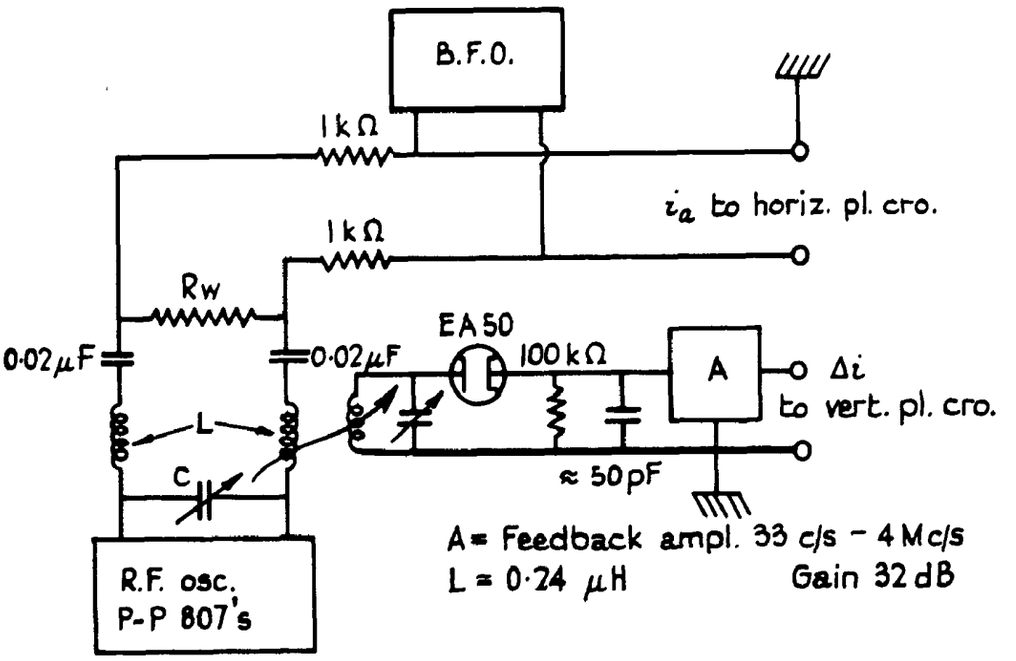

FIG. 69.

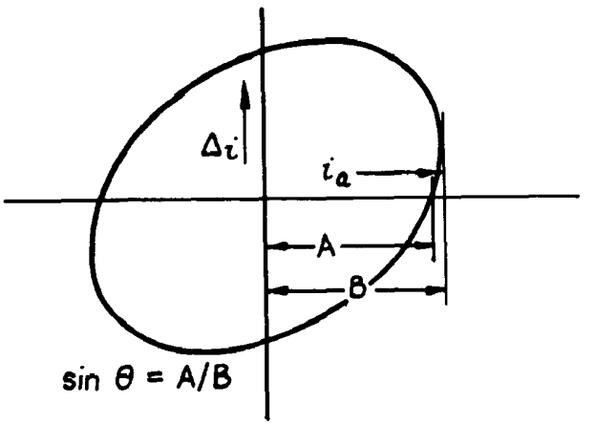

FIGS. 70 & 71.

FIG. 70.

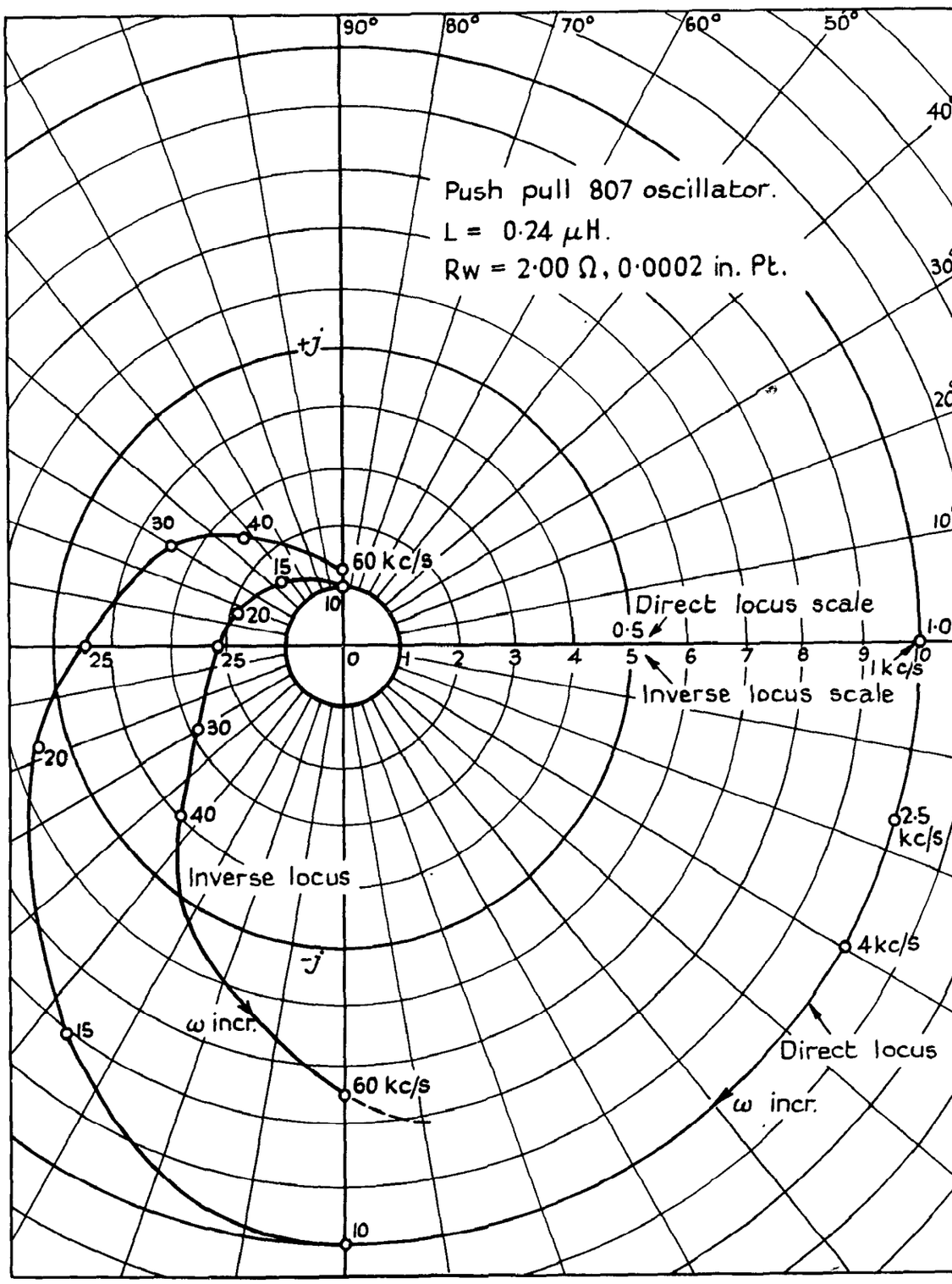

FIG. 71.

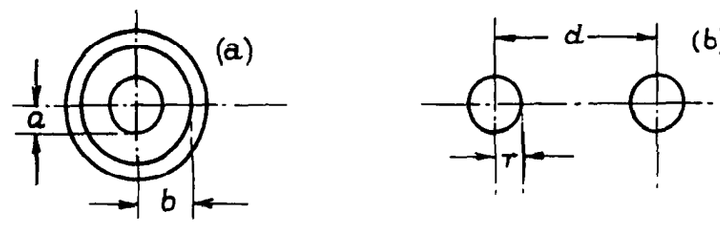

FIGS. 72 & 73.

FIG. 72.

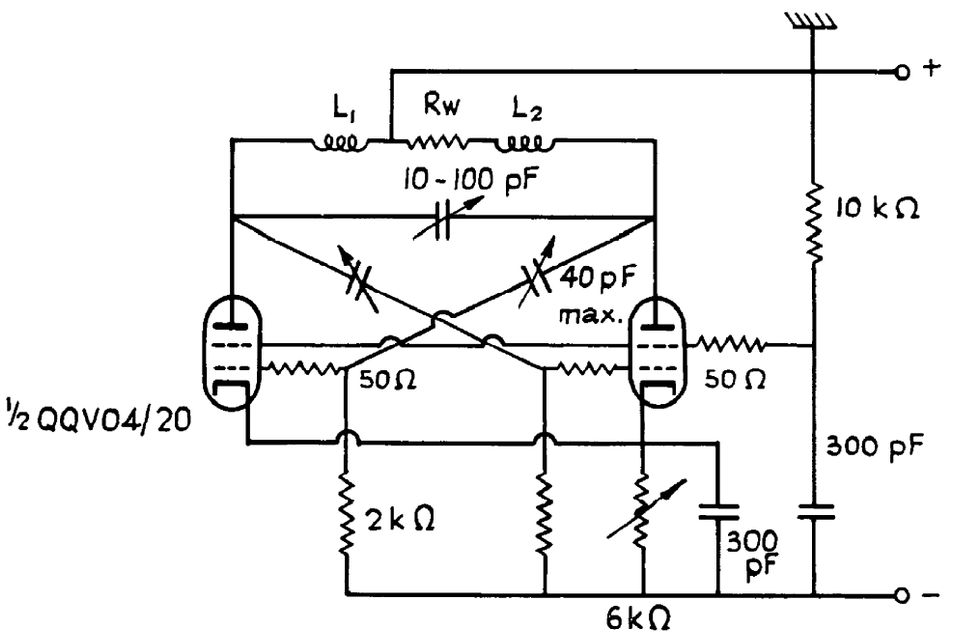

FIG. 73.

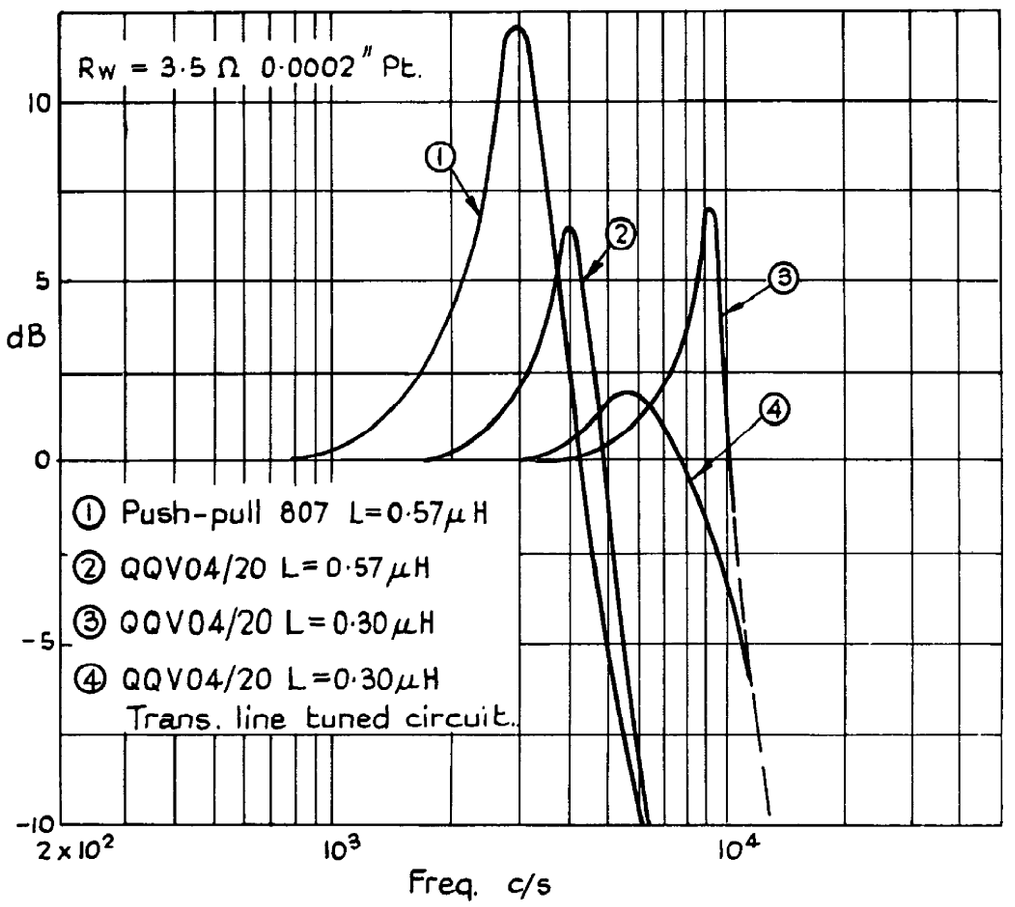

FIGS. 74 & 75.

FIG. 74.

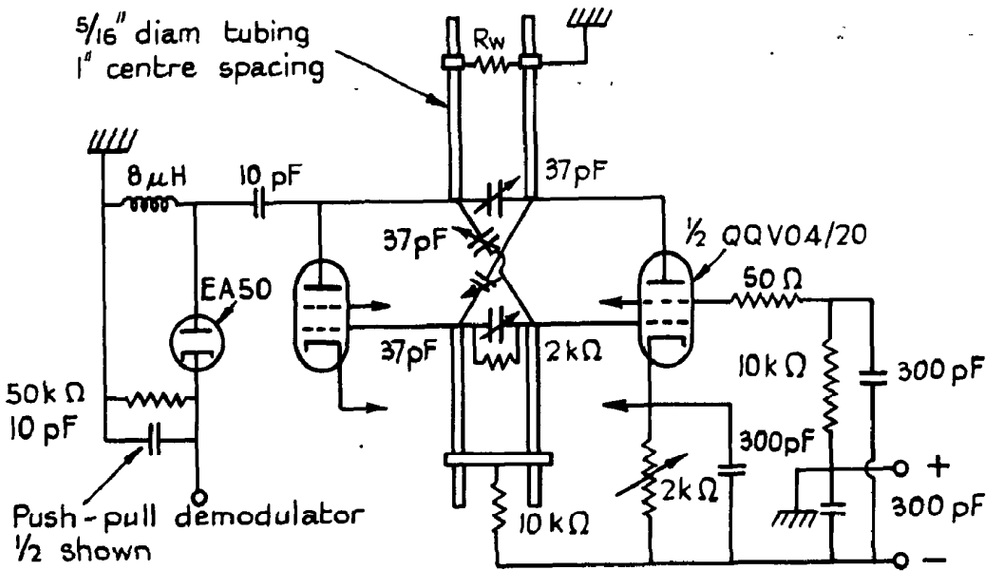

FIG. 75.

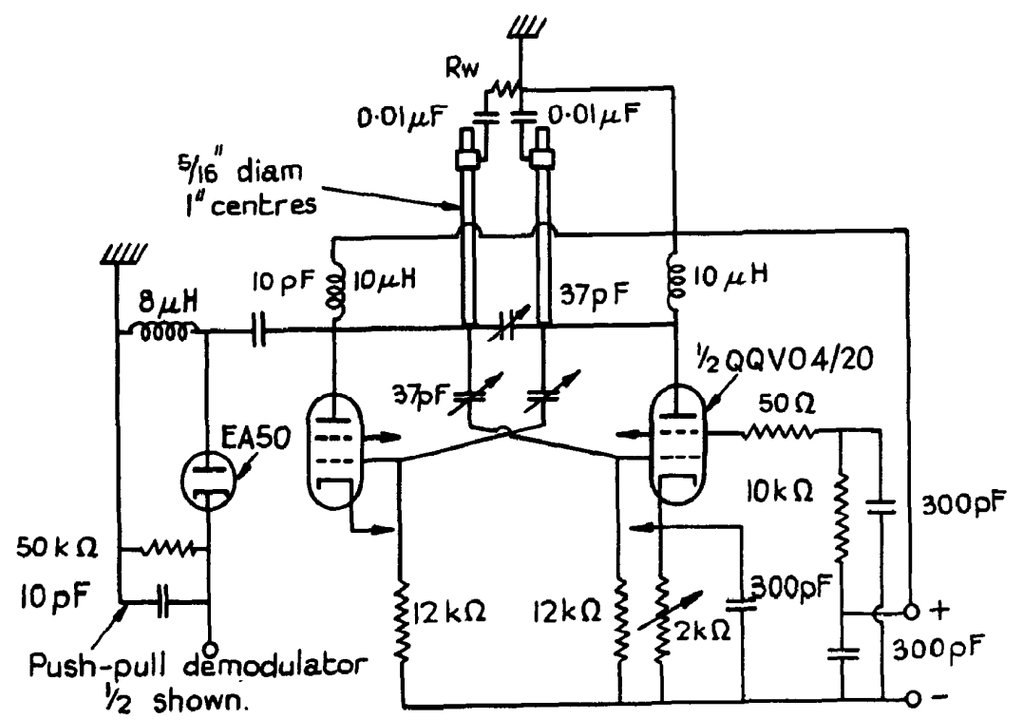

FIGS. 76 - 78.

FIG. 76.

Scale: 4 x full size

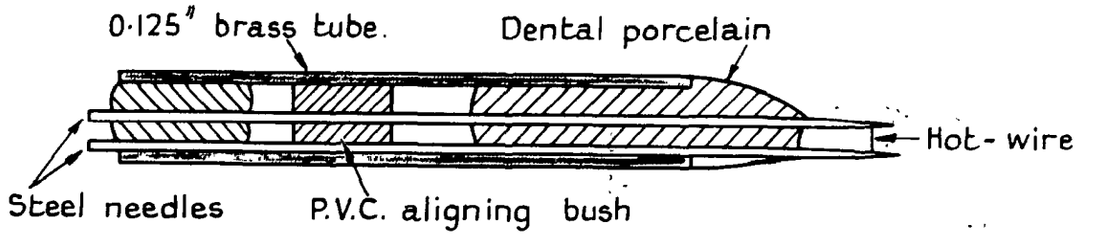

FIG. 77.

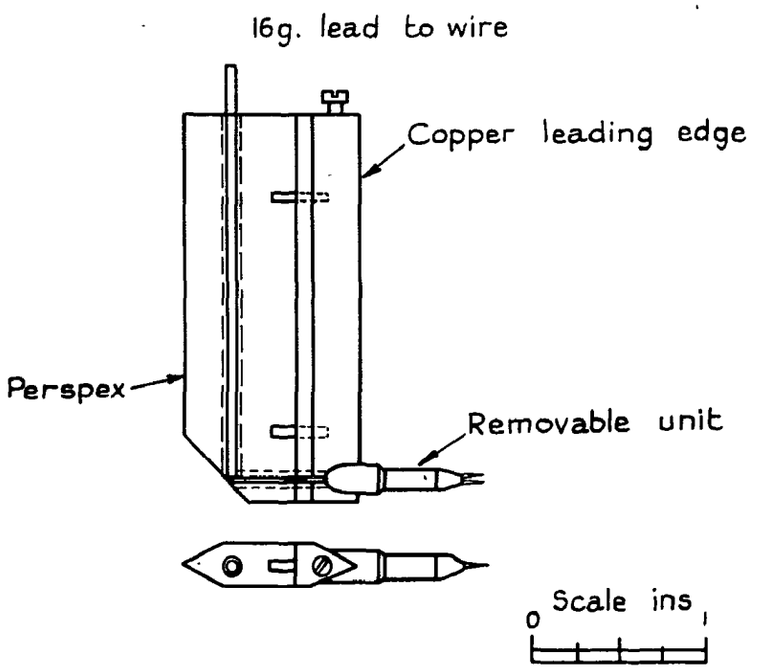

FIG. 78.

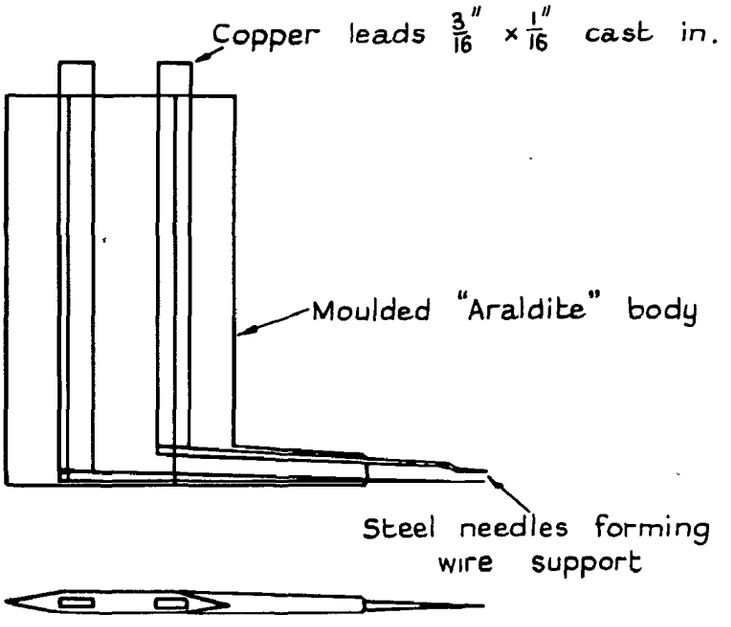

Anemometer probes.

FIGS. 79 & 80.

FIG. 79.

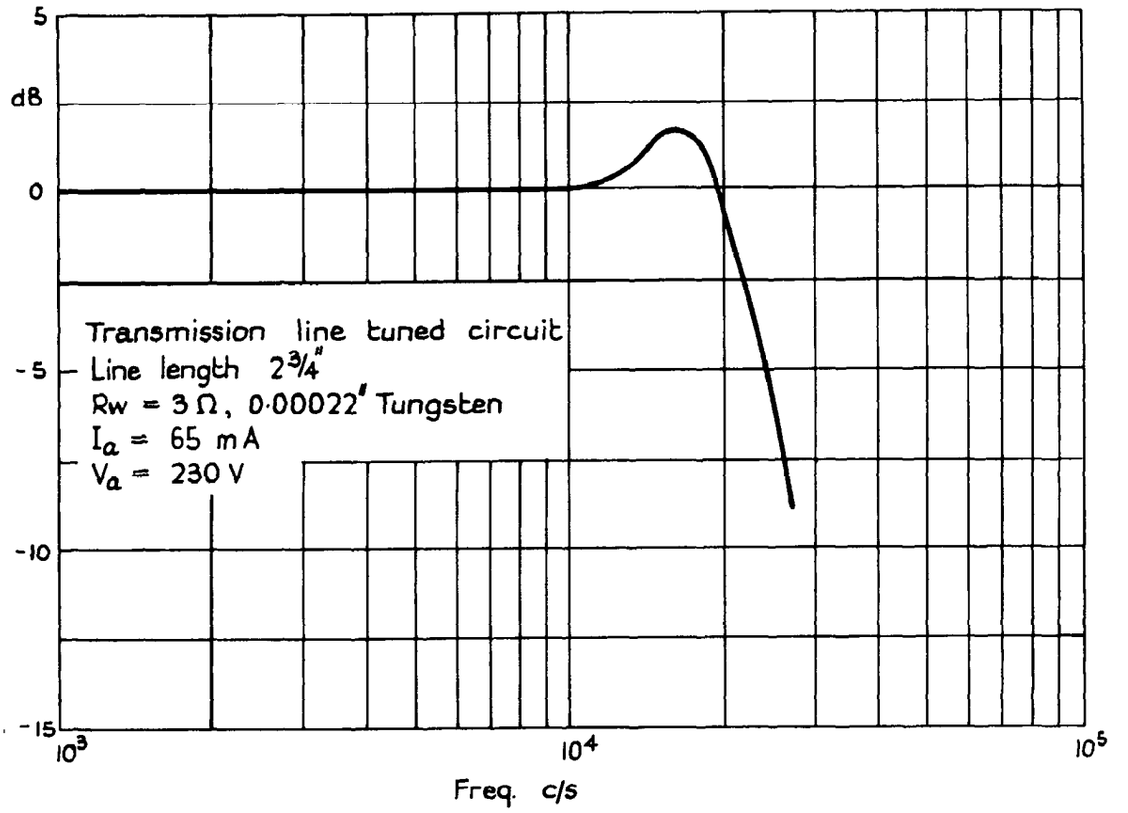

FIG. 80.

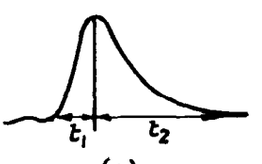

(a)

t_1 = 65 μ sec
t_2 = 200 μ sec

(b)

t_1 = 70 μ sec
t_2 = 70 μ sec

C.P. No. 275
(16,679)
A.R.C. Technical Report

Printed and published by
HER MAJESTY'S STATIONERY OFFICE

To be purchased from
York House, Kingsway, London W.C.2
423 Oxford Street, London W.1
P.O. Box 569, London S.E.1
13A Castle Street, Edinburgh 2
109 St. Mary Street, Cardiff
39 King Street, Manchester 2
Tower Lane, Bristol 1
2 Edmund Street, Birmingham 3
80 Chichester Street, Belfast
or through any bookseller

Printed in Great Britain

S.O. Code No. 23-9089-75
C.P. No. 275